227-8

CR-152031

(NASA-CR-152031) SPACE ELECTRIC POWER DESIGN STUDY (Joint Center for Graduate Study) 126 p HC A07/MF A01 CSCL 10A

N78-21590

Unclas
G3/44 09886

SPACE ELECTRIC POWER DESIGN STUDY

By

W. R. Martini

Joint Center for Graduate Study
Richland, Washington

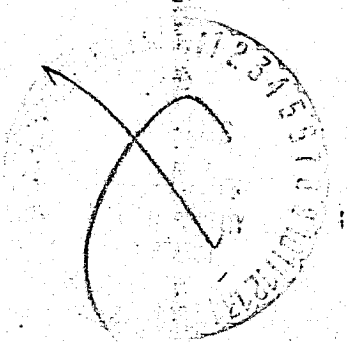

Task 2 of Order Number

A-29674-B (DG)

from NASA Ames Research Center

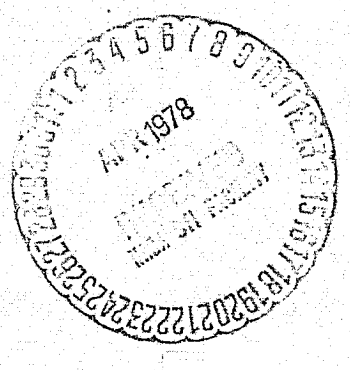

ABSTRACT

This study evaluates different ways laser energy can be converted to electrical energy by means of a heat engine. Heat engines in which the laser heats the gas inside the engine through a window as well as heat engines in which the gas is heated by a thermal energy storage reservoir which has been heated by laser radiation are both evaluated. Also the necessary energy storage, transmission and conversion components needed for a full system are evaluated. Preliminary system concepts are presented and a recommended development program is outlined briefly. It now appears possible that a free displacer Stirling engine operating directly a linear electric generator can convert 65% of the incident laser energy into electricity.

TABLE OF CONTENTS

TABLE OF CONTENTS (continued)

LIST OF FIGURES

LIST OF FIGURES (continued)

LIST OF TABLES

1. INTRODUCTION

With lasers for the first time it is possible to beam energy over long distances--like several times the earth-moon distance--through space with very little divergence or attenuation (Ref. 11). However, for such an energy transportation system to be practical, efficient ways of converting to and from laser energy are needed. Ref. 11 discusses some of these ways as well as the technology of beaming the energy.

Using present technology there are a number of means for converting from laser radiation to electrical energy. Photovoltaic cells are used for almost all of the solar electric power sources in space. But for high power lasers there would have to be an entirely different type of semiconductor material developed. Nevertheless, the potential may be very good (Ref. 11). Thermoelectric converters can conceivably convert laser radiation to electricity but after many years of development the best system efficiencies are about 10% (Ref. 12). Closed Brayton cycle power sources for space applications have been well developed to be the next step beyond thermoelectrics. Turbines have been tested for 32500 hours and overall efficiencies of about 27% are claimed for 750 w(e) output (Ref. 13). This type of hardware is now available for application. For an advanced power source development project to be attractive it must offer substantially increased efficiency, a low specific weight and a very high reliability.

The purpose of this study is to evaluate the feasibility of using a Stirling engine or another type of positive displacement heat engine to produce 750 w(e) of electrical energy from concentrated laser radiation. The goal is 50% efficiency computed as electric power out divided by laser radiation applied to the engine. It is assumed that concentrated laser radiation will be available at 10 Kw/cm^2 either pulsed or continuous. A CO_2 or a CO laser will be assumed although in

most cases the kind of laser will not be important. The possibilities will now be identified and then evaluated quantitatively. Based upon this evaluation the best apparent power source concept will be chosen based upon the lightest power source that will reliably produce 750 w(e) at 50% overall efficiency with a long life expectancy.

2. POWER SOURCE POSSIBILITIES

Figure 1 shows the possibilities for converting laser radiation either pulsed or continuous into electrical energy.

There are two main paths to mechanical power. One takes advantage of the fact that laser radiation can be absorbed efficiently and directly by the working gas of the engine. Once absorbed it is not easily re-radiated. Engines related to the internal combustion or Otto cycle engine can be used to employ heat source temperatures generated by laser radiation through a window in the engine cylinder which are far higher than any solid material can stand. This very high temperature leads to a high efficiency. The other main path leads through a black body cavity energy receiver. The receiver converts energy from any radiant energy source to heat and stores it by melting an appropriate salt. The thermal energy storage is insulated and so is the black body receiver insulated when it is not receiving energy. A Stirling type cycle, which can be much more efficient for the temperature than an Otto type cycle, is then used for producing pressure-volume (PV) energy.

Once PV is produced by an engine, there are a number of viable paths to electrical energy suitable for space craft power. The heat engine can produce a high pressure gas which can be let down through a turbine directly connected to an electric generator. The heat engine can convert its output into hydraulic power which can operate a hydraulic turbine or a positive displacement hydraulic

Figure 1

Power Source Options to be Evaluated

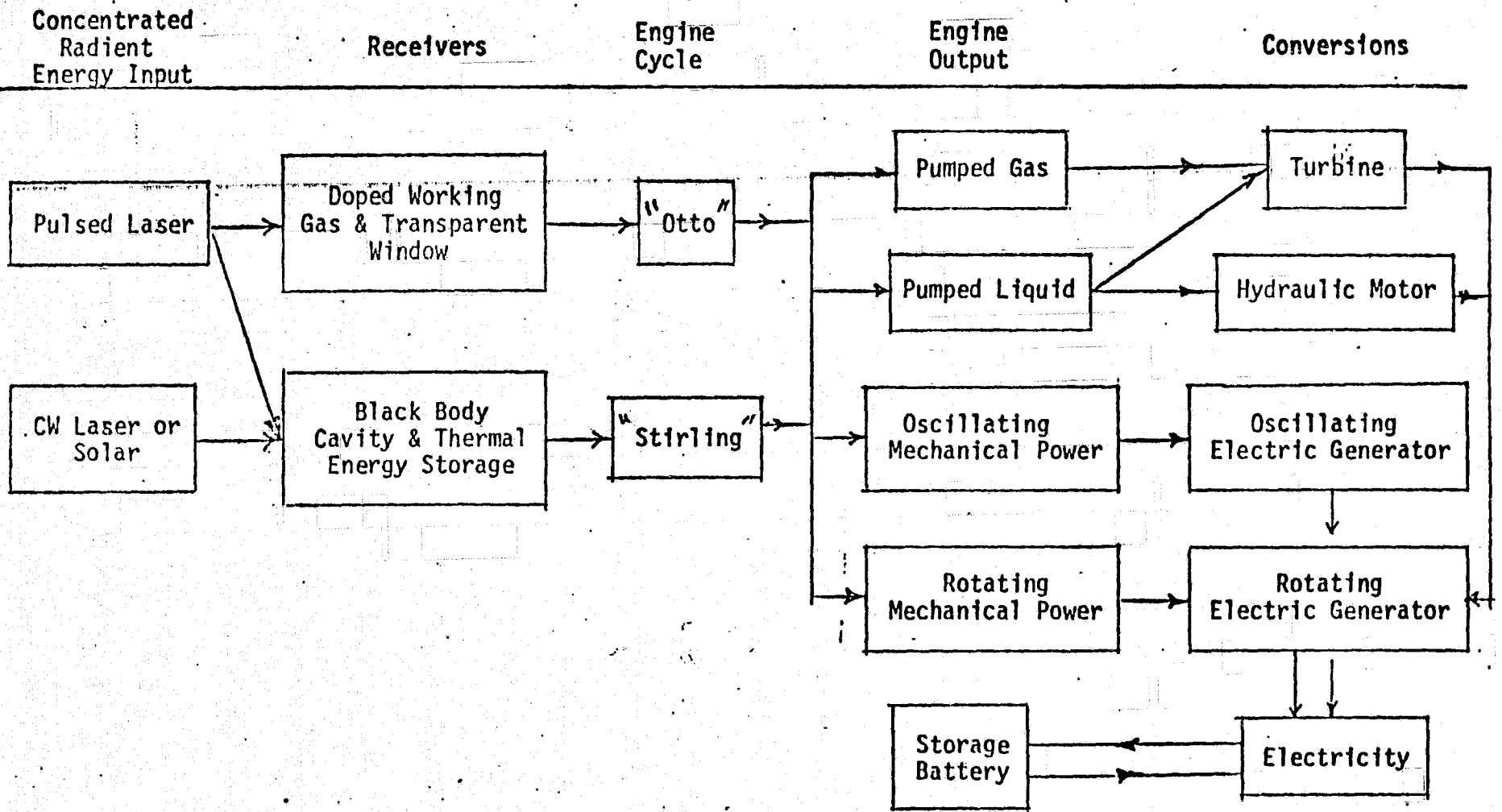

motor connected to a rotating electric generator. Since both "Otto" and "Stirling" engines are both positive displacement type, one can conceive of an oscillating electric generator directly connected to or possibly incorporating the power piston of the heat engine. Intermediate machinery is therefore eliminated. Finally, the conventional approach is to convert piston motion to shaft power to drive a conventional rotary electric generator.

Space craft power is probably best supplied by batteries which are kept re-supplied by the laser engine-generator. This arrangement makes it easier to control voltage and can allow for power surges and breaks in engine output due to interruption of the laser beam. It also can be used in conjunction with and compliment thermal energy storage.

3. COMPONENT EVALUATION

The components that could be included in the power source discussed above will now be discussed quantitatively so that a well informed choice can be made.

3.1 Laser Energy Acceptance

The laser energy must be either transmitted through a window into the working gas where it is absorbed (internal heating) or it is absorbed in a cavity which is part of an insulated thermal energy storage container which is in good thermal contact with the engine (external heating).

3.1.1 Internal Heating

3.1.1.1 Windows

The window must be transparent to the laser radiation and be able to stand the thermal stresses and the pressure stresses of use. Garbuny and Pechersky (Ref. 1) have evaluated from a theoretical standpoint the feasibility of a laser

engine using a window and absorption in the gas phase. Table 1 presents the results of their evaluation. High power CO_2 lasers are available but the window material is difficult. Sapphire is apparently an ideal window material which can be used for CO and other lasers. CO lasers exhibit large powers but as yet do not lase at quite the right wavelength to escape atmospheric attenuation.

Since the window is a crucial part of one possible type of engine, additional research was made into the extensive literature on laser windows. These windows will be heated internally by absorption of some of the laser energy. This will cause the core of the window to try to expand and place the circumference of the window in tension. The circumference is also cooled. Good thermal conductivity helps keep these thermal stresses down. Also, in a laser engine the window is subjected to additional thermal stress due to contact with the hot gas generated inside the engine. In addition, pressure stress is generated by the gas pressure. In an engine where refraction is not critical, one can gain considerably by pre-stressing the window by shrinking a metal rim around it and keeping the window always in compression since most nonconductive materials are much stronger in compression than they are in tension. Horrigan et al. (Ref. 14) recommends KCl and GaAs as window materials for CO_2 lasers. This reference presents a figure of merit which is a reasonable way of rating a window's ability to stand the thermal stress of use in an engine. Thus,

$$FM = \sigma_c K/\beta\alpha E$$

where

σ_c = critical fracture stress or modulus of rupture, psi

K = thermal conductivity, w/cm ^oC

β = absorption coefficient, cm^{-1}

α = linear coefficient of thermal expansion, $^oC^{-1}$

E = Young's Modulus, psi

TABLE 1

RECOMMENDATIONS FOR WINDOWS AND GAS ABSORBERS FOR LASER ENGINES (REF. 1)

Laser Type	Wavelength	Window Material	Absorbing Gas	Saturation Temp. ^{o}K	Estimated Max. Temp. ^{o}K
CO_2	10.6 m	diamond (1)	SF_6	1380	1500
CO	4.7 m	sapphire	CO	3100	> 2500
HCl	3.5 m	sapphire	HCl	4100	~ 2500
HF	2.8 m	sapphire	HF	5100	~ 2500
I	1.3 m	sapphire	I_2	10,900	

(1) also antireflection coated CdSe

All of these window materials need antireflection coatings on both surfaces which will reduce the reflection loss to ~0.5% (Ref. 15). Table 2 gives additional information on the figure of merit for common available windows for the CO_2 laser. Galium arsenide is the best. The use of diamond for this purpose is being investigated. Diamonds are found to have quite variable absorption coefficients.

3.1.1.2 Gas Absorption

Reference 1 presents theoretical evaluation of the process of absorbing laser radiation by a gas. An estimate of the maximum temperature attainable in the gas is made (see Table 1). The absorbing gas will be mostly helium colored by the absorbing gas shown in Table 1 (i.e., SF_6, CO, etc). The reason for this is to keep from having all the radiation absorbed right next to the window and have the heat be deposited more nearly in the volume of the gas.

Calculations indicate that interesting effective temperatures can possibly be attained. However, so far no experiments have been reported in which laser energy is applied to gas in a capsule containing an appropriate window. A pressure transducer on the capsule can record the effective temperature as a function of time. Data of this sort are needed before engine designs can be made with confidence.

3.1.2 External Heating

3.1.2.1 Cavity Absorption

The cavity absorber does not have a window to absorb or reflect the radiant energy but it does have the ability to re-radiate energy back out. Assume that 10 KW/cm^2 of absorption cavity opening is being applied by laser. The black body re-radiation would be:

$$Q_R = 5.67 \times 10^{-12} (T_H^4)$$

TABLE 2

COMPARISON OF WINDOWS SUITABLE FOR TRANSMISSTION OF CO_2 LASER RADIATION INTO AN ENGINE

(Ref. 14 except as noted)

Window Material	σ_c psi	K w/cm^{o}C	β cm^{-1}	α $^{o}C^{-1}$	E psi	FM W
Potassium Chloride	640	0.0653	0.001	36×10^{-6}	4.3×10^{6}	270
KRS-5[1]	18,100	0.0054	0.005	58×10^{-6}	2.3×10^{6}	146
Gallium Arsenide	20,000	0.3705	0.02	5.7×10^{-6}	12.3×10^{6}	5284
Diamond						

[1] Thalium Bromide-Iodide

where Q_R = re-radiation heat flux, w/cm^2

T_H = heat source temperature, ^oK

The heat absorption efficiency therefore is

$$\eta_A = 1 - \frac{5.67 \times 10^{-12}(T_H)^4}{10{,}000} = 1 - 5.67 \times 10^{-16}(T_H)^4$$

For reasonable temperatures for heat engine, η_A is:

T_H ^oC	T_H ^oK	η_A
600	873	0.99967
700	973	0.99949
800	1073	0.99925
1000	1273	0.99851
1200	1473	0.99733
1500	1773	0.99440
2000	2273	0.98487
3000	3273	0.93493

From the above it is seen that re-radiation is entirely negligible in the region of 600 to 800°C where super alloys could be used. It is still negligible in the region of 1700 to 1900°C which is the limit for refractory metals like tungsten alloys.

3.1.2.2 Thermal Energy Storage

Thermal energy storage has the advantage of allowing for breaks in the transmission of laser energy without stopping the engine. It will also be shown that energy storage as heat is more efficient, lighter, more rugged than energy storage in electrochemical batteries. Borucka (Ref. 2) has made a wide survey of possible salts for use in thermal energy storage. Four of the best salts in terms of calories/gram heat of fusion are listed in Table 3. These

TABLE 3

PROPERTIES OF THERMAL ENERGY STORAGE SALTS

Salt	Use Range °C	Melting Point °C	Liquid Density gm/cc	Heat Storage Capacity KWH(th)/kg
37) 44.9 w/o LiF - 55.1 w/o MgF_2	641 - 841	741	2.16	0.374
16) LiF	742 - 942	842	1.83	0.422
22) MgF_2	1170 - 1370	1270	2.43	0.333
33) 49.1 w/o LiF - 50.9 w/o NaF	552 - 752	652	1.89	0.362

salts may be contained in either stainless steel or refractory metal, provided all water is excluded. A practical way of gettering water in these chemical systems is to add a few % of alumium powder to the melt just before casting (Ref. 3).

These salts have a low thermal conductivity in the solid phase, typically 1/3 that of stainless steel (Ref. 2). Therefore, the salt must be cast into small enough diameter cylinders so that at the rate of discharge planned, this temperature drop is not serious.

3.1.2.3 Thermal Insulation

Heat in the thermal storage can leak off through the engine, out the cavity hole or through the thermal insulation. The engine can support the thermal storage and have a low static heat loss. The engine cylinder can support a number of free-standing radiation shields (see Figure 2). Between the stationary radiation shields are pivoting radiation shields actuated by a bimetallic strip. The strip is heated by the fringes of the incoming laser radiation which causes the pivoting radiation shield to turn to expose the absorption cavity. When the laser radiation stops, the strip cools and the hole closes.

High vacuum, multi-foil insulation has been used successfully for high temperature insulation where a very low effective thermal conductivity is mandatory such as in artificial heart engines (Ref. 4, 5). Table 4 gives some of the very low thermal conductivities achieved. Ref. 4 achieves this low thermal conductivity by electro-plating a series of nickel cups onto aluminum mandrals. The cup thickness is only 0.0005 to 0.0008 inch thick when the mandral is etched away with caustic. Then by using a mask, an array of ZrO_2 dots are flame sprayed onto the cup to act as spacers. The cups are then nested with a radial clearance of 0.003 to 0.004". These ZrO_2 dots degrade the effective emissivity of the cups but do allow for a practical close packing of the foils to achieve a very low thermal conductivity. Ref. 4 achieves approximately the same effect by winding together 0.0005 inch thick

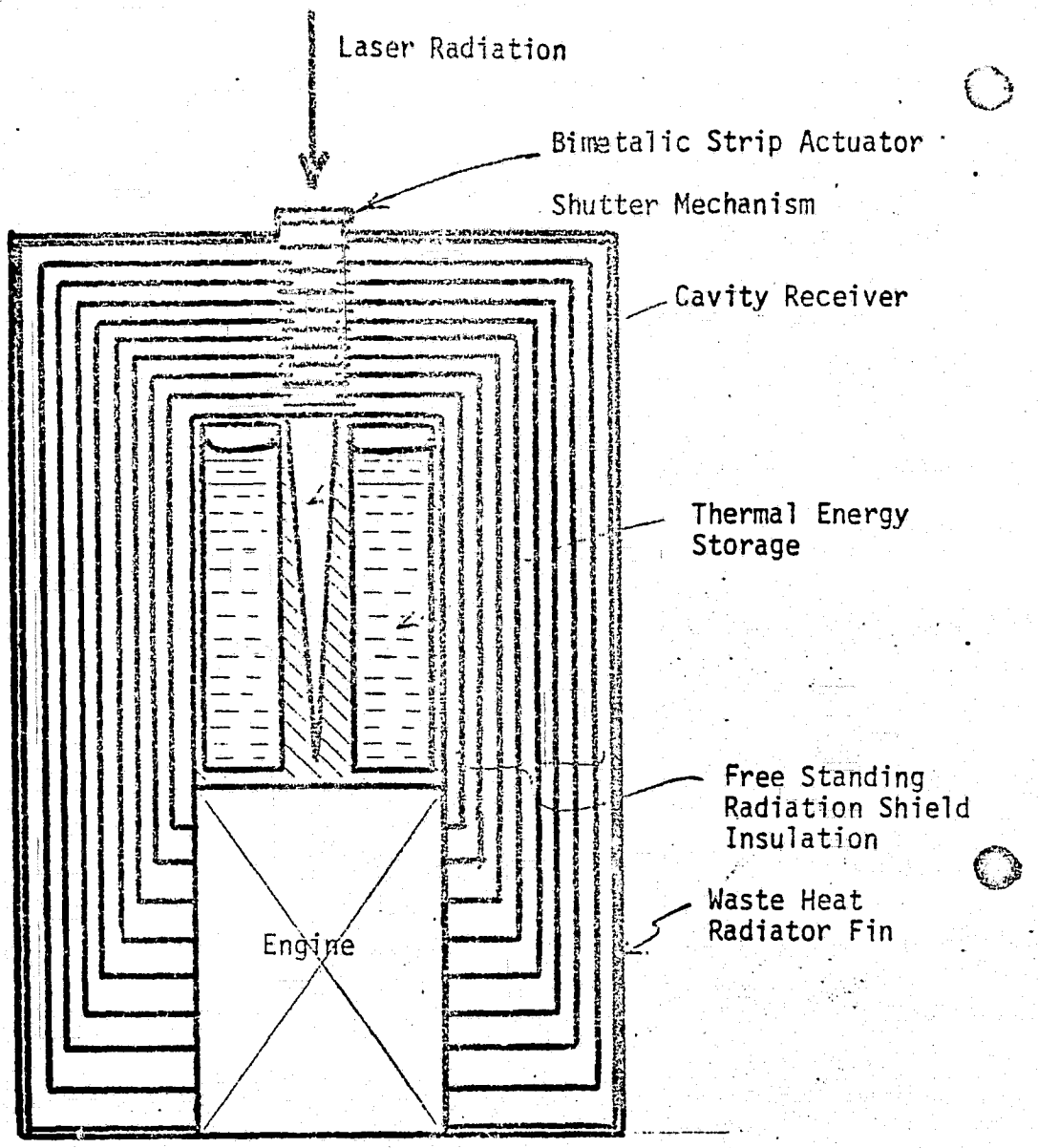

Figure 2. Concept for External Heating of Engine.

TABLE 4

HEAT LOSS RATES FOR MULTIFOIL INSULATION

Ref.	Heat Source Temp. ^{o}K	Heat Sink ^{o}K	Number of Foils	Foil Emissivity	Spacer	Measured Heat Flux w/cm^2	Measured Thermal Cond. $w/cm\ ^{o}C$
4	1140	300	4	.5	flame sprayed ZrO_2	0.29	1.40×10^{-5}
4	1140	300	40	.5	flame sprayed ZrO_2	0.0228	1.11×10^{-5}
	1140	300	4	0.265	none	0.29	
				0.018		0.0173	
	1140	300	40	0.018		0.0021	
			40	0.18		0.0230	
5	988	311	15	0.018 (gold)	.0025" silica paper	0.0169	7.61×10^{-6}
--	988	311	15	0.018	none	0.0030	
	988	311	15	0.0962	--	0.0169	

gold foil with 0.0025 inch silica paper. A step miter joint is used at the corner between the cylindrical surface and the end cap.

In a spacecraft application where weight is much more important than volume, the radiation shields can be spaced out so that each shield is free-standing being supported by attachment to the engine cylinder at a point where the temperature is the same as the shield. The basic equation for heat transmission through a series of radiation shields all with the same emissivity is:

$$q = \frac{(T_H^4 - T_C^4)\,\sigma}{(\frac{2}{\varepsilon} - 1)(n + 1)}$$

where q = heat flux w/cm^2

$\sigma = 5.67 \times 10^{-12}\ w/cm^2\ (^oK)^4$

T_H, T_C = heat source, heat sink temperature, ^oK

ε = emissivity of surfaces

n = number of radiation shields

This equation was used to determine the effective emissivity for the radiation shield system due to the need for spacing material. This equation also shows (see Table 3) that the number of radiation shields needed for a given amount of insulation can be greatly reduced if the emissivity of each shield is as low as possible (such as highly polished gold) and no spacing material is needed.

3.1.2.4 Heat Transport

Heat must be transported from the receiver cavity to the engine or to the thermal energy storage. Liquid metal heat pipes are commonly used for this purpose. Waters (Ref. 16) indicates that a potassium filled heat pipe will be useful from 400 to 800°C with super alloys. A calcium filled heat pipe can be used from 1100 to 1900°C with refractory metal alloys. The heat

flux at the receiver cone will be high but should be no problem for a heat pipe since the burnout heat flux for sodium is 0.3 to 0.8 Kw/cm^2 (Ref. 17) and other liquid metals would be similar. The transition from 10 KW/cm^2 incident laser flux to say 0.5 KW/cm^2 is accomplished by using a narrow receiver cone.

3.2 Heat Engines

After the laser energy is accepted and converted to heat, an engine is needed to convert heat to pressure-volume energy. Two types are being considered. One is variations on the "Otto" cycle that employs a laser heated gas. The other is the "Stirling" cycle which efficiently uses heat from a solid receiver. Brayton cycle machines (Ref. 13) do not have sufficient efficiency.

3.2.1 "Otto" Cycles

Three "Otto" cycles will be discussed in a manner analogous to Ref. 1. The same nomenclature will be used. These are diagramed in Figure 3.

3.2.1.1 Non-Compression Cycle

In Figure 3a, a very old type of internal combustion engine with no pre-compression is brought back for evaluation. The gas charge is brought into the cylinder at low pressure (stroke 4-1). The inlet valve closes and the laser fires (1-2). Adiabatic expansion occurs (2-3). Outlet valve opens and hot gas is forced into cooler loop (3-4). Cold gas enters the cylinder again (stroke 4-1 again).

For all engine cycles take as a basis:

1) Maximum effective gas temperature 3000^{o}K.
2) Maximum gas volume in cylinder, 1 liter (10^{-3} m^3)
3) Minimum gas pressure in cylinder, 1 atm (1×10^5 N/m^2).
4) Helium working gas (assume no effect of colorant gas).

C_p = 4.97 cal/^{o}K g mol = 20.867 j/^{o}K g mol

C_v = 2.983 cal/g mol ^{o}K = 12.481 j/^{o}K g mol

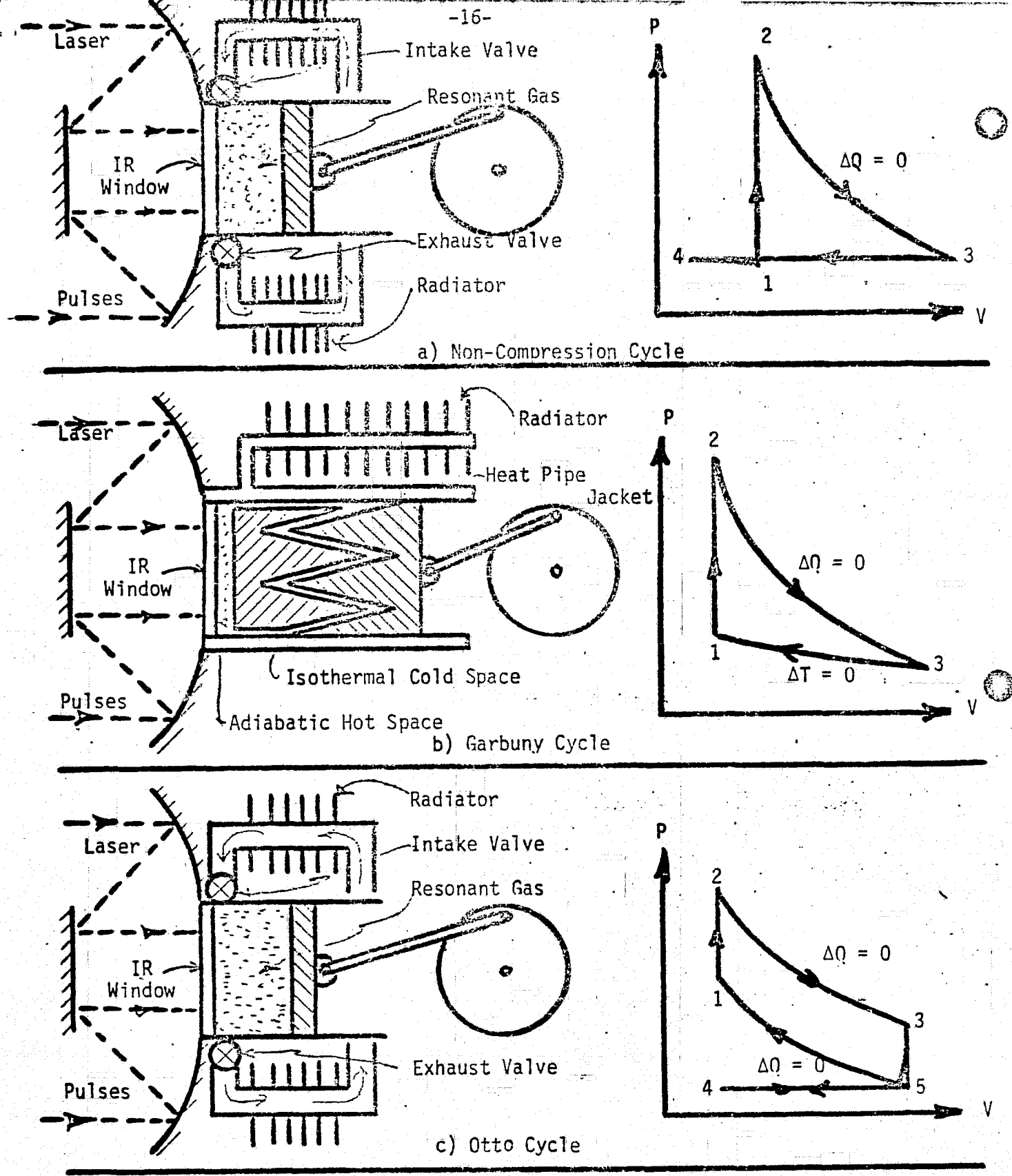

Figure 3. "Otto" Cycle Engines.

$R = 1.987$ cal/g mol $^{o}K = 8.314$ j/g mol ^{o}K

$k = C_p/C_v = 1.666$

5) Minimum gas temperature $300^{o}K$.

For the non-compression cycle:

$V_3 = 10^{-3}\ m^3$ $\qquad P_3 = 1 \times 10^5\ N/m^2 = P_4 = P_1$

$T_2 = 3000^{o}K$ $\qquad T_1 = 300^{o}K$

For the heating process at constant volume (1-2):

$$\frac{P_2}{P_1} = \frac{T_2}{T_1} = \frac{3000}{300} = \frac{P_2}{10^5}\ ,\ P_2 = 10^6\ N/m^2$$

For the adiabatic expansion process:

$$\frac{P_3}{P_2} = \left(\frac{V_2}{V_3}\right)^k\ ,\ \frac{10^5}{10^6} = \left(\frac{V_2}{10^{-3}}\right)^{1.666}$$

$$0.2511 = \frac{V_2}{10^{-3}}\ ,\ V_2 = 2.51 \times 10^{-4}\ m^3$$

The amount of gas involved per cycle is:

$$P_1V_1 = nRT_1$$

$$10^5\ (2.51 \times 10^{-4}) = n(8.314)(300)$$

$$n = 1.01 \times 10^{-2}\ \text{g mol}$$

The heat input per cycle is:

$$Q_{in} = nC_V\Delta T = 1.01 \times 10^{-2}\ (12.481)(3000-300) = 3.404 \times 10^2\ \text{joules}$$

Work out per cycle:

$$W_{out} = \frac{-nRT_2}{k-1}\left(\left(\frac{P_3}{P_2}\right)^{\frac{k-1}{k}} - 1\right)$$

$$= \frac{-1.01 \times 10^{-2}\ (8.314)(3000)}{0.666}\left(\left(\frac{10^5}{10^6}\right)^{\frac{0.666}{1.666}} - 1\right)$$

$$= 2.277 \times 10^2\ \text{joules}$$

Work in per cycle

$$W_{in} = P_3(V_2 - V_3) = 10^5 (2.51 \times 10^{-4} - 10^{-3})$$
$$= -7.490 \times 10^1$$

Net work = $2.277 \times 10^2 - 7.490 \times 10^1 = 1.527 \times 10^2$ joules

Thus cycle efficiency is:

$$\eta = \frac{\text{Net Work}}{Q_{in}} = \frac{1.527 \times 10^2}{3.404 \times 10^2} = 44.85\%$$

This efficiency is too low and therefore this cycle will not be considered further.

3.2.1.2 Garbuny Cycle

Garbuny and Pechersky (Ref. 1) proposed a cycle to use a laser heated gas but did not present a way that an isothermal compression which is part of this cycle can be carried out. Figure 3b shows the phase diagram and the engine schematic. Figure 4 shows in more detail how the engine can be made. Starting at point 3, the isothermalizer is open and is held open by a spring. During the isothermal compression (3 to 1) the two meshing fins come closer and closer. The fins absorb the heat of compression as it is generated. From 1 to 2 the fins are completely meshed by a magnet which overcomes the spring. Right after the fins mesh and the gas is transferred to the adiabatic space, the laser should fire and heat the gas and therefore greatly increase the pressure. From 2 to 3 expansion proceeds adiabatically until the gas temperature drops to heat sink temperature. At 3' the compression of the spring creates enough force to overcome the force of the magnet. After the break, the magnet force decreases faster than the spring force so one fin plate flies back to the original position for another cycle.

Using the same basis as the previous cycle, for the 2-3 process:

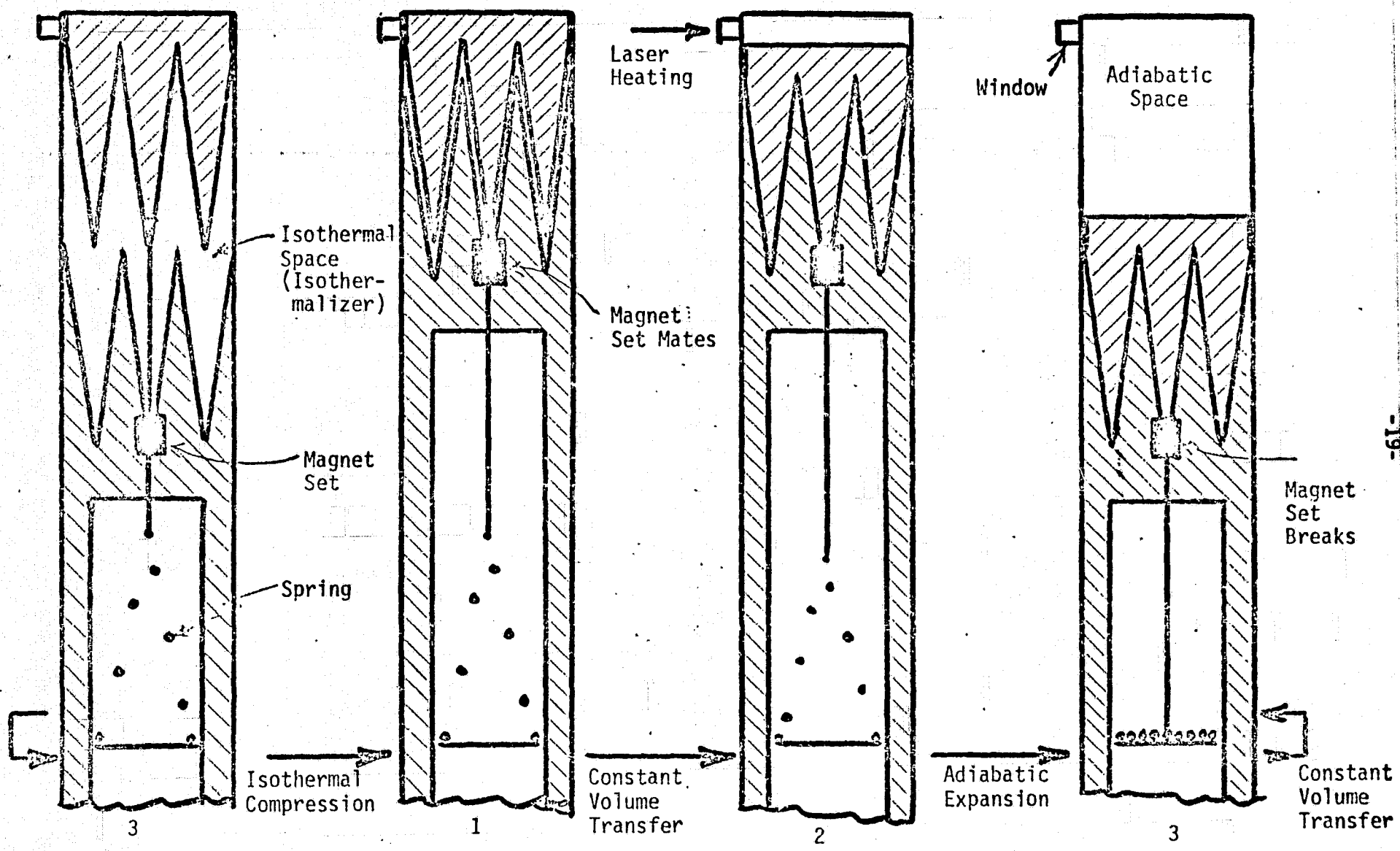

Figure 4. A Possible Laser Engine Using the Garbuny Cycle.

$$\frac{T_3}{T_2} = \left(\frac{V_2}{V_3}\right)^{k-1}, \quad \frac{300}{3000} = \left(\frac{V_2}{10^{-3}}\right)^{0.666}, \quad V_2 = 3.15 \times 10^{-5}\ m^3$$

$$\frac{T_3}{T_2} = \left(\frac{P_3}{P_2}\right)^{\frac{k-1}{k}}, \quad 0.1 = \left(\frac{10^5}{P_2}\right)^{0.4}, \quad P_2 = 3.16 \times 10^7\ N/m^2$$

For the 3-1 process:

$$\frac{P_3}{P_1} = \frac{V_1}{V_3}, \quad V_1 = V_2$$

$$\frac{10^5}{P_1} = \frac{3.15 \times 10^{-5}}{10^{-3}}, \quad P_1 = 3.17 \times 10^6\ N/m^2$$

The amount of gas involved per cycle is:

$$P_3V_3 = nRT_3$$

$$10^5\ (10^{-3}) = n(8.314)(300)$$

$$n = 4.01 \times 10^{-2}\ g\ mol$$

The heat input per cycle is:

$$Q_{in} = nC_v\Delta T = 4.01 \times 10^{-3}\ (12.481)(3000 - 300) = 1351\ joules$$

Work out per cycle is:

$$W_{out} = \frac{-nRT_2}{k-1}\left[\frac{T_3}{T_2} - 1\right] = \frac{-4.01 \times 10^{-2}\ (8.314)3000}{0.666}\left[\frac{300}{3000} - 1\right]$$

$$= 1351.6\ joules$$

Work in per cycle is:

$$W_{in} = -nRT_1 \ln \frac{V_3}{V_1} = -4.01 \times 10^{-2}\ (8.314)(300) \ln \frac{10^{-3}}{3.15 \times 10^{-5}}$$

$$= -345.84\ joules$$

Net work = 1351.6 - 345.84 = 1005.76

Cycle efficiency, η = 1005.76/1351 = 0.744

This is quite good,therefore the cycle will be considered further. The maximum possible cycle efficiency for the assumptions given is 1 - 300/3000 = 0.90.

3.2.1.3 Otto Cycle

This cycle is the same as that used in the familiar 4 stroke internal combustion engine except that a burst of laser energy through a window takes the place of spark ignited internal combustion. Also an external cooling loop is used instead of open cycle exhaust and intake. Refering to Figure 3c the process is as follows:

a) 5 to 1, adiabatic compression of 1 liter of gas originally at $300^{o}K$.

b) 1-2, constant volume heating of gas to $3000^{o}K$ by laser.

c) 2-3, adiabatic expansion of hot gas back to original volume.

d) 3-4, exhaust valve opens and piston strokes to expel hot gas into external heat exchanger.

e) 4-5, exhaust valve closes, inlet valve opens, piston draws in cooled gas from the external heat exchanger.

f) 5-1, inlet valve closes, adiabatic compression starts again to repeat the cycle.

As in 2 cycle internal combustion engines, it is possible to flush out the hot gas and replace it with cold at the end of the power stroke and thus have a power stroke every revolution.

In calculating this cycle, the minimum gas volume, V_1, will be chosen to give the best efficiency.

For adiabatic compression 5 → 1,

$$\frac{P_1}{P_5} = \left(\frac{V_5}{V_1}\right)^{k}, \quad P_1 = 10^5 \left(\frac{10^{-3}}{V_1}\right)^{1.667}$$

$$\frac{T_1}{T_2} = \left(\frac{V_5}{V_1}\right)^{k-1}, \quad T_1 = 300 \left(\frac{10^{-3}}{V_1}\right)^{0.667}$$

$$W_{in} = \frac{-nRT_5}{k-1}\left(\left(\frac{V_5}{V_1}\right)^{k-1} - 1\right)$$

$$W_{in} = \frac{-4.01 \times 10^{-2} (8.314)(300)}{0.6667} \left(\left(\frac{10^{-3}}{V_1} \right)^{0.667} - 1 \right)$$

$$= -150.03 \left(\frac{1.00 \times 10^{-2}}{V_1^{.667}} - 1 \right)$$

For laser heating 1-2,

$$Q_{in} = nC_v\Delta T = 4.01 \times 10^{-2} (12.481)(3000 - T_1)$$

$$= 5.00 \times 10^{-1} (3000 - T_1)$$

Also,

$$P_2V_2 = nRT_2, \; V_2 = V_1$$

$$P_2 = 4.02 \times 10^{-2} (8.314)(3000)/V_1$$

$$P_2 = 1000/V_1$$

For the adiabatic expansion work stroke 2 → 3,

$$W_{out} = \frac{-nRT_2}{k - 1} \left(\left(\frac{V_1}{V_5} \right)^{k - 1} - 1 \right)$$

$$= \frac{-4.01 \times 10^{-2} (8.314)(3000)}{0.6667} \left(\left(\frac{V_1}{10^{-3}} \right)^{0.667} - 1 \right)$$

$$= -1500.4 \left(\frac{V_1^{0.667}}{0.0100} - 1 \right)$$

Also,

$$\frac{P_3}{P_2} = \left(\frac{V_2}{V_3} \right)^k, \; P_3 = \frac{1000}{V_1} \left(\frac{V_1}{10^{-3}} \right)^{1.666}$$

Therefore, the net work is,

$$W_{net} = -1500 \left(\frac{V_1^{0.667}}{0.01} - 1 \right) - 150 \left(\frac{0.01}{V_1^{0.667}} - 1 \right)$$

and the cycle efficiency is

$$\eta = \frac{W_{net}}{1500 - \frac{1.5}{V_1^{0.667}}}$$

Both these equations are graphed in Figure 5. Note that at the maximum power point $V_1 = 1.8 \times 10^{-4}$ m^3 (compression ratio of 5.56) and $\eta = 0.68$. This result agrees with the formula for the optimum Otto cycle given by Martini (Ref. 6), that is:

$$\eta_{oo} = 1 - \left(\frac{T_C}{T_H}\right)^{\frac{1}{2}} = 1 - \left(\frac{300}{3000}\right)^{\frac{1}{2}} = 0.68$$

This cycle produces 700 joules/power cycle. But in between each power cycle is a pumping cycle which theoretically requires no work and actually requires a small amount. Therefore, the work per engine revolution is only 350 joules. The Otto cycle is a reasonable one to use. It has adequate efficiency and a very convenient cooling mechanism. The valving could be troublesome, but one can call on many years of experience with similar engines to solve these kinds of problems. Also, a two cycle machine can be built analogous to a two cycle internal combustion engine. The flushing out of the cylinder with cold gas at the end of the power stroke can be very thorough since no fuel would be lost.

3.2.1.4 Comparison of Cycles

The three cycles considered are therefore compared as follows:

Cycle	Cycle Efficiency	Work/Engine Revolution (joules)
Non-Compression	0.449	153
Garbuny	0.744	1006
Otto -- 4 cycle	0.68	350
2 cycle	0.68	700

The PV diagrams for the reference Garbuny and Otto cycles are graphed in Figure 6. Note that the Garbuny cycle required extreme pressure, 3.17×10^7 N/m^2 (317 atm) and very high compression ratio, ~32. Also note that the last half

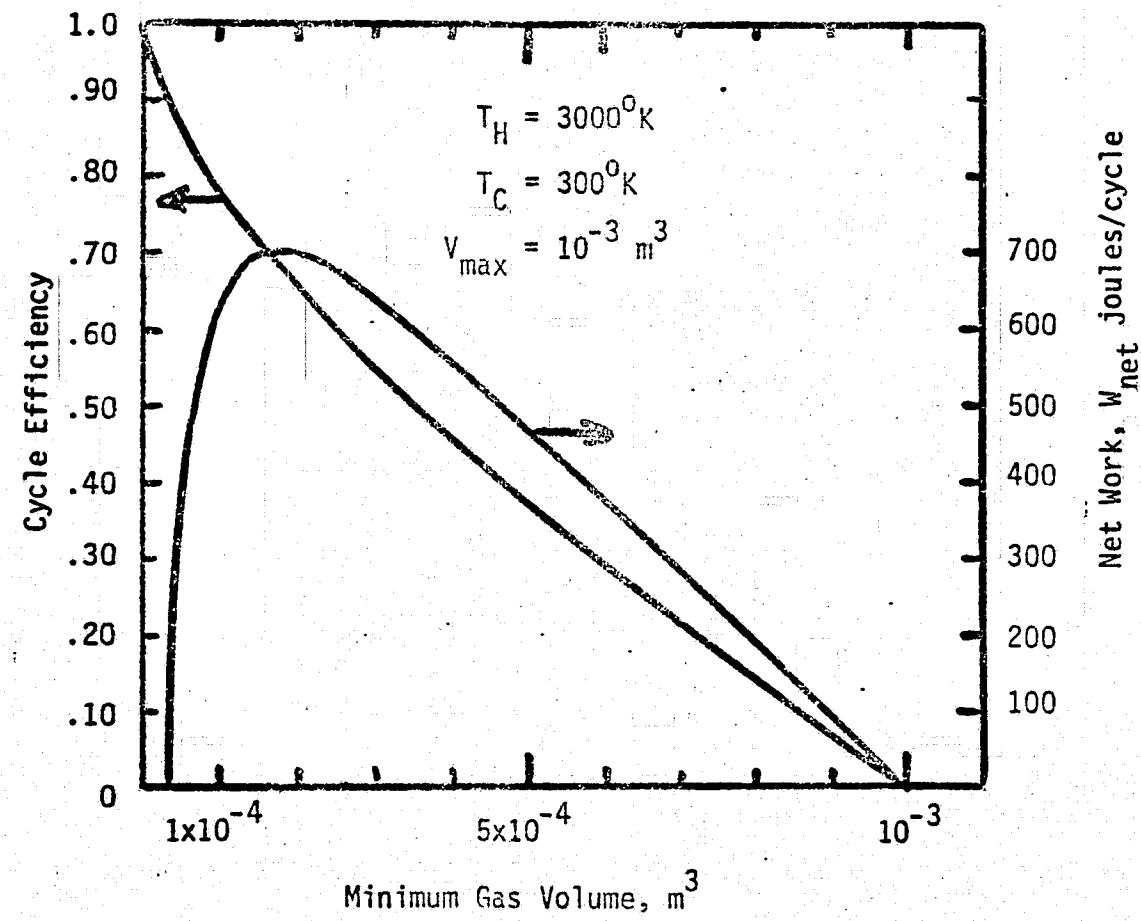

Figure 5. Net Work and Cycle Efficiency for the Otto Cycle.

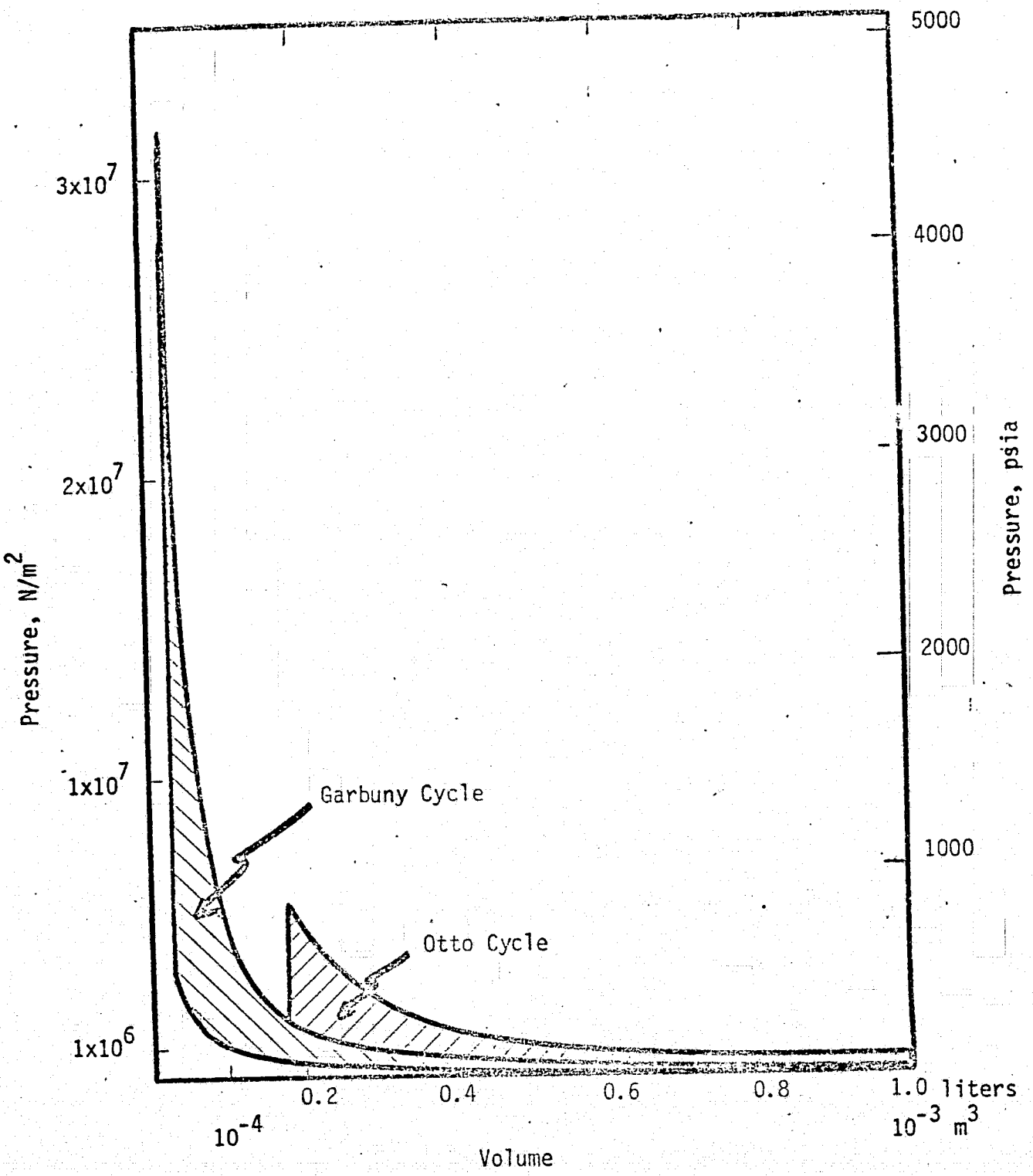

Figure 6. Work Diagrams for Garbuny and Otto Cycles.

of the expansion produces essentially no work. The Otto cycle has nearly the same efficiency with much less required in gas pressure on the window. With a two cycle approach the power density is also reasonable.

3.2.1.5 Conceptual Designs

In order to gain a better understanding about what would be involved in executing a 1 HP engine using the above concepts, a rough conceptual design will be described for both the Garbuny and the two cycle Otto engines. Table 5 gives the estimates of the sizes needed to make initial estimates.

3.2.1.5.1 Garbuny Cycle.

Figure 7 shows full scale how the Garbuny cycle engine might look using the dimensions from Table 5. Due to space limitations the spring assembly as shown in Figure 4 is not shown. The left hand side of Figure 7 shows the same position as position 2 of Figure 4. The power piston is at top dead center (TDC) and the magne has pulled down the displacer to move the isothermally compressed gas into the expansion space. The laser energy pulse enters through a small window in the side. This arrangement was thought to be necessary because of the extremely high pressure and the thinness of the compression space. All sides of the expansion space are plated with a specular gold plate. Input energy reflects several times off the walls until it is absorbed nearly evenly in the gas. There is a worry about the gas in this small size expansion chamber losing its heat before it expands. This will be investigated in the next section.

After TDC the gas expands. The displacer remains meshed with the power piston until it nearly reached bottom dead center (BDC) as shown on the right of Figure 7. At this point the conical spring stacks up on the spring base and forces the magnet set apart (see Figure 4, position 3'). The spring then pushes the conical displacer to the top of

TABLE 5

INITIAL SIZING OF GARBUNY
AND OTTO CYCLE ENGINES

	Garbuny	2 Cycle Otto
Reference Engine		
Maximum cylinder volume, m^3	10^{-3}	10^{-3}
Indicated work, joules	1006	700
Indicated efficiency	0.744	0.68
Estimated electric generator efficiency	0.85	0.85
Estimated mechanical efficiency	0.80	0.80
Estimated overall efficiency	0.51	0.46
Assumed frequency, Hz	20	20
Calculated output power, watts	13,682	9,520
Compression ratio	31.75	5.56
1 HP engine		
Output power, watts	750	750
Maximum cylinder volume, m^3	5.48×10^{-5}	7.80×10^{-5}
Minimum cylinder volume, m^3	1.73×10^{-6}	1.40×10^{-5}
Displacement, m^3	5.31×10^{-5}	6.40×10^{-5}
Piston stroke, m	0.1	0.1
Piston diameter, cm	2.60	2.85
Gas thickness at TDC, mm	3.3	21.9
Minimum pressure, N/m^2	10^5	10^5
Minimum pressure, atm	1	1
Maximum pressure, N/m^2	3.17×10^7	5.56×10^6
Maximum pressure, atm	317	55.6

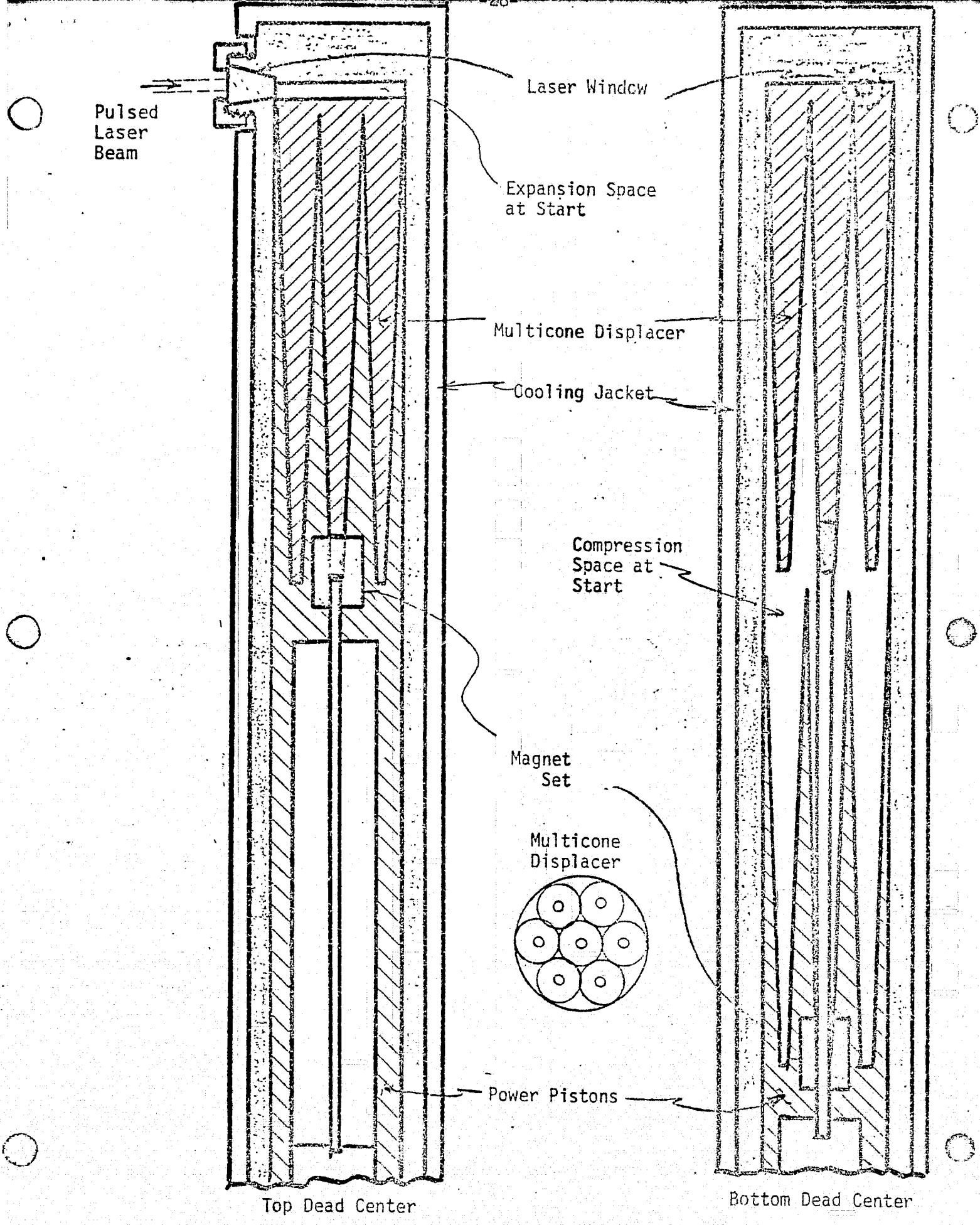

Figure 7. 750 w(e) Garbuny Cycle Engine Concept (Full Scale).

its stroke as shown in the right hand side of Figure 7. The displacer helps cool the expansion cylinder and the gas it contains and so does the cooling jacket surrounding the whole engine.

During the compression stroke, from BDC to almost TDC the gas is supposed to give up its heat as fast as it forms. However, as drawn in Figure 7 the geometry at the start of the compression stroke is not as good as at the end when the two conical surfaces are close together. The cycle now repeats.

3.2.1.5.2 Otto Cycle.

Figure 8 shows a conceptual design of a possible Otto cycle engine. At top dead center (TDC) on the left the laser pulse fires through the window-lens. As shown in Ref. 1, this method concentrates the laser heat into the center of the space where it is least likely to be conducted away before expansion can take place. Note that the gas space is about as deep as it is wide (diameter). However, the gas will probably be whirling from being introduced into the cylinder. An estimate of how gas conduction may affect this engine is given in the next section.

At the end of the power stroke (see the right of Figure 8) the exhaust manifold opens up. The 3 atm gas pressure remaining in the engine cylinders starts a vigorous flow to the exhaust cooler through a check valve (not shown). The momentum of this flow creates a partial vacuum in the cylinder to help bring in fresh, cold gas through a check valve in the piston. As in most two cycle gasoline engines, the crank case acts as a pump to force new gas into the engine. Since the gas does not contain the fuel the old hot gas can be thoroughly washed out before the exhaust ports are closed by the rising piston and compression starts. During the compression back to TDC any gas conduction due to the small size of the engine and due to the use of helium gas working fluid would be beneficial and may help to compensate for the power loss by gas conduction in the power stroke.

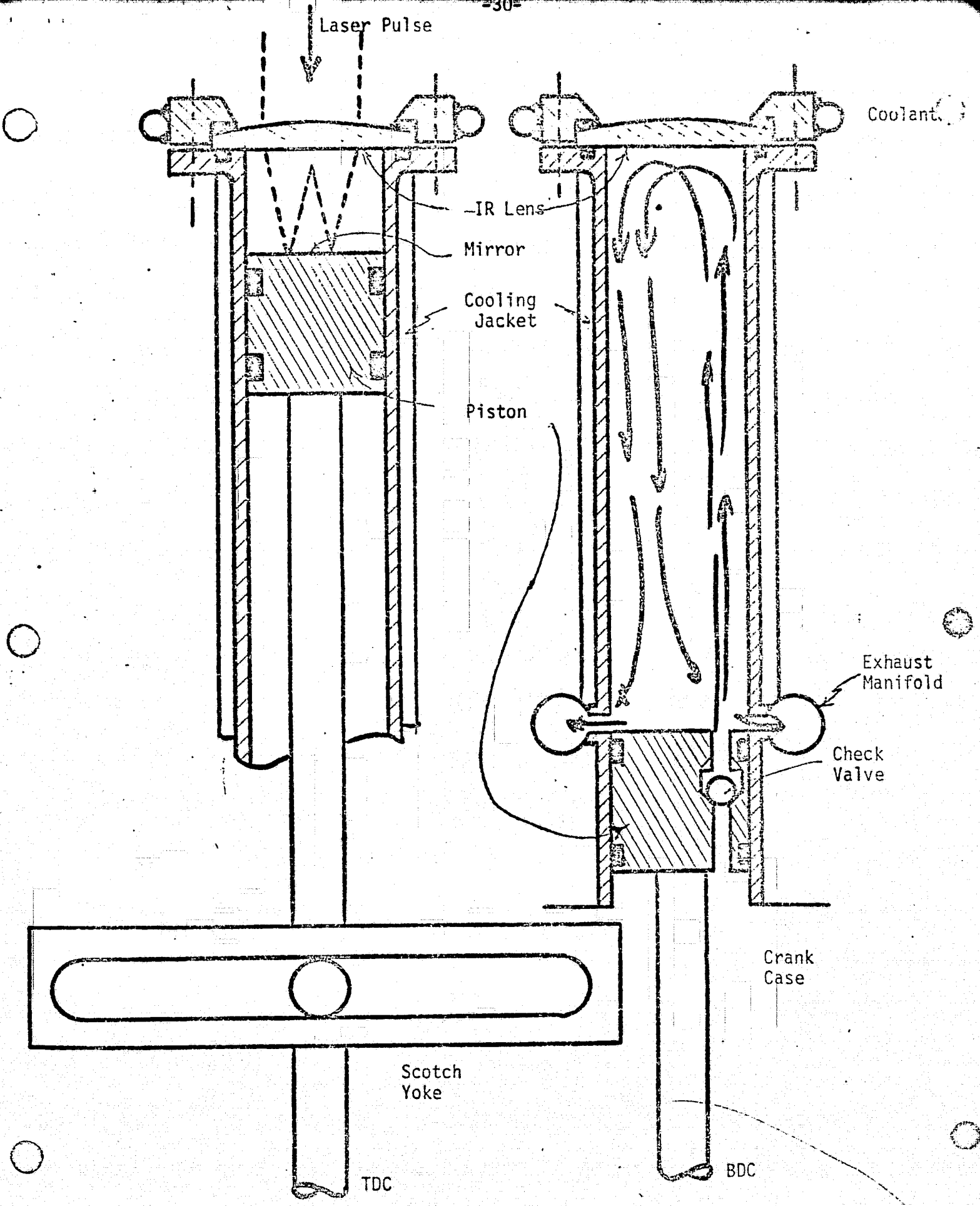

Figure 8. 750 w(e) Otto Cycle Engine Concept. Full Scale.

3.2.1.6 Gas Conduction Analysis

For the specific conceptual designs given in the previous section, the specific effect of gas conduction on the effective work diagram of these two machines will be evaluated. During compression and expansion, heat will be generated and absorbed uniformly. It is also assumed that laser energy input is uniform throughout the gas space. In the Garbuny cycle engine this is probably reasonably accurate. In the Otto cycle engine the laser heat starts in the core but gas turbulence soon distributes it. Although gas turbulence is acknowledged there is no way to compute what will happen with gas turbulence without experimental data to go on. Therefore, it will be assumed that the gas space acts as if it were stagnant. Therefore, if these calculations show a problem, there is a very serious problem indeed.

In Appendix A the equations are derived for gas conduction from a layer and a cylinder. Using these equations a work diagram will be calculated with cycle angle intervals of 10 degrees. During each interval the effect of heat transfer to the walls on the otherwise adiabatic process is calculated and added in. The gas pressure is then calculated. The calculation proceeds by an alternate adiabatic increment and then a temperature equilibration at constant volume (Ref. 18). The shape of the work diagram corrected for heat transfer will be compared with the idealized work diagram (Figure 6) to determine the difference.

3.1.2.6.1 Garbuny Cycle Analysis.

Table 6 summarizes these calculations. At a cycle increment of 10^{o}, $\Delta\theta = 1/20\ (10/360) = 1.389 \times 10^{-3}$ seconds. The gas volume in the engine at any angle θ is:

$$V_{\theta} = 1.73 \times 10^{-6} + \frac{5.31 \times 10^{-5}}{2} (1 - \cos \theta)$$

The gas inventory is:

TABLE 6

GARBUNY CYCLE ANALYSIS WITH HEAT TRANSFER

θ	V_o	T_o, T_1	T_1'	P
0	1.730×10^{-6}	3000		3.173×10^{7}
10	2.134×10^{-6}	2608	2579	2.211×10^{7}
20	3.334×10^{-6}	1915	1901	1.043×10^{7}
30	5.294×10^{-6}	1397	1389	4.802×10^{6}
40	7.953×10^{-6}	1059	1054	2.426×10^{6}
50	1.123×10^{-5}	838	834	1.359×10^{6}
60	1.503×10^{-5}	687	684	8.331×10^{5}
70	1.923×10^{-5}	580	578	5.502×10^{5}
80	2.37×10^{-5}	503	501	3.87×10^{5}
90	2.83×10^{-5}	445	443	2.86×10^{5}
100	3.29×10^{-5}	401	400	2.22×10^{5}
110	3.74×10^{-5}	367	366	1.79×10^{5}
120	4.16×10^{-5}	341	340	1.50×10^{5}
130	4.54×10^{-5}	321	321	1.29×10^{5}
140	4.87×10^{-5}	306	306	1.15×10^{5}
150	5.14×10^{-5}	295	295	1.05×10^{5}
160	5.33×10^{-5}	288	288	9.90×10^{4}
170	5.45×10^{-5}	284	285	9.55×10^{4}
180	5.49×10^{-5}	283	283	9.44×10^{4}
190	5.45×10^{-5}	285	289	9.70×10^{4}
200	5.33×10^{-5}	293	295	1.01×10^{5}
210	5.14×10^{-5}	303	302	1.08×10^{5}
220	4.87×10^{-5}	313	309	1.16×10^{5}
230	4.54×10^{-5}	324	316	1.27×10^{5}
240	4.16×10^{-5}	335	323	1.42×10^{5}
250	3.74×10^{-5}	347	329	1.61×10^{5}
260	3.29×10^{-5}	358	334	1.86×10^{5}
270	2.83×10^{-5}	370	338	2.20×10^{5}
280	2.37×10^{-5}	381	339	2.62×10^{5}
290	1.92×10^{-5}	390	337	3.20×10^{5}
300	1.50×10^{-5}	397	331	4.03×10^{5}
310	1.12×10^{-5}	402	322	5.25×10^{5}
320	7.95×10^{-6}	406	312	7.19×10^{5}
330	5.29×10^{-6}	410	304	1.05×10^{6}
340	3.33×10^{-6}	414	301	1.65×10^{6}
350	2.13×10^{-6}	405	300	2.57×10^{6}
360	1.73×10^{-6}	345	300	3.17×10^{6}

$$N = \frac{PV}{RT} = \frac{(10^5\ N/m^2)\ (5.48 \times 10^{-5}\ m^3)}{8.314\ j/g\ mol\ ^oK\ (300\ ^oK)}$$

$$= 2.197 \times 10^{-3}\ g\ mol$$

The adiabatic temperature change for helium due to volume change is given by the formula

$$\frac{T_1}{T_o} = \left(\frac{V_o}{V_1}\right)^{2/3}$$

The rate of heat transfer to the flat ends of the gas space is given by the formula (Appendix A, Equation A-11)

$$Q_{WF} = \frac{6kA}{s}\ (LMTD)$$

where

Q_{WF} = heat absorbed by the flat wall, watts

k = gas thermal conductivity, helium

= 0.151 w/m ^oK

s = thickness of gas space = $V_1/5.31 \times 10^{-4}$

A = area of both flat walls = $1.062 \times 10^{-3}\ m^2$

LMTD = log mean temperature difference between gas and metal

$$LMTD = \frac{T_1 - T_M - (T_1' - T_M)}{\ln \frac{T_1 - T_M}{T_1' - T_M}} = \frac{T_1 - T_1'}{\ln \frac{T_1 - T_M}{T_1' - T_M}}$$

where T_1' = gas temperature after heat transfer.

The rate of heat transfer to the cylindrical walls of the gas space is (see Appendix A, Equation A-22),

$$Q_{WC} = 8\pi sk(LMTD)$$

The total heat transferred from the gas space is:

$$Q_W = Q_{WF} + Q_{WC}$$

And due to the heat capacity of the gas

$$Q_W = NC_v \frac{(T_1 - T_1')}{\Delta\theta}$$

Combining the above equations, substituting constants and solving for T_1' one obtains

$$T_1' = 300 + (T_1 - 300)/\exp\left(\frac{2.588 \times 10^{-8}}{V_1} + 3.620 \times 10^2 V_1\right)$$

Then T_1' becomes T_o and the process repeats until the multicone displacer flips at the end of the expansion stroke. When the gas is between the cones and the conical holes, the flat walls become conical surfaces with greater area and the thickness of the gas space is also greatly reduced. Thus for 6 truncated cones with a base radius of 4.5×10^{-3} m, top radius of 1×10^{-3} m and a height of 0.1 m,

$$A = 1.062 \times 10^{-3} - 14\pi(4.5 \times 10^{-3})^2 + 4\pi(1 \times 10^{-3})^2 + 14\pi(5.5 \times 10^{-3}) \sqrt{(0.1)^2 + 3.5 \times 10^{-3})^2}$$

$$= 2.442 \times 10^{-2} \text{ m}^2$$

and

$$s = \frac{V_1(r_1 - r_2)}{5.31 \times 10^{-5}(h)} = \frac{V_1 (3.5 \times 10^{-3})}{5.31 \times 10^{-4} (0.1)} = \frac{V_1}{1.517 \times 10^{-2}}$$

Again combining the above equations, substituting constants and solving for T_1', one obtains,

$$T_1' = 300 + (T_1 - 300)/\exp\left(\frac{1.700 \times 10^{-5}}{V_1} + 3.620 \times 10^2 V_1\right)$$

Note that the equation is the same except that one constant is increased by 657 times.

The above computation was programmed for an HP-65 computer (see program in Appendix B). Table 6 tabulates the results of this calculation and Figure 9 compares the resultant work diagram with the ideal cycle. Note that the calculation predicts that for the dimensions of this engine only a small amount of power is lost by cooling during expansion. During compression some additional

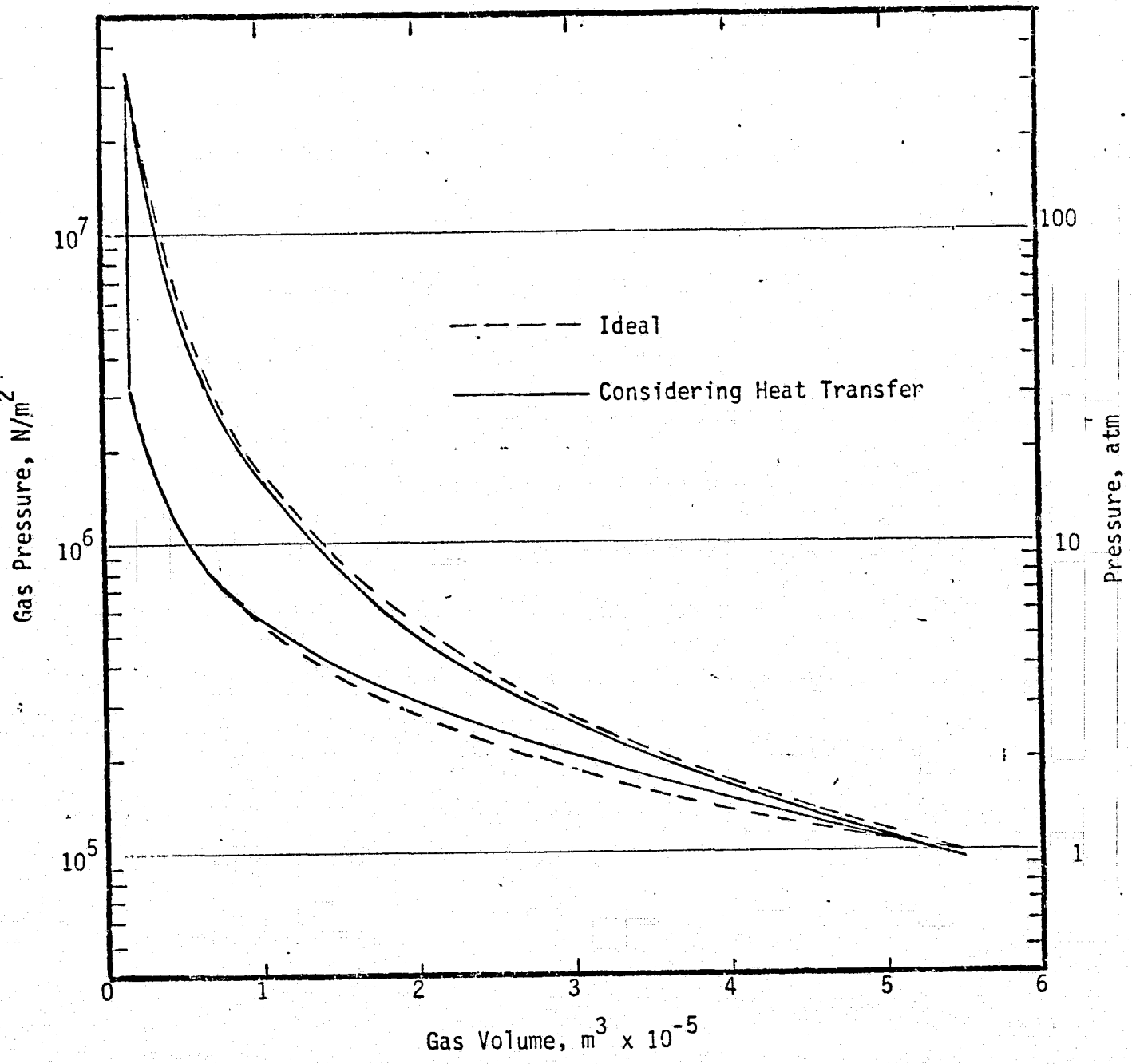

Figure 9. Effect of Real Heat Transfer on the Garbuny Cycle.

power is needed in the first part of compression. But, as the cones nearly mesh, very good isothermalizer action makes the calculated curve follow the ideal.

These calculations show that a reasonably practical Garbuny engine is possible. However, the effect of gas turbulence both on gas cooling by the walls and gas heating by the laser is quite important. Experimental measurements are needed.

3.2.1.6.2 Otto Cycle Analysis.

The Otto cycle will be computed using the same computer program. The different dimensions will result in different constants. The constants for gas conduction will not change but the gas temperature will be changed to 300^{o}K at the end of the expansion stroke. A $\Delta\theta$ of 10^{o} will still be used. The gas volume in the engine at any angle θ is:

$$V_\theta = 1.40 \times 10^{-5} + \frac{6.40 \times 10^{-5}}{2} (1 - \cos \theta)$$

The gas inventory is

$$N = \frac{PV}{RT} = \frac{10^5 (7.80 \times 10^{-5})}{8.314 (300)} = 3.127 \times 10^{-3} \text{ g mol}$$

The same heat transfer equations are used, but the constants are evaluated differently.

$$S = \frac{V_1}{6.40 \times 10^{-4}} \quad \text{and} \quad A = 1.28 \times 10^{-3} \text{ m}^2$$

Therefore, the temperature equilibration equation is:

$$T_1' = 300 + (T_1 - 300)/\exp\left(\frac{2.641 \times 10^{-8}}{V_1} + 216.6\, V_1\right)$$

The pressure is computed by

$$P = \frac{NRT}{V} = 3.127 \times 10^{-3} (8.314) \frac{T}{V} = 0.026\, T/V$$

Table 7 shows the results of this calculation. Figure 10 shows the results plotted and compared with the theoretical Otto cycle. There is a difference but if the results were plotted on linear paper instead of log paper, the difference would be hard to see.

This calculation shows that the Otto cycle in the size presented for a 750 w(e) power source is essentially not affected by heat transfer to the cooled walls. Also it shows that the Otto cycle engine produces power over its full stroke. In contrast, the Garbuny cycle produces no power at all over the last 20% of the stroke.

3.2.2 "Stirling" Cycles

All "Stirling" engines have the following characteristics:

1. No valves - a single gas space at a common pressure for each point in the cycle.
2. Compression chiefly in the cold space of the engine.
3. Expansion chiefly in the hot space of the engine.
4. Transfer of gas back and forth between the two spaces through a regenerator to attain high efficiency.

Figure 11 shows the main types of Stirling engines. These types differentiate between the different ways that the gas may be transferred between the hot and cold spaces. Heating and cooling of the gas can take place in passages between the expansion (hot) space and the compression (cold) space. By special arrangement it can take place in the body of these spaces.

A theoretically perfect Stirling engine will now be evaluated. Then the effect of dead volume, adiabatic spaces and sinusoidal motion will be evaluated separately. Next examples of 5 real Stirling engines will be given. Finally, some conclusions will be drawn about Stirling engines.

TABLE 7. OTTO CYCLE ANALYSIS WITH HEAT TRANSFER

θ ^{o}	V_θ m^3	T_o, T_1 ^oK	T_1' ^oK	P N/m^2
0	1.40×10^{-5}	3000	--	5.57×10^6
10	1.45×10^{-5}	2932	2919	5.24×10^6
20	1.59×10^{-5}	2740	2728	4.45×10^6
30	1.83×10^{-5}	2488	2476	3.52×10^6
40	2.15×10^{-5}	2224	2213	2.68×10^6
50	2.54×10^{-5}	1978	1967	2.01×10^6
60	3.00×10^{-5}	1761	1751	1.52×10^6
70	3.51×10^{-5}	1578	1567	1.16×10^6
80	4.04×10^{-5}	1425	1414	9.09×10^5
90	4.60×10^{-5}	1298	1288	7.28×10^5
100	5.16×10^{-5}	1193	1183	5.97×10^5
110	5.69×10^{-5}	1107	1097	5.01×10^5
120	6.20×10^{-5}	1036	1026	4.30×10^5
130	6.66×10^{-5}	979	969	3.78×10^5
140	7.05×10^{-5}	932	922	3.40×10^5
150	7.37×10^{-5}	896	886	3.12×10^5
160	7.61×10^{-5}	868	858	2.93×10^5
170	7.75×10^{-5}	847	838	2.81×10^5
180	7.80×10^{-5}	835	825	2.75×10^5
Change		300		1.00×10^5
190	7.75×10^{-5}	301	301	1.01×10^5
200	7.61×10^{-5}	305	305	1.04×10^5
210	7.37×10^{-5}	311	311	1.10×10^5
220	7.05×10^{-5}	321	320	1.18×10^5
230	6.66×10^{-5}	333	332	1.30×10^5
240	6.20×10^{-5}	348	348	1.46×10^5
250	5.69×10^{-5}	368	367	1.68×10^5
260	5.16×10^{-5}	392	391	1.97×10^5
270	4.60×10^{-5}	422	421	2.38×10^5
280	4.04×10^{-5}	459	457	2.94×10^5
290	3.51×10^{-5}	503	501	3.72×10^5
300	3.00×10^{-5}	556	554	4.80×10^5
310	2.54×10^{-5}	619	617	6.30×10^5
320	2.15×10^{-5}	690	688	8.32×10^5
330	1.83×10^{-5}	766	763	1.08×10^6
340	1.59×10^{-5}	837	834	1.36×10^6
350	1.45×10^{-5}	888	886	1.59×10^6
360	1.40×10^{-5}	906	903	1.68×10^6

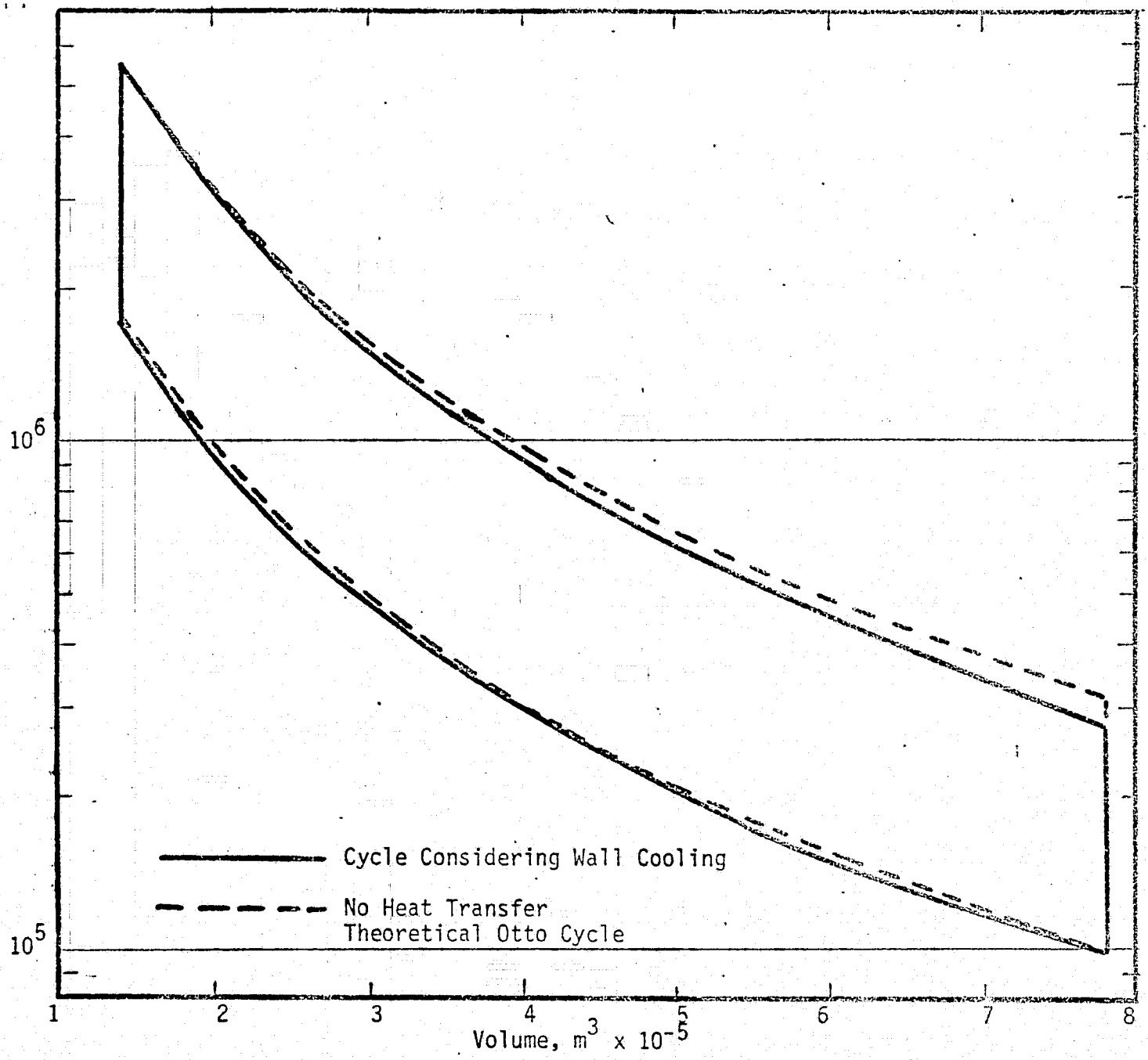

Figure 10. Effect of Real Heat Transfer on the Otto Cycle.

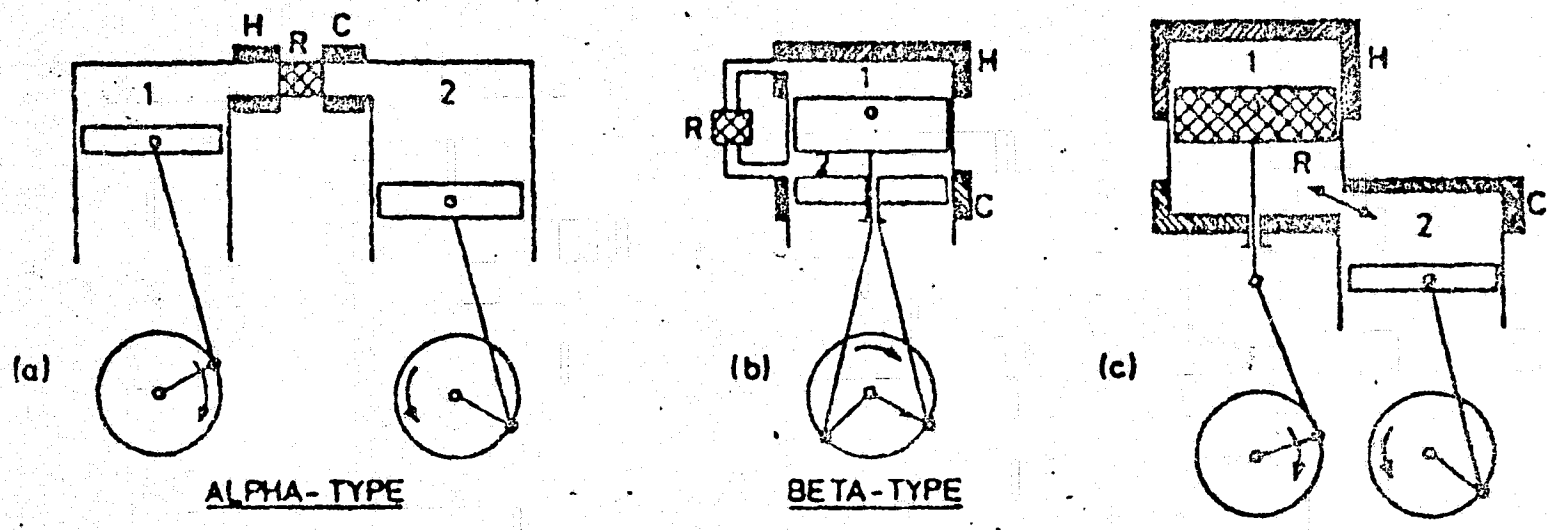

Figure 11. The Main Types of Stirling Engine (Ref. 34).

3.2.2.1 Theoretically Perfect Stirling Engine

Simple analyses for Stirling engines assume that the gas is compressed isothermally at the low temperature and expanded isothermally at the high temperature even though most present Stirling engines cannot even approximate this process. Some engines can however. Figure 12 shows the thermodynamically defined Stirling cycle. The processes are:

1-2. Isothermal compression at low temperature.

2-3. Transfer of gas from cold space to hot space through a perfectly efficient regenerator with no dead volume.

3-4. Isothermal expansion at high temperature.

4-1. Transfer back through the same regenerator.

1-2. Isothermal compression again--cycle repeats.

In order to make a comparison with the Otto cycle machines make the following assumptions:

1. Maximum effective gas temperature 1600°K. (down from 3000°K to allow refractory metal and MgF_2 TES to be used).
2. Maximum gas volume in cylinder, 1 liter (10^{-3} m^3 -- same as before).
3. Minimum gas pressure in cylinder, 1 atm (1×10^5 N/m^2 -- same as before).
4. Helium as working gas (same as before).
5. Minimum effective gas temperature, 300°K (same as before).

As in the analysis of the Otto cycle, one has a choice on the degree of compression.

For isothermal compression $1 \rightarrow 2$,

$$\frac{P_2}{P_1} = \frac{V_1}{V_2}, \quad P_2 = 10^5 \left(\frac{10^{-3}}{V_2}\right) = \frac{100}{V_2}$$

$$W_{in} = -nRT_1 \ln \frac{V_1}{V_2}$$

$$= -4.01 \times 10^{-2} (8.314)(300) \ln\left(\frac{10^{-3}}{V_2}\right)$$

$$= -100 \ln\left(\frac{10^{-3}}{V_2}\right)$$

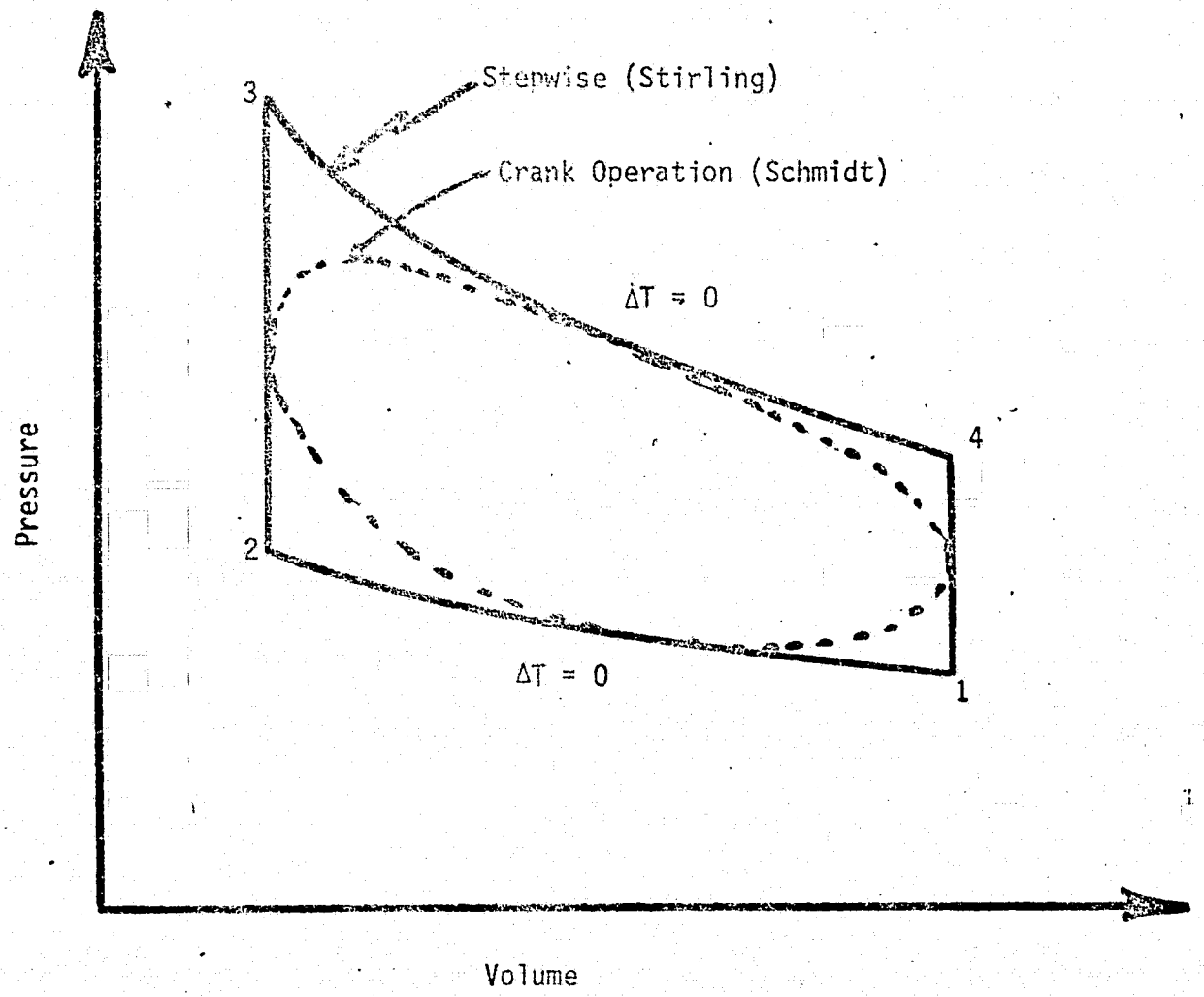

Figure 12. The Stirling Cycle (Thermodynamic Definition).

Constant volume heating 2→3 and constant volume cooling 4 → 1, if both perfect, cancel each other out and need not be considered at this stage of the analysis.

For isothermal expansion 3 → 4,

$$P_3 = \frac{nRT_3}{V_3} = \frac{4.01 \times 10^{-2} (8.314)(1600)}{V_2}$$

$$= 533.4/V_2$$

$$Q_{in} = W_{out} = -nRT_3 \ln \frac{V_3}{V_4}$$

$$= -4.01 \times 10^{-2} (8.314)(1600) \ln\left(\frac{V_2}{10^{-3}}\right)$$

$$= -533.4 \ln\left(\frac{V_2}{10^{-3}}\right)$$

Thus, the net work per cycle is:

$$W_{net} = -533.4 \ln\left(\frac{V_2}{10^{-3}}\right) - 100 \ln\left(\frac{10^{-3}}{V_2}\right) = -433.4 \ln\left(\frac{V_2}{10^{-3}}\right)$$

And the efficiency is:

$$\eta = \frac{W_{net}}{Q_{in}} = \frac{-433.4}{-533.4} = 0.8125 \text{ for any } V_2$$

The Carnot efficiency for these conditions is:

$$\eta_o = 1 - \frac{T_c}{T_H} = 1 - \frac{300}{1600} = 0.8125.$$

Therefore, the theoretical Stirling engine has the same efficiency as the Carnot cycle.

The net work per cycle for the theoretical Stirling cycle is large in comparison to other cycles (see Figure 13). Note that in contrast to the Otto cycle, the Stirling cycle benefits from higher and higher compression ratios. However, in the Otto cycle, the compression space is isolated with valves and high compression ratios are possible. The Stirling engine, on the other hand, has a heater, cooler and regenerator all which enclose space which cannot be

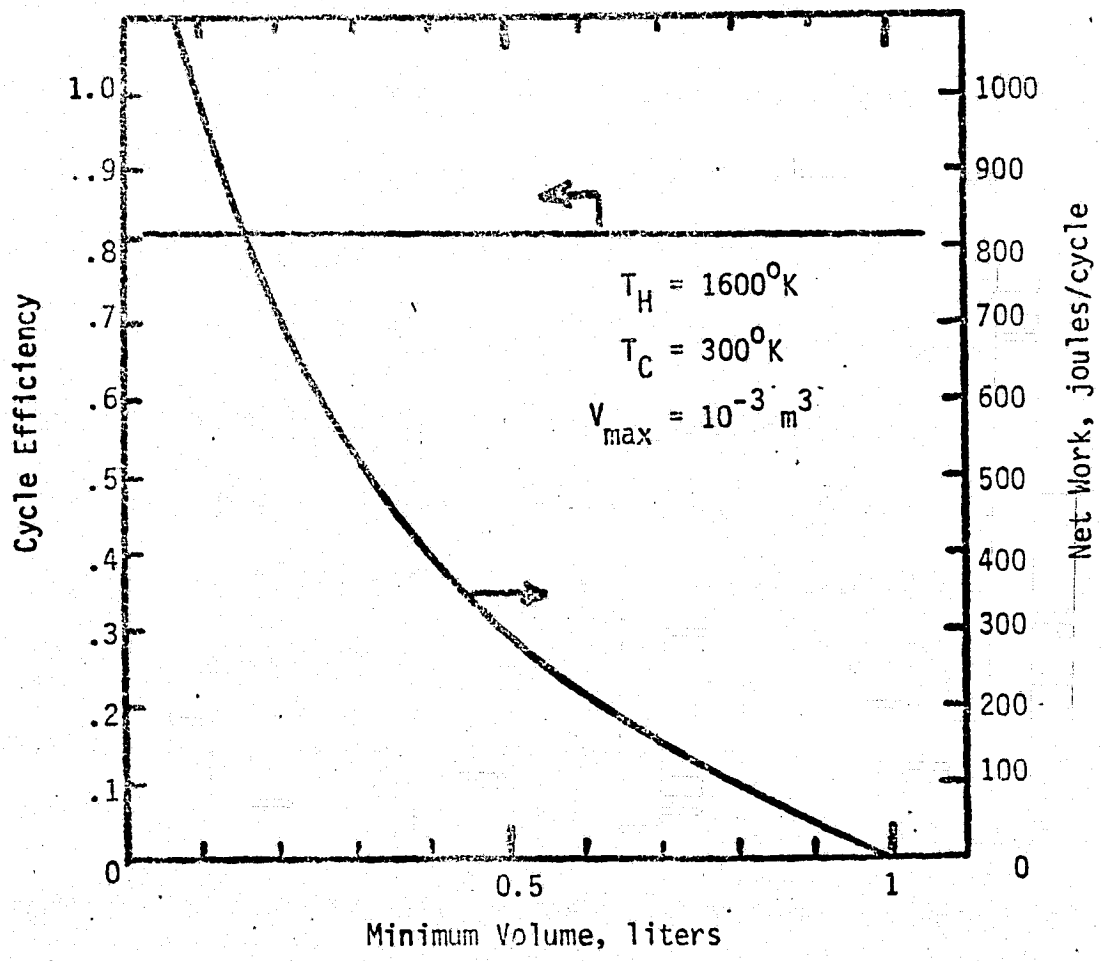

Figure 13. Net Work and Cycle Efficiency for Stirling Cycle.

displaced (dead volume). These components limit the compression ratio that is practically possible.

3.2.2.2 Effect of Dead Volume

Dead volume is the gas space in the regenerator and in any heater and cooler connected with it. Dead volume also includes the clearances in the hot and cold and power piston spaces. Dead volume reduces power available from the engine by making the gas more springy than it would otherwise have to be. It does not reduce efficiency directly but in a real engine the lower power means that the losses are more important and therefore the efficiency does decrease. Dead volume is inevitable in every real Stirling engine design because there is a trade-off between dead volume and heat transfer and fluid flow losses. In conventional Philips Stirling engines dead volume is about 3 times the piston displacement (Ref. 6). The displacer displacement is usually the same as the power piston. Therefore, conventional Philips Stirling engines have about 150% dead volume expressed as a fraction of the live volume. Martini (Ref. 18) found that power was reduced 0.83% for every percent increase in dead volume expressed as a fraction of the live volumes. Thus, at 15% dead volume (the maximum considered) power is reduced 12%.

As a further evaluation of dead volume, consider the step-wise process shown in Figure 14. Here the displacer and the power piston have the same displacement and the maximum volume of gas in the cylinders (1.43 liters) is equal to the dead volume (100% dead volume). Table 8 shows the conditions at the corner points and Figure 15 shows the work diagram. (Consider the one labeled isothermal spaces.) Table 9 and Figure 16 shows the same engine with an assumed zero dead volume. For isothermal spaces, the area of the work diagram in Figure 15 is 99 joules and is 440 joules in Figure 16. This means that when the dead volume is increased to 100% (based upon the live volume) that the

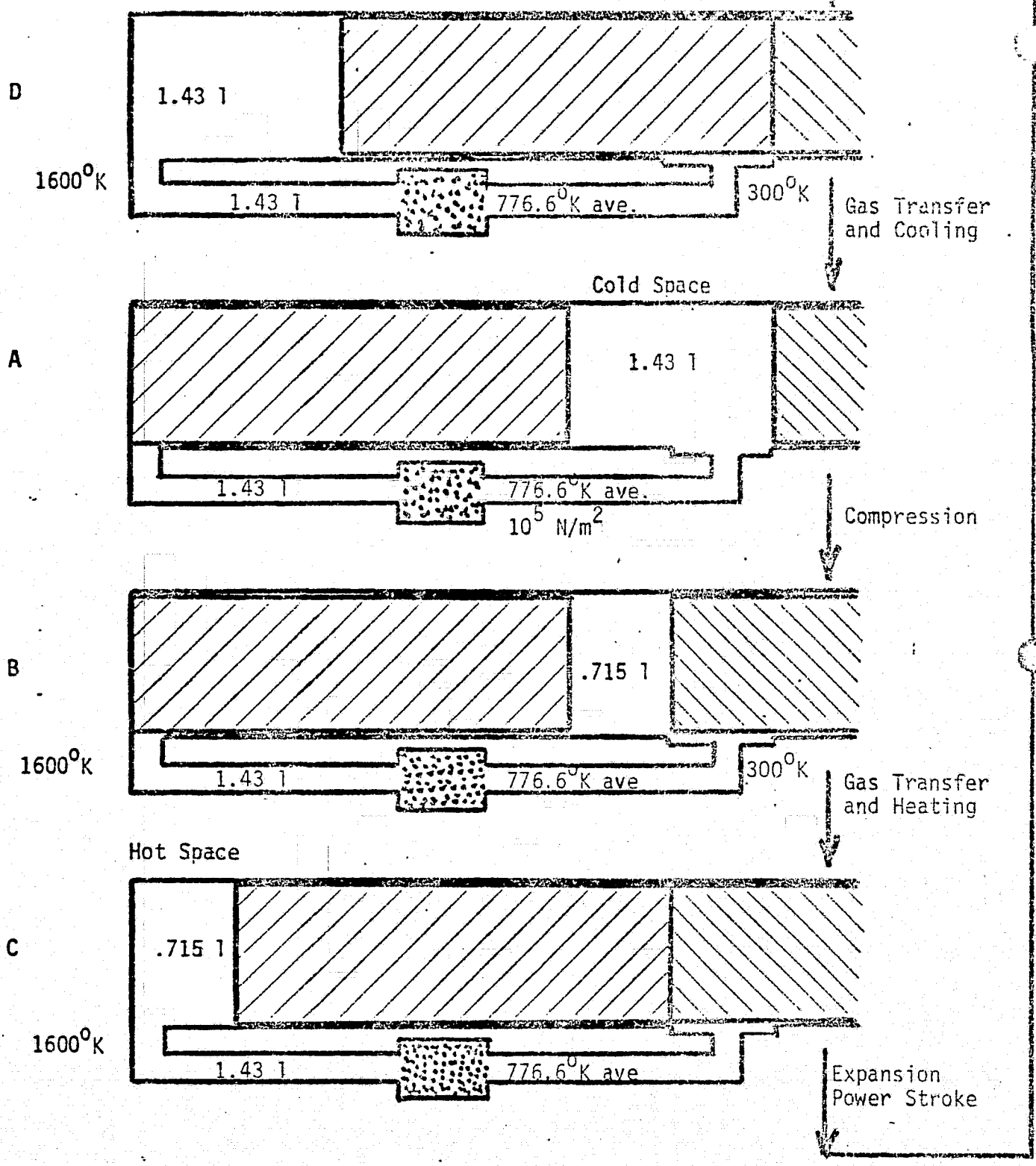

Figure 14. Stepwise Engine Calculation Example.

TABLE 8

ENGINE CALCULATION FOR ISOTHERMAL LIVE VOLUMES
(100% Dead Volume)

A		B		C		D	
T_C ^oK	P, N/m^2	T_C ^oK	P, N/m^2	T_H ^oK	P, N/m^2	T_H ^oK	P, N/m^2
300	1×10^5	300	1.546×10^5	1600	2.888×10^5	1600	2.416×10^5

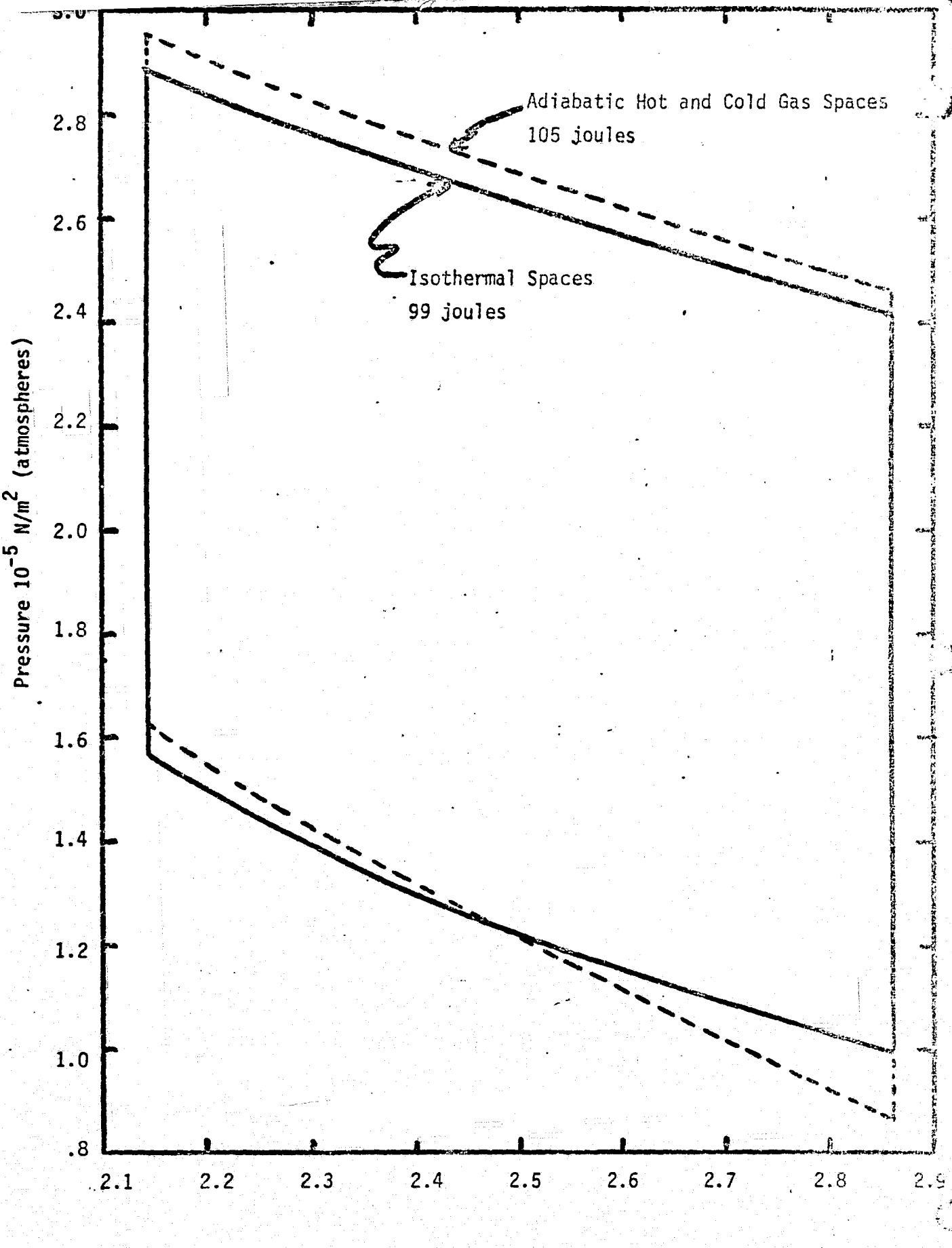

Figure 15. Sample Stepwise Engine Work Diagrams with 100% Dead Volume (based upon live volume).

TABLE 9

ENGINE CALCULATION, ISOTHERMAL LIVE VOLUMES
(0% Dead Volume)

A		B		C		D	
T_C ^oK	P, N/m^2	T_C ^oK	P, N/m^2	T_C ^oK	P, N/m^2	T_C ^oK	P, N/m^2
300	1×10^5	300	2×10^5	1600	10.67×10^5	1600	5.33×10^5

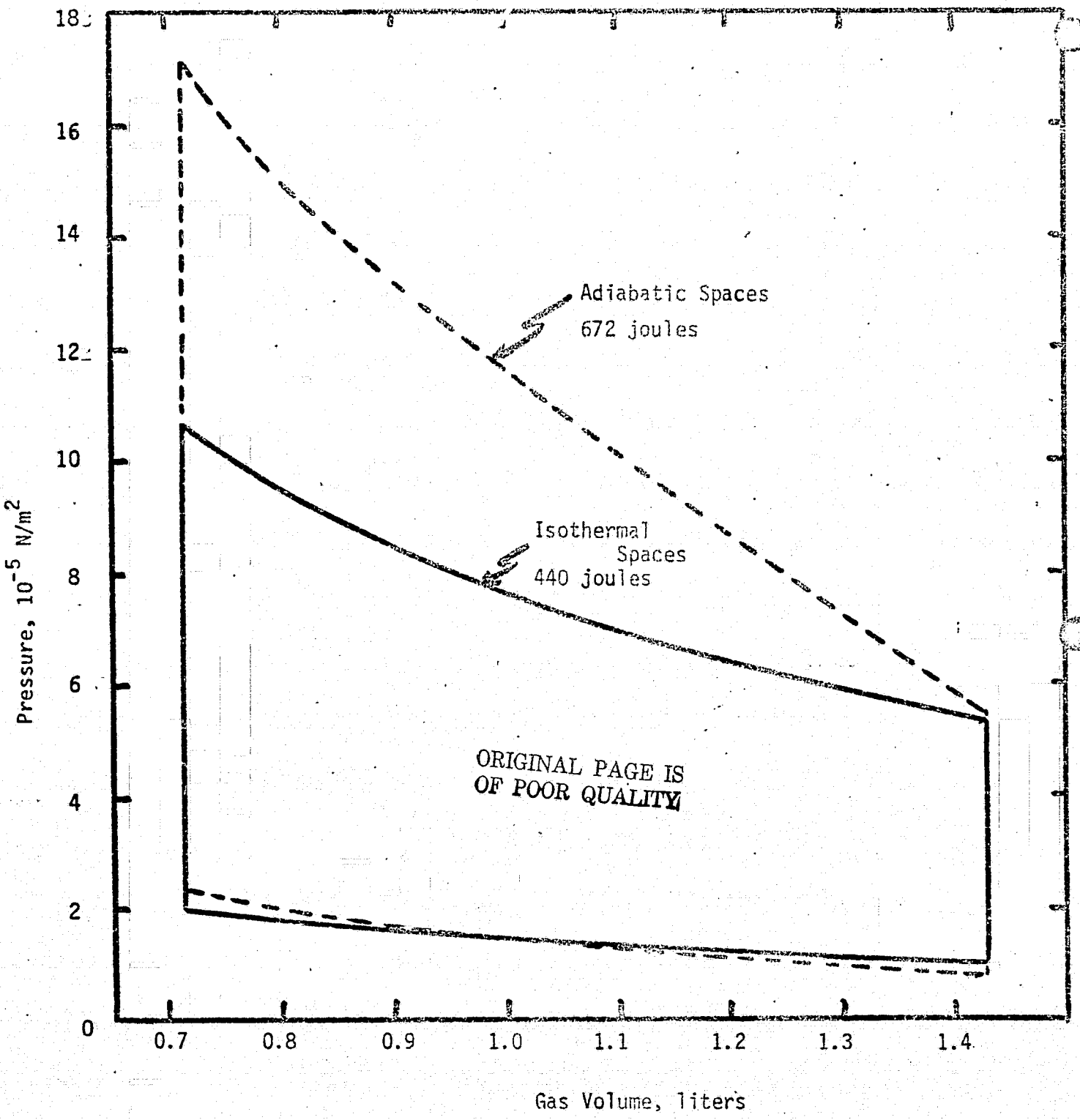

Figure 16. Sample Stepwise Engine Work Diagrams with 0% Dead Volume.

potential work per cycle is reduced 77.5%. Thus approximately the same ratio seems to hold. Potential work per cycle is reduced about 0.8% for every percent increase in dead volume. This is not a general rule but seems to hold between zero and 100% dead volume (based upon live volume).

3.2.2.3 Effect of Adiabatic Spaces

If the hot and cold spaces of the Stirling engine are open as they usually are, then compression and expansion in these spaces takes place essentially adiabatically (see analysis in section 3.2.1.6.2). Adiabatic compression and expansion and constant volume heating and cooling defines the Otto cycle. The Otto cycle of Figure 6 and the Stirling cycle with the same compression ratio are compared. For the temperatures used in the "Stirling" engines, the optimum compression ratio for the Otto cycle is (Ref. 6):

$$C_{opt} = \tau^{\left(\frac{1}{2 - 2k}\right)} = 3.51 = \frac{1 \times 10^{-3}\ m^3}{V_{min}}$$

where C_{opt} = compression ratio, V_{max}/V_{min}

τ = temperature ratio, T_C/T_H, absolute units

= $300/1600 = 1.875 \times 10^{-1}$

$k = C_p/C_v$ = 5/3 for helium

Thus, V_{min} = 0.285 liters

Figure 17 shows that for zero dead volume and for the same maximum and minimum gas temperatures, the Stirling cycle work diagram is much bigger than the Otto cycle. Figures 13 and 17 both show that the net work for the Stirling cycle is 550 joules. Figure 17 shows that the net work for the Otto cycle is 270 joules. (Figure 5 cannot be used because it is for a higher compression ratio.) Thus, for zero dead volume and for the same gas temperature swing the use of open hot and cold spaces reduces the power output to 49% of what it could be with fully

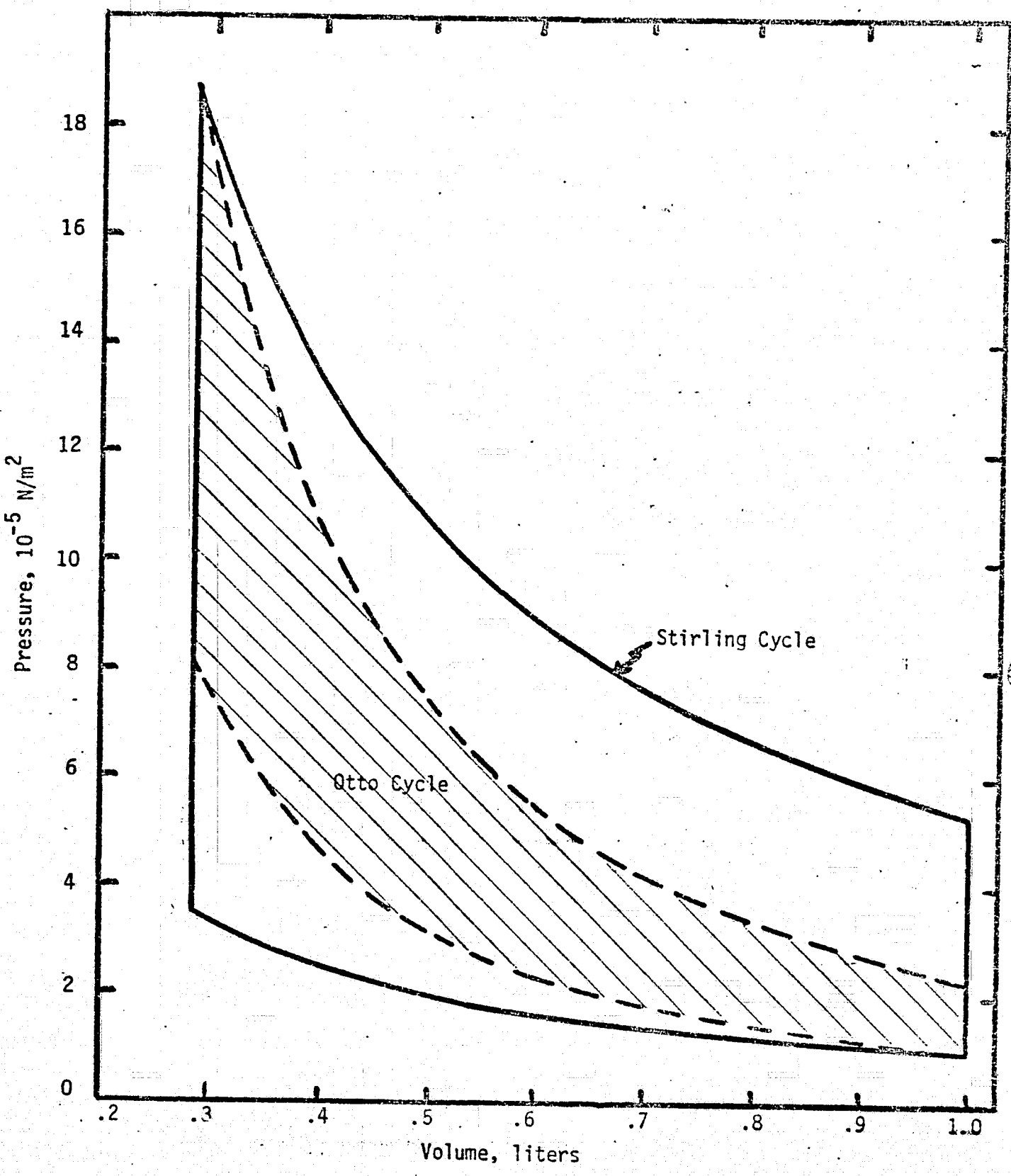

Figure 17. Comparison of Otto and Stirling Cycles.

isothermalized spaces.

However, if one assumes that the heat exchangers are in series with the regenerator and make the working gas being transferred closely approach the heat source and heat sink temperatures, then the average gas temperature in the hot space can run higher than the heat source temperature and the average gas temperature in the cold space can be below the heat sink temperature. Thus more power can be generated with the open gas spaces than with isothermal gas spaces WITH THE SAME DEAD VOLUME FRACTION. The isothermalized machine will have substantially less dead volume and therefore more power. This surprising phenomenom which has been observed in real engines will now be explained more fully and a method of calculating will be presented.

Starting with Figure 14A with the gas in the cold space at $300^{o}K$ and the gas in the regenerator and heat exchanger at $776.6^{o}K$ effective average temperature the gas inventory is first computed

$$P\left(\frac{V_R}{T_R} + \frac{V_c}{T_c}\right) = nR \text{ j/}^{o}K$$

$$nR = 10^5\left(\frac{1.43 \times 10^{-3}}{776.6} + \frac{1.43 \times 10^{-3}}{300}\right) = 0.6608 \text{ j/}^{o}K$$

From Figure 14A to 14B with adiabatic compression in the cold space and isothermal compression in the regenerator, two laws apply. The gas law:

$$nR = P_B\left(\frac{1.43 \times 10^{-3}}{776.6} + \frac{0.715 \times 10^{-3}}{T_{BC}}\right) = 0.6608$$

And the adiabatic compression law:

$$\frac{T_2}{T_1} = \left(\frac{P_2}{P_1}\right)^{\frac{k-1}{k}}, \quad \frac{T_{BC}}{300} = \left(\frac{P_B}{10^5}\right)^{0.4}$$

These 2 equations in 2 unknowns are solved. The result is:

$$T_{BC} = 376.7^{o}K, \; P_B = 1.767 \times 10^5 \text{ N/m}^2$$

From B to C gas is transferred. The gas from the cold space is cooled down to 300°K in the cold heat exchanger. Then it is heated to 1600°K in the regenerator and the hot heat exchanger. As elements of gas enter the hot space, pressure increases. Those elements that first enter are compressed and increase in temperature above 1600°F. The average temperature in the hot space at the end of the transfer is assumed to obey the equation:

$$\frac{T_{HC}}{T_{HB}} = \tfrac{1}{2}\left(\left(\frac{P_C}{P_B}\right)^{\frac{k-1}{k}} + 1\right), \quad \frac{T_{HC}}{1600} = \tfrac{1}{2}\left(\left(\frac{P_C}{1.767 \times 10^5}\right)^{0.4} + 1\right)$$

Also by the gas law:

$$nR = P_C\left(\frac{.715 \times 10^{-3}}{T_{HC}} + \frac{1.43 \times 10^{-3}}{776.6}\right) = .6608$$

Solution as before gives:

$$T_{HC} = 1782^{\circ}K, \; P_C = 2.947 \times 10^5 \; N/m^2$$

From C to D gas is expanded using the same formulas as for the compression from A to B. Table 10 shows the results. The transfer from D back to A is calculated in the same way as the transfer from B to C. However, Table 10 shows that the process does not return to the initial conditions. One more cycle is needed for practical convergence.

Figure 15 compares this calculated result with the corresponding isothermal case. The corner points were calculated in Table 10 and the curves inbetween were estimated. About 6% more work per cycle is realized for this level of dead volume.

If one could attain this effect without dead volume devoted to heat exchangers, then one could produce an even larger effect. Table 11 shows 3 cycles of computing the corner points and practical convergence is obtained. The results are graphed on Figure 16. Fifty-three percent more power could be obtained by using adiabatic gas spaces if zero dead volume could in reality be obtained.

TABLE 10

ENGINE CALCULATION FOR ADIABATIC LIVE VOLUMES
(100% Dead Volume).

Revolution	A		B		C		D	
	T_C ^oK	P, N/m^2	T_C ^oK	P, N/m^2	T_H ^oK	P, N/m^2	T_H ^oK	P, N/m^2
1	300	1×10^5	376.7	1.767×10^5	1782	2.947×10^5	1653	2.442×10^5
2	249.4	8.722×10^4	319.5	1.620×10^5	1818	2.957×10^5	1688	2.458×10^5
3	249.1	8.715×10^4						

TABLE 11

ENGINE CALCULATION FOR ADIABATIC LIVE VOLUMES
(0% Dead Volume)

Revolution	A		B		C		D	
	T_C ^oK	P, N/m^2	T_C ^oK	P, N/m^2	T_H ^oK	P, N/m^2	T_H ^oK	P, N/m^2
1	300	1×10^5	472.6	3.175×10^5	2303	1.535×10^6	1451	4.836×10^5
2	220.6	7.354×10^4	350.2	2.335×10^5	2578	1.719×10^6	1624	5.412×10^5
3	217.1	7.236×10^4	344.7	2.298×10^5	2593	1.729×10^6	1634	5.446×10^5

The analysis in Section 3.2.1.6.2 shows that open spaces even about 3 cm in diameter and filled with helium are very close to adiabatic. The analysis in Section 3.2.1.2.1 shows that by subdividing the space into thin layers one can approach an isothermal compression or expansion. Therefore, one can employ either kind of space. Isothermal spaces are expected to be better because they eliminate the dead volume and flow resistance of heat exchangers in series with the regenerator which is probably a larger advantage than the effect just discussed above. However, both concepts need to be evaluated for a particular application and the best concept chosen. However, it is quite clear that using isothermal compression and expansion spaces and gas heaters and coolers too would be detrimental.

3.2.2.4 Effect of Sinusoidal Motion

Real engines don't move in jumps as the previous analysis implies. As a mechanical convenience as well as to allow maximum time for heat transfer, the displacer and the power piston both move sinusoidally or nearly so. Figure 18 shows how the parts really move in a crank operated Stirling engine. Free piston Stirling engines have more freedom in arranging for motion but for best efficiency, they need to move as shown in Figure 18. This motion rounds the corners on the step-wise work diagram (see Figure 12). The work diagram can be computed for a specific case by assuming that the pressure is the same throughout the engine at each point in time and that the gas temperatures throughout are known and that the gas inventory remains constant. The line integral of the work diagram is then computed. Over a hundred years ago Gustav Schmidt (Ref. 35) solved the problem and obtained a formula. A useful form of his equation was presented in Ref. 26 (see below).

$$W = mR\,T_c\,\frac{2\pi b V_p}{b^2+c^2}\left[\frac{a}{(a^2 - b^2 - c^2)^{\frac{1}{2}}} - 1\right]$$

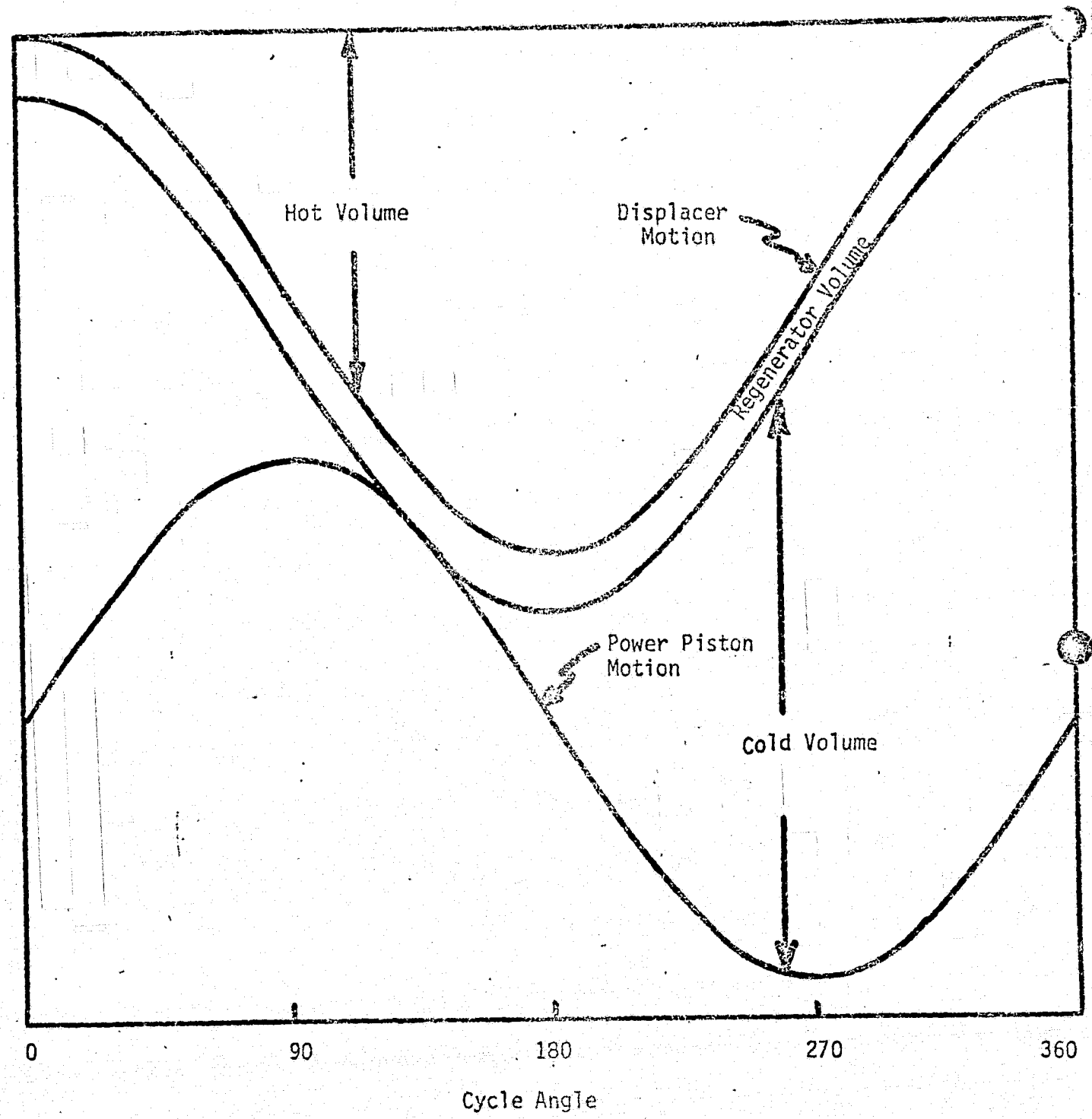

Figure 18. Stirling Engine Parts Motion.

where W = ideal work output per cycle (joules)

m = amount of contained working fluid (gram-moles)

R = gas constant ($8.316 \frac{\text{joules}}{\text{gram-mole}^{\circ}K}$)

T_H, T_C = hot, cold gas temperature ($^{\circ}K$)

$\tau = T_C/T_H$

$a = V_{CO} + V_{HO}$, (m^3)

V_{CO} = volume between midpoint of regenerator travel and midpoint of power piston or pump diaphragm travel, (m^3)

V_{HO} = volume between hot surface and midpoint of regenerator travel (m^3)

$b = V_R(1 - \tau)$, (m^3)

$c = V_P$, (m^3)

These expressions for b and c are only valid for the conventional engine when the power piston lags the regenerator by 90°. For an arbitrary phase lag, ϕ, $b = V_R(1 - \tau) \sin \phi$ and $c = V_P - V_R(1 - \tau) \sin \phi$.

V_R, V_P = the volume swept out by the regenerator, power piston or pump diaphragm, as is moves from the midposition to either extreme position (m^3)

For instance, for the engine described in Figure 14 and 15,

$m = 7.946 \times 10^{-2}$ g mol

$T_H = 1600^{\circ}C$, $T_C = 300^{\circ}K$

$\tau = 300/1600 = 0.1875$

$V_R = 0.715 \times 10^{-3}\ m^3$

$V_P = 0.3575 \times 10^{-3}\ m^3$

$V_{HO} = 0.715 \times 10^{-3} + \underbrace{0.715 \times 10^{-3}}_{\text{split dead volume}} = 1.43 \times 10^{-3}\ m^3$

$V_{CO} = (.715 - .3575 + .715) \times 10^{-3} = 1.0725 \times 10^{-3}\ m^3$

$a = 1.0725 \times 10^{-3} + 0.1875\ (1.430 \times 10^{-3}) = 1.3406 \times 10^{-3}$

$b = 0.715 \times 10^{-3}\ (1 - .1875) = 5.8094 \times 10^{-4}$

$c = 0.3575 \times 10^{-3}$

Therefore, W = 89.85 joules which is about 90% of the step-wise work diagram. Therefore, not much is lost by going to sinusoidal motion and it is essentially necessary anyway to allow time for heat transfer.

3.2.2.5 Example of Gas Pumping Engine (Thermocompressor)

A simple, light-weight form of Stirling engine is now called the thermocompressor. It was once used in the McDonnell Douglas artificial heart program (Ref. 7) and is still used in the Aerojet program (Ref. 8, 9). Basically, this engine works by using the pressure change realized by heating and cooling a gas to pump part of that same gas. Its operation is diagrammed in Figure 19 which shows the engine at the end of each of the four phases of its operation and relates these phases to points on a pressure-volume (PV) diagram and a pressure-regenerator displacement diagram. Note that the regenerator is attached to the plunger of a gas spring, and inlet and outlet check valves are installed in the cold plate of the engine. Note too that at Position A, the gas pressure A in the engine is greater than the pressure A' in the gas spring; thus the regenerator is forced down. As the regenerator moves down toward Position B, the pressure in the engine increases faster than in the gas spring. After Position B, the outlet valve opens and the gas spring pressure becomes equal to the engine pressure at B'. The area A' A B B' is a measure of the work applied to move the regenerator. After B', the force applied by the spring reverses to bring the regenerator to a stop at C. The area B' C C' is a measure of the work stored in the spring. The process is the same on the return stroke. This analysis indicates that the area A B C D in the graph of gas pressure versus regenerator position is a measure of the work-per-cycle applied by the engine to maintain regenerator motion. In the graph of gas pressure versus gas volume, the gas is pressurized from A to B with no volume change. From B to C, the gas is expelled into the high-pressure line at no change in pressure. From C to D, the gas is depressurized with no volume change. Finally, from D to A*, gas is drawn in from the low-

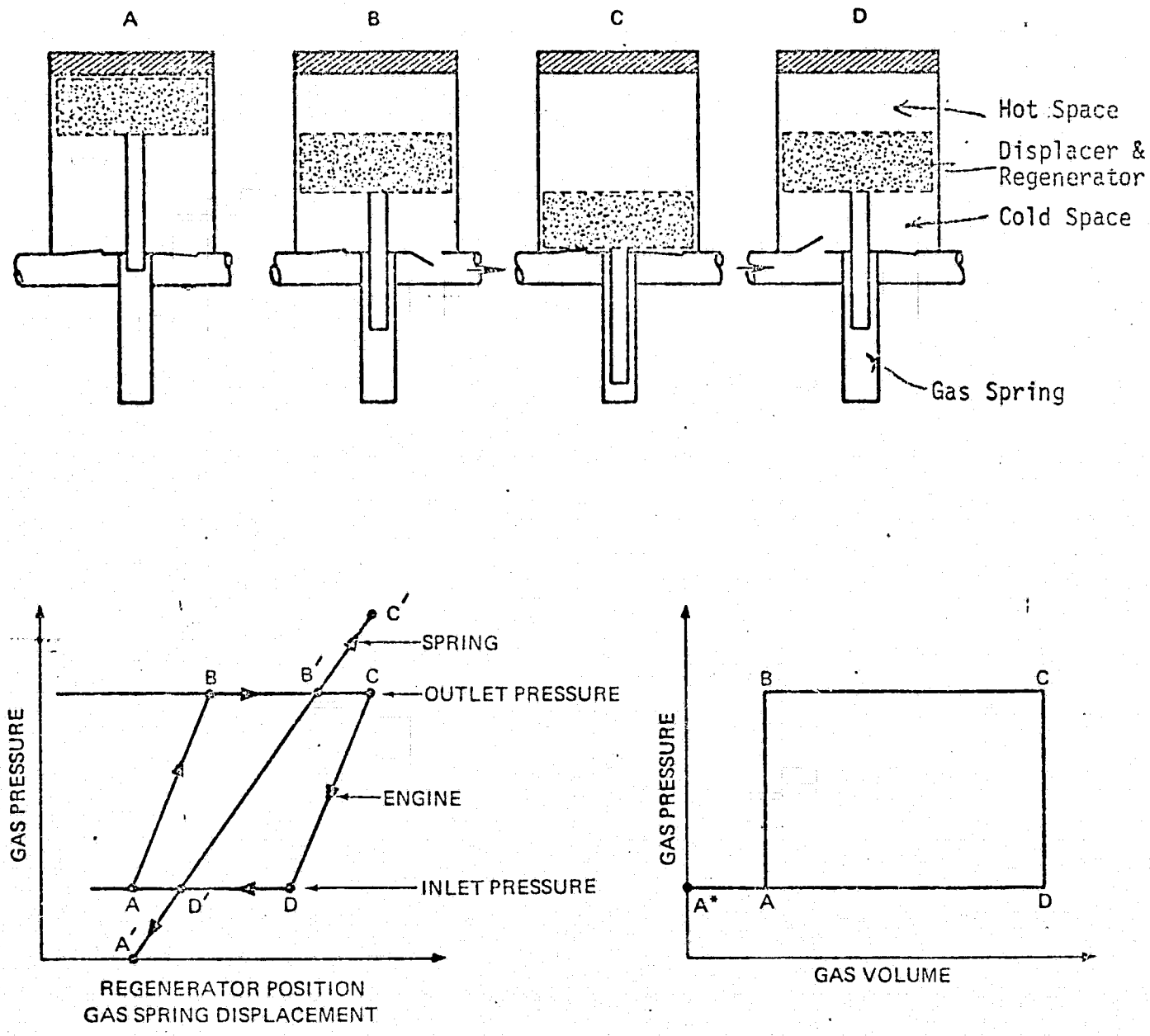

Figure 19. Principle of Operation of Thermocompressor.

pressure line at no change in pressure. Because of the compressibility of the gas, a greater volume must be drawn in than is expelled, but no difficulty is encountered because the system is redefined in the usual way for flow processes at the start of each cycle.

The inlet and outlet valves can be either in the hot space or in the cold space.

Since the engine simply pumps gas, it is necessary to decide how the pumped gas will be used to produce electricity. The most reasonable way is to use a high speed turbine directly attached to an electric generator. This turbine approximates isentropic expansion.

In order to roughly compare the thermocompressor with Otto cycle machines and other Stirling cycle machines which will be described, assume similar specifications:

1. Maximum effective gas temperature of $1600^{o}K$.
2. Gas volume inside thermocompressor, 1 liter (10^{-3} m^3 --- when cold space is at zero volume).
3. Minimum gas pressure in thermocompressor, 1 atm (10^5 N/m^2)
4. Helium as working gas.
5. Minimum effective gas temperature, $300^{o}K$.

In addition, there must inevitably be some fraction of the gas volume that must be used in the regenerator and in some cases in the gas heater and cooler and cannot be displaced. Let this dead volume fraction be 10%. If this dead volume fraction is evenly distributed between the two temperature extremes, then its effective gas temperature is the log mean.

$$T_r = \frac{T_H - T_C}{\ln\left(\frac{T_H}{T_C}\right)} = \frac{1600 - 300}{\ln \frac{1600}{300}} = 776.6^{o}K$$

Also, it is necessary to move the displacer with a rod. The fluctuating engine pressure operating on the rod area produces the work needed to keep the displacer

moving against windage and friction. This drive rod also detracts from the power output because the volume of gas leaving the cold space is less than the volume of gas entering the hot space by the volume of the drive rod. Let the drive rod volume be 5% of the cold volume.

In order to have a clear understanding of what is happening in a thermocompressor, consider that a power piston is immediately adjacent to the thermocompressor (Figure 20). From A to B the gas is pressurized. From B to C pressurized gas is expelled from the thermocompressor into the power piston. From C to D additional work is done as gas expands. The most reasonable assumption is an adiabatic expansion. From D to D' gas expands further as heat is added to the gas to bring it back up to heat rejection temperature. Also for C to D the displacer moves part way back to reduce the pressure in the thermocompressor from P_C back to $P_A = 10^5$ N/m^2. Finally, the displacer returns and all the gas returns into the thermocompressor. The cycle then repeats. With the assumptions given above, the volumes for the reference case are:

Point	C	A
V_H	0.9×10^{-3} m^3	0
V_R	0.1×10^{-3} m^3	0.1×10^{-3} m^3
V_C	0	0.81×10^{-3} m^3

Based upon the previous assumptions the gram moles of gas, N, in the engine at point A is

$$P_A\left(\frac{V_R}{T_R} + \frac{V_C}{T_C}\right) = N_A R$$

$$10^5\left(\frac{0.1 \times 10^{-3}}{776.6} + \frac{0.81 \times 10^{-3}}{300}\right) = N_A(8.314)$$

$$N_A = 3.402 \times 10^{-2} \text{ g mol}$$

If no gas is allowed to escape the pressure at point C would be:

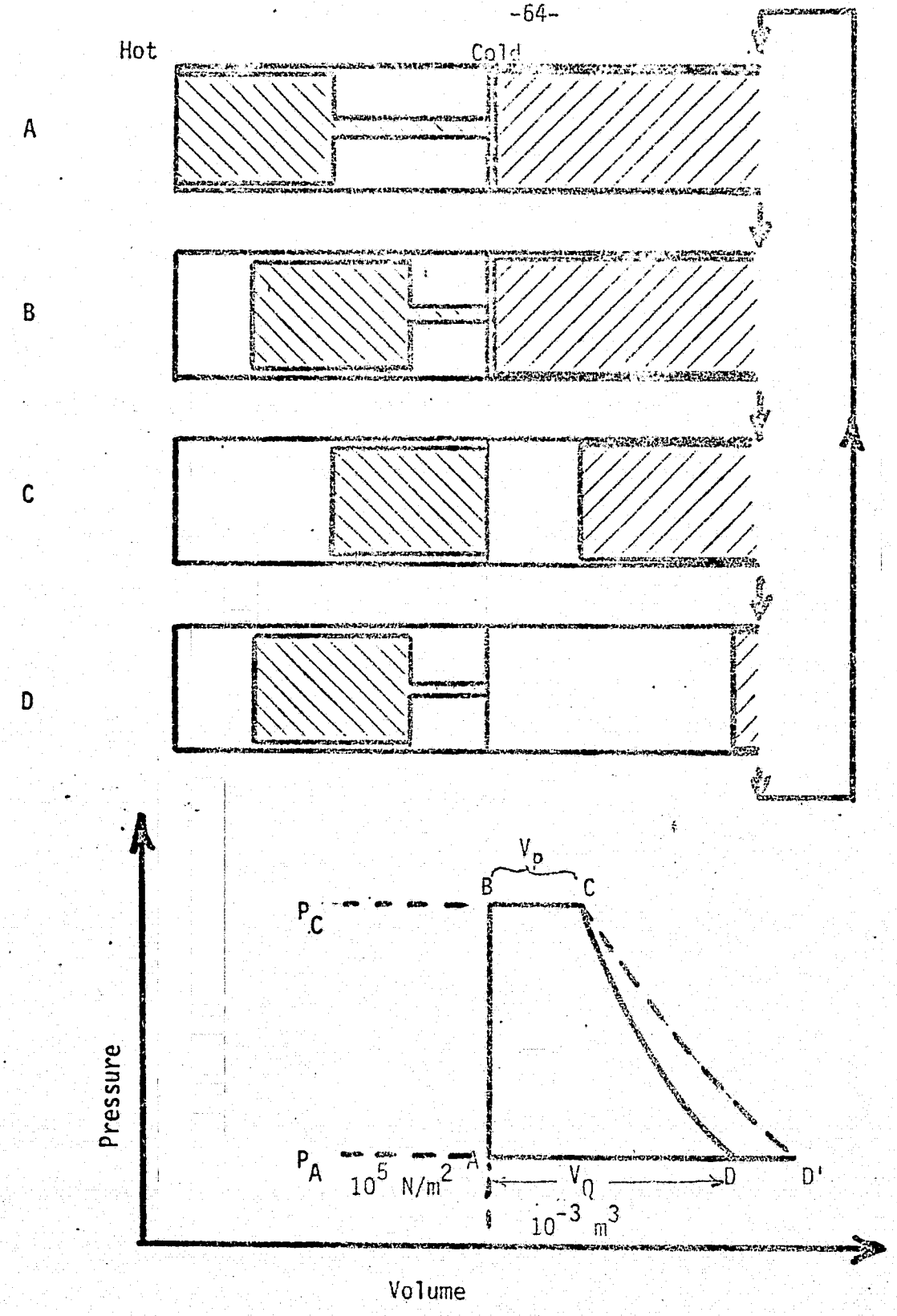

Figure 20. Analysis of Thermocompressor Process.

$$P_{C_{max}}\left(\frac{V_H}{T_H} + \frac{V_R}{T_R}\right) = N_A R$$

$$P_{C_{max}}\left(\frac{0.9 \times 10^{-3}}{1600} + \frac{0.1 \times 10^{-3}}{776.6}\right) = 3.402 \times 10^{-2}\ (8.314)$$

$$P_{C_{max}} = 4.092 \times 10^{5}$$

For the maximum power out:

$$P_C = (P_{C_{max}} + P_A)/2$$

$$P_C = (4.092 \times 10^{5} + 1 \times 10^{5})/2$$

$$P_C = 2.546 \times 10^{5}$$

Employing this pressure the gas in the engine is:

$$P_C\left(\frac{V_H}{T_H} + \frac{V_R}{T_R}\right) = N_C R$$

$$2.546 \times 10^{5}\left(\frac{0.9 \times 10^{-3}}{1600} + \frac{0.1 \times 10^{-3}}{776.6}\right) = N_C(8.314)$$

$$N_C = 2.117 \times 10^{-2}\ \text{g mol}$$

The amount of gas pumped per cycle is:

$$N_A - N_C = N_P$$

$$3.402 \times 10^{-2} - 2.117 \times 10^{-2} = 1.285 \times 10^{-2}\ \text{g mol}$$

The volume of gas pumped, V_P is:

$$V_P = \frac{N_P R T_C}{P_C} = \frac{(1.285 \times 10^{-2})(8.314)(300)}{2.546 \times 10^{5}}$$

$$= 1.259 \times 10^{-4}\ m^2$$

The volume, V_Q, after the gas is expanded adiabatically back to the original pressure is:

$$\frac{P_A}{P_C} = \left(\frac{V_P}{V_Q}\right)^k$$

$$\frac{10^5}{2.546 \times 10^5} = \frac{(1.259 \times 10^{-4})^{1.667}}{V_Q^{1.667}}$$

$$V_Q = 2.206 \times 10^{-4}\ m^3$$

The temperature after expansion is:

$$\left(\frac{P_A}{P_C}\right)^{\frac{k-1}{k}} = \frac{T_D}{T_C}$$

$$\left(\frac{10^5}{2.546 \times 10^5}\right)^{0.4} = \frac{T_D}{300}\ ,\ T_D = 206.4^oK$$

The output work is:

$$W_{out} = P_C V_P - N_P R T_C \left(\left(\frac{P_A}{P_C}\right)^{0.4} - 1\right)$$

$$= 2.546 \times 10^5\ (1.259 \times 10^{-4}) - 1.285 \times 10^{-2}\ (8.314)(300)\left(\left(\frac{1}{2.546}\right)^{0.4} - 1\right)$$

$$= 42.05 \text{ joules}$$

The input work is:

$$W_{in} = P_A V_Q = 10^5\ (2.206 \times 10^{-4}) = 22.06 \text{ joules}$$

Thus, $W_{net} = 42.05 - 22.06 = 19.99$ joules

The heat input is equal to the pressure volume integral in the hot space of the engine. Let x be the fraction of the displacer stroke. During the pressurizing stroke the pressure, P_x, is:

$$P_x\left(\frac{x(0.9 \times 10^{-3})}{1600} + \frac{0.1 \times 10^{-3}}{776.6} + \frac{(1 - x)(0.81 \times 10^{-3})}{300}\right) = 3.401 \times 10^{-2}(8.$$

$$P_x = \frac{2.818 \times 10^{-1}}{2.829 \times 10^{-6} - 2.138 \times 10^{-6} x}$$

During the depressurizing stroke the pressure, P_x, is:

$$P_x = \left(\frac{x(0.9 \times 10^{-3})}{1600} + \frac{0.1 \times 10^{-3}}{776.6} + \frac{(1 - x)(0.81 \times 10^{-3})}{300}\right) = 2.117 \times 10^{-2}(8.314)$$

$$P_x = \frac{1.760 \times 10^{-1}}{2.829 \times 10^{-6} - 2.138 \times 10^{-6}x}$$

The engine pressure is plotted against the displacer stroke in Figure 21. The area of this curve, 4.68×10^4 N/m^2, is multiplied by the maximum hot space volume of 0.9×10^{-3} m^3 to give the heat input Q_{in}. So,

$$Q_{in} = 4.68 \times 10^4(0.9 \times 10^{-3}) = 42.12 \text{ joules}$$

Thus, the cycle efficiency for a thermocompressor operating between 1600°K and 300°K with 10% of the gas volume in regenerator and with the cold space reduced by 10% to allow for the drive rod is:

$$\eta = \frac{19.99}{42.12} = 0.47$$

Because this efficiency is less than 50%, the idea of a thermocompressor connected to a cold gas turbine or other type of cold gas expander will not be considered further. Considerably more power and efficiency can be obtained if the expansion were from the hot gas side but valves and a turbine operating at 1600°K (2420°F) are not considered practical.

3.2.2.6 Example of a Liquid Pumping Engine

One possibility of an engine with some compression is the kind currently used by McDonnell Douglas in their heart assist machines (Ref. 8, 10). It is related to the thermocompressor because it appears to work the same way but a vital ingredient has been added--inertia. First, the engine principle will be explained in general using a valve controlled free-displacer, free-piston engine concept. This could be used to power an electric generator directly. Next it will be shown schematically how it can produce hydraulic power. This kind of machine was tested at the 500 w scale (Ref. 37).

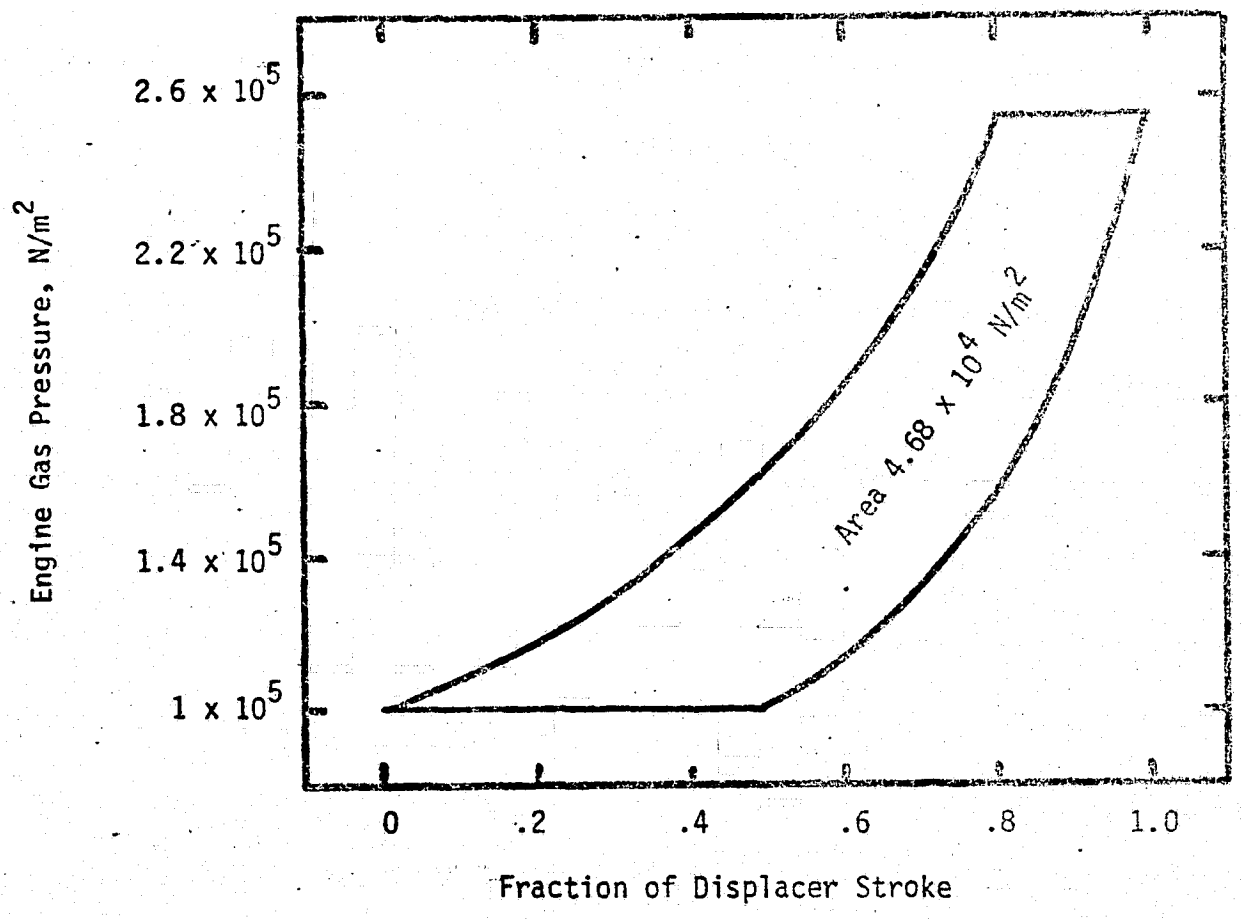

Figure 21. Engine Pressure in a Standard Thermocompressor.

The principle of operation is as follows. Starting at position 1, (Figure 22) the displacer has moved most of the gas to the cold end of the engine, and the power piston is compressing this gas in the cold portion using energy stored in the gas reservoir from a previous cycle. Gas reservoir pressure is higher than engine pressure so that the power piston is being accelerated to the left. At time 1A, engine compression has proceeded to the point where the engine pressure is now higher then gas reservoir pressure, requiring piston inertia to conclude the compression stroke. This pressure difference also causes a force to be developed across the displacer drive piston to cause the displacer to be moved to the right. As it moves to the right, compressed cold gas is moved through an annular gas regenerator into the hot portion of the engine and rapidly increases engine pressure. At point 2, this process has been completed, and high engine pressure has started the power piston back to the right. At point 3A, this power stroke is continuing with the gas being expanded from the hot zone of the engine. At point 3A, expansion has proceeded to the point where gas pressure in the engine now becomes less than gas reservoir pressure.

This changed pressure difference causes a force to be developed across the displacer drive piston to move the displacer to the left. This displacer motion causes the remaining gas in the hot zone to be transferred into the cold zone which rapidly reduces engine pressure, and at 4, this reduced pressure has reversed the motion of the power piston and has again started the compression stroke. The process then repeats. For stable operation, power must be removed from the power piston either by coupling to an electromagnetic generator, a liquid pump, or some other sink for mechanical energy. For most efficient operation of the engine, the displacer should take most of the time between 1A and 3A to move to the right and most of the time from 3A back to 1A to move to the left. This allows maximum time for heat to be transferred by the regenerator as gas moves from one end of the displacer to the other. The area of the displacer

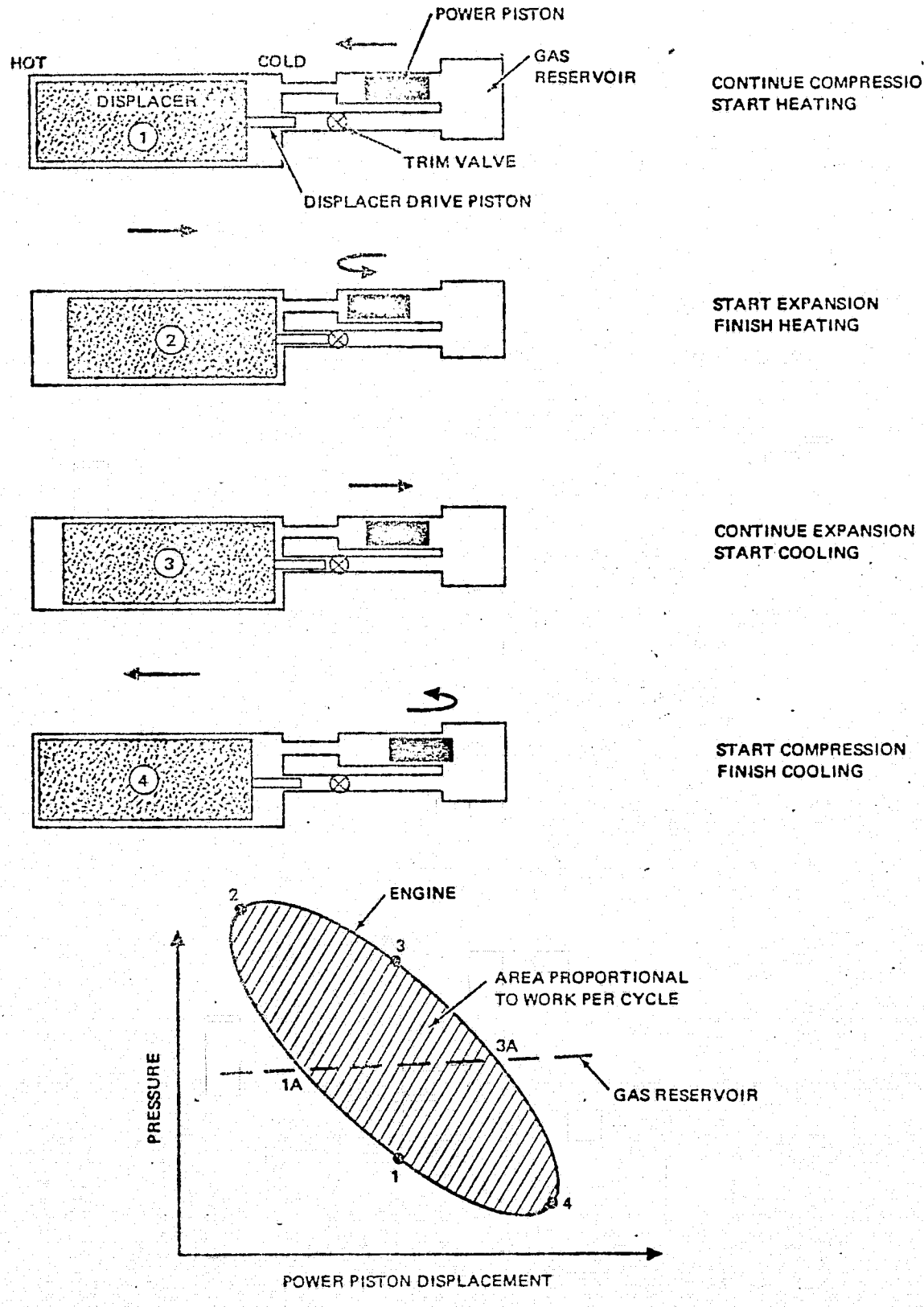

Figure 22. Free-Displacer, Free-Piston Stirling Engine Principle of Operation.

drive piston and the setting of the control valve is adjusted to ensure this condition. Experimental tests have shown that once the engine is hot, the control valve can smoothly regulate engine output power. As the control valve is cracked, the displacer starts moving at a low amplitude and low frequency, and as the control valve is further opened, both frequency and amplitude increase until the desired power level is obtained.

Application to Hydraulic Power

Figure 23 shows how this type of machine can be applied directly to produce hydraulic power without any intervening shaft power being produced. A basic hydraulic Stirling module consists of an engine and converter. The engine utilizes a free displacer centered with springs that cushion the displacer at the ends of each stroke. The displacer moves helium working gas from the hot space, through the heater, regenerator, and cooler to the cold space, then back again. This process changes engine pressure with very little heat loss, and allows displacer motion to be self-starting.

An external heater, regenerator, and cooler may be necessary for larger machines. A displacer counterweight is indicated but is not necessary where minor vibration can be tolerated or for multiple displacer engines. A double acting hydraulic pump is shown as one type of energy takeoff from the engine. The converter piston is the primary inertial member. The diaphragm seals between the gas and the hydraulics are fitted with supports at each end of the travel so that accidental overpressurization in either direction will not harm the diaphragms.

Based upon McDonnell Douglas experience with the heart power source and upon calculations of 1 HP size machines elsewhere, the efficiency of the engine itself operating from $1600^{o}K$ to $300^{o}K$ can be about 70% (about 90% of Carnot). The converter is about 90% efficient. Thus an expected overall heat to hydraulic

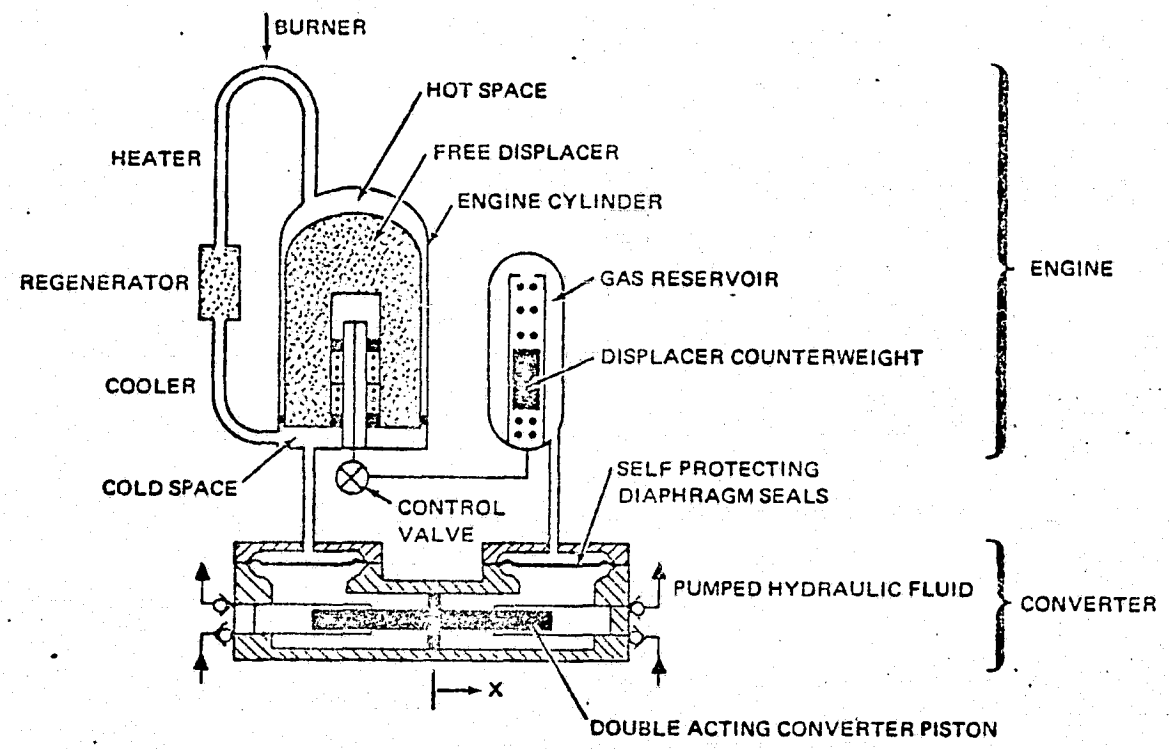

Figure 23. Principle of Hydraulic Stirling Engine Operation.

power efficiency of 63% is expected. The engine and converter is expected to weigh about 2 to 3 pounds in the 1 HP size.

3.2.2.7 Example of a Conventional Philips Stirling Engine

Nobody outside the Philips organization and licensees knows how the Philips engine is designed or what its critical dimensions are. However, if an engine is needed, the Philips organization will produce it to order. Therefore, the latest published performance numbers for the Philips engine by Michels will be presented (Ref. 38). The engine is a beta type engine (see Figure 11). It is a one cylinder rhombic drive machine with a 98 cm^3 swept volume for the power piston and about the same for the displacer. This design is 10 years old and about 30 engines were built and are still in use by various licensees of Philips. A schematic of this engine with its burner and air preheater is shown in Figure 24.

The following is quoted from Ref. 38:

> Using the Philips Stirling optimization computer program, a large number of engines were calculated to determine the influence of heater and cooler temperature and working fluids on the efficiency. The following parameters were chosen and assumptions made during the runs:
>
> --The engine size was chosen to be equal to that of the 1-98 engine, and the same stroke and piston dimensions were taken.
>
> --Three different heater tube temperatures were used, viz., 850, 400 and 250°C.
>
> --Two different cooler temperatures were used, viz., 100 and 0°C.
>
> --Three different working fluids were used: hydrogen, helium and nitrogen.
>
> --Only the heat exchangers were optimized, i.e., dimensions of the coolers, regenerators, and heater. Further, the necessary mechanical "fitting" requirements were obeyed.
>
> By "fitting" requirements it is meant, e.g., that the sum of the lengths of coolers, regenerators and the second part of the heater must be equal to the sum of the lengths of the cylinder and the first part of the heater. Another dimensional restriction is that ranges have to be specified within which parameters like lengths, diameters, etc. can be varied.
>
> For every combination of temperatures and working fluids and at a number of speeds, the pressure and dimensions were determined such that maximum efficiency was obtained. The results are given in Figure 25

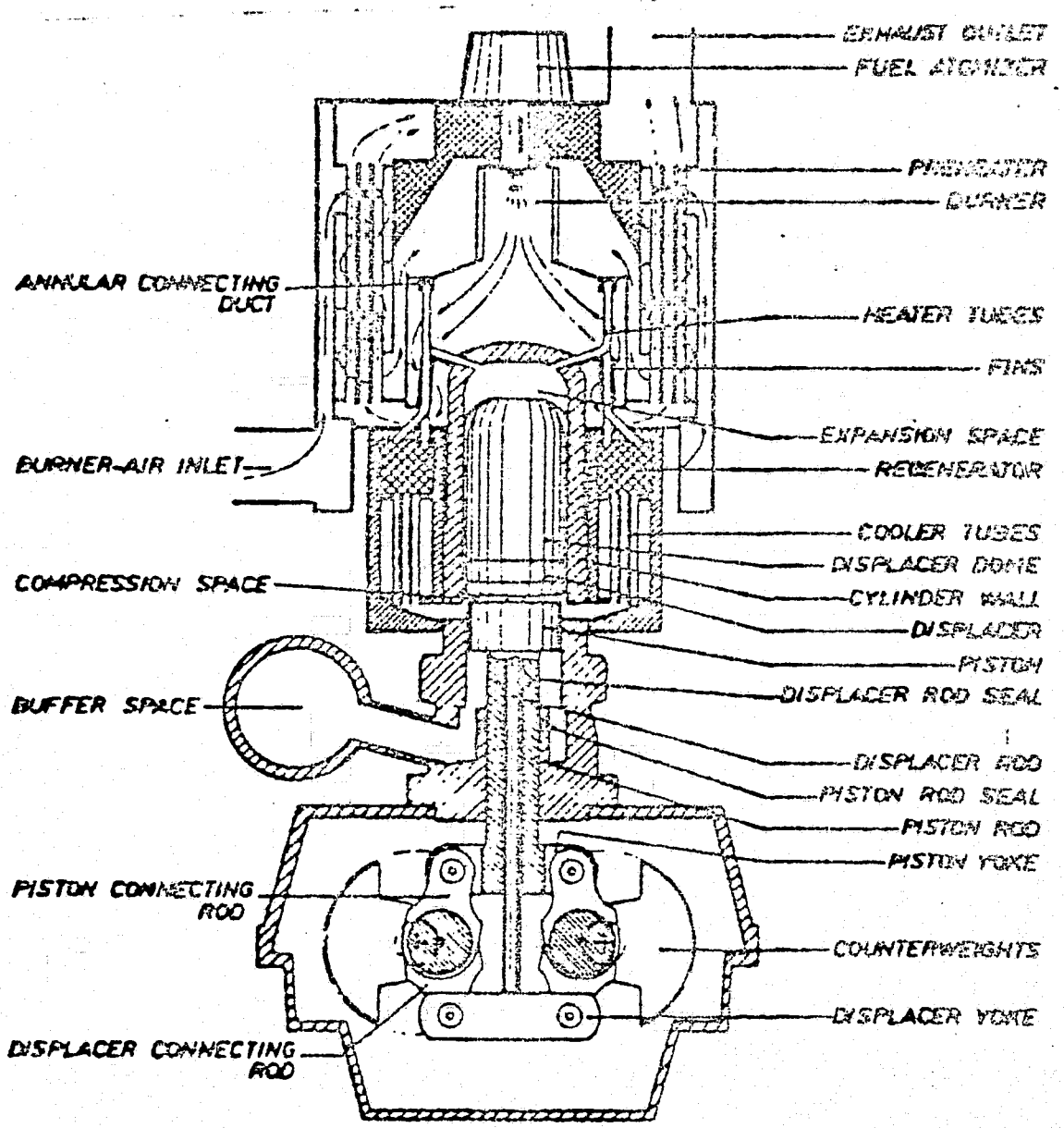

Figure 24. Cross-Section of the Philips Rhombic Drive Engine. (Ref. 38)

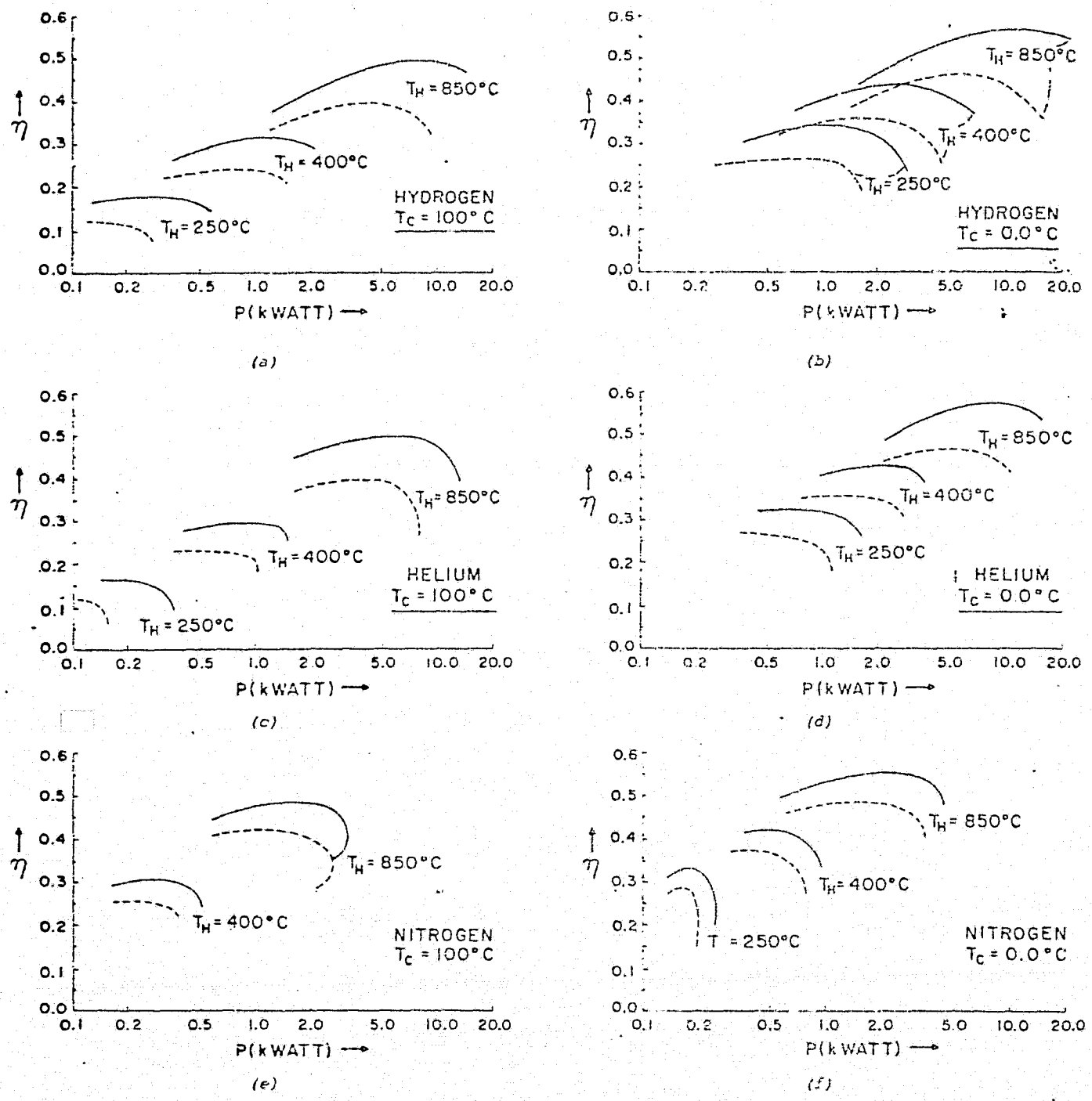

Figure 25. Efficiency vs. Indicated Power for an Engine with 98 cm^3 Displacement at Different Heater Temperatures T_H and Cooler Temperatures T_C. Hydrogen, Helium, and Nitrogen are Used as the Working Fluids. The Heater Efficiency is Not Included. (Ref. 38)

———— Indicated Efficiency
- - - - - - - - - - Shaft Efficiency

where the indicated efficiencies are plotted as a function of indicated power. The indicated power output is defined as the engine power assuming no mechanical friction; the indicated efficiency is the ratio of this power to the heat delivered to the heater. The engine speed increases from left to right along the curves.

For the 750 w(e) space power source helium should probably be used because it can be contained permanently in metal. Assume 85% efficiency for a 750 w(e) low speed electric generator to be driven directly by the engine. Assume about 83% mechanical efficiency (Ref. 38). Therefore, the required indicated engine power is:

$$\frac{750}{0.85(0.83)} = 1063 \text{ watts}$$

The cold temperature should be 100°C to allow for a reasonably sized radiator. Heater temperature of 850°C (1123°K) is much lower than the 1600°K used as standard in the Stirling engine section so far. The 1123°K is as hot as stainless steel will go. Engines can be made with refractory metals at up to 1600°K. The 98 cm^3 displacement engine is too big for this application (see Figure 25C). A smaller engine could be designed to attain about 75% of Carnot for these temperatures.

To attain the goal of 50% overall efficiency, one must consider Stirling engines specially made from refractory metals. One must also use as low a heat sink temperature as practical.

One study and experimental program was sponsored by the Air Force at Allison Division of General Motors to build a 3 KW(e) solar heated space electric power source (Ref. 39). An engine was built on this program but was not very successful because sealing problems were not then worked out. The engine design showed heating by a liquid metal loop and cooling to a space radiator. The engine was a single cylinder rhombic drive machine operating two counter rotating electric generators inside the sealed crankcase tank.

Since that early development there have been no programs in conventional

Stirling engines where weight was particularly important.

General Motors (Ref. 40) shows a 11 HP Stirling engine which operated at 3600 rpm and about 21% efficiency (fuel to brake power). It was 15" long, 16" wide and 29" high and weighed 90 lb. (8.2 lb/HP).

3.2.2.8 Example of a Flight Weight Free-Displacer Stirling Engine

As a predecessor to the current ERDA program on Stirling Electric Generators, McDonnell Douglas adapted the work they did on the artificial heart and on a 500 w(m) engine design to propose on a free-displacer engine operating the MTI linear electric generator. The power source involved 2 engines each with the characteristics listed in Table 12. The engine operates as shown in Figure 22 and uses current McDonnell Douglas heart power source technology.

3.2.2.9 Example of an Isothermalized Engine

An isothermalized engine design was presented in Ref. 17 and in an errata sheet that was distributed at the meeting (see Appendix C). This design uses interleaving fins in all variable volume spaces to assure isothermal compression and expansion and to reduce dead volume and flow resistance. During cruise, the displacer only moves a small fraction of the total available travel and therefore, efficiently produces the power needed. During acceleration maximum torque is produced but at a lower efficiency. The example given in Appendix C is abstracted in Table 13 to show how 87% of Carnot efficiency is obtained for the cruise case. This table shows that a large engine lightly loaded can have a high efficiency if it is a Stirling engine.

Stirling engines are quite complex to design because there are so many important trade-offs that all must be considered together.

3.2.2.10 Conclusion on Stirling Engines

1) Stirling engines can be made to take full advantage of the energy of a

TABLE 12

FLIGHT-WEIGHT FREE DISPLACER ENGINE CHARACTERISTICS

Dimensions, in.	
Diameter	2.00
Gas Heater Length	1.75
Gas Heater Annular Gap	0.020
Regenerator Length	2.64
Number of Regenerator Annuli	3
Gap of Each Annulus	0.014
Gas Cooler Length	2.27
Gas Cooler Annular Gap	0.020
Displacer Stroke	0.30
Overall Length (internal)	7.26
Operating at	
Frequency, Hz	60
Maximum Pressure, psia	135
Hot Metal Temperature, ^{o}C	871
Cold Metal Temperature, ^{o}C	93
Output Power, watts	
Gross	260
Windage	10
Net	250
Input Heat, watts	
Carnot	400
Heat Conduction	29
Reheat Loss	92
Total	521
Efficiency, %	48
Weight, lb.	15
Specific Weight, lb/HP	45

TABLE 13

EXAMPLE OF AN ISOTHERMALIZED AUTOMOTIVE STIRLING ENGINE
(Ref. 17 and Appendix C)

Dimensions	
Number of Displacers and Power Pistons	4 each
ID of Displacer Cylinder	27.9 cm
Maximum Stroke of Displacer	2.5 cm
Working Stroke of Displacer	8.3% of maximum
Length of Displacer Cylinder	30.5 cm
Effective Diameter of Power Pistons	27.9 cm
Stroke Power Pistons	2.5 cm
Regenerator annuli	20
Thickness Each Annuli	0.25 mm
Interleaving Square Fins with Slight Taper as Isothermalizers	
Fin Thickness	1.27 mm
Fin Length	2.5 cm
Operating at:	
Frequency	7.74 Hz
Hot Metal	992°K
Cold Metal	339°K
Maximum Pressure	13.6 atm
Output Power, watts	
Gross	3,980
Windage	90
Net	3,890
Heat Required, watts	
Carnot Heat	6,300
Reheat Loss	140
Shuttle Conduction	10
Metal Conduction	150
Gas Conduction	200
Insulation Loss	110
Regenerator Windage	-30
Isothermalizer Windage	-20
Total	6,860
Efficiency, %	57
% of Carnot Efficiency	87

laser beam in a space electric power source. However, the technology for building a Stirling engine at least part from refractory metals or ceramics to stand the high temperature will need to be developed in order to get the indicated efficiency well over 50% so that the overall efficiency can be 50%.

2) The most efficient Stirling engines have a low power density. Therefore, a ground rule must be agreed upon relating efficiency to system weight before design optimization can start.

3) Stirling engines can be designed up to about 90% of Carnot efficiency or $0.9(1 - \frac{300}{1600}) = 73\%$ for the maximum and minimum temperature assumed in this study. However, the engine will be large and heavy. An indicated efficiency of 75% of Carnot or 61% is current state-of-the-art.

4) There are many options for the internal design of a Stirling engine. Because of the conflicting effects, it is necessary to specify a specific engine requirement and then evaluate the design options discussed herein to determine the best design for the purpose.

3.2.3 Conclusions on Heat Engines

The potential for developing a high efficiency heat engine to convert laser energy is not clearly with either "Otto" or the "Stirling" cycle engine. The higher usable heat source temperature of the "Otto" cycles approximately balances the higher percent of Carnot efficiencies of the "Stirling" engines. Choice of the best engine is clouded by uncertainties on both sides.

Uncertainties for the "Otto" cycle engines are:

1. Ignorance of how hot a laser can heat a confined gas and how fast this gas cools off.
2. Laser window durability.
3. Seal life and friction in small engine sizes.
4. Engine control to get the laser pulse at the right time in the cycle.

The uncertainties in the Stirling engine area are:

1. Design optimization at about 1 KW(m) indicated power.
2. Very high input temperature and refractory metals for Stirling engines.
3. Seal life and friction in small engine sizes.

The deciding factor may very well be in the full system design. For instance the thermal energy storage used with the Stirling engine may be lighter and less troublesome than the electrochemical batteries required for the "Otto" cycle machines. Power control may be a much bigger problem for the "Otto" cycle machine than it would be for the "Stirling" cycle machines.

3.3 Engine Output

In the previous section the thermodynamic part of the engine has been discussed. That is, gas pressure has been applied to an oscillating piston, in most cases, to generate net work each cycle. The engine output column in Figure 1 shows the different ways that the thermodynamic engine can be utilized. These are:

Pumped gas

Pumped liquid

Oscillating mechanical power

Rotating mechanical power

The technology germane to each of these components will now be discussed.

3.3.1 Gas Pump

Section 3.2.2.5 showed that gas pumping using a thermocompressor gives low power and insufficient efficiency. However, harnessing the piston of a free piston engine to compress gas is a reasonable coupling mechanism which has been proposed and used previously (Ref. 19).

Compression can take place adiabatically at low frequency to suit the engine. A miniature turbine wheel can be powered to turn at high speed to suit the

generator. Positive displacement gas compressors are known to be quite efficient. An indicated efficiency of 90% is regularly obtained (Ref. 20a).

3.3.2 Liquid Pump

A liquid pump has the advantage of not having to deal with the compressibility of gas. Dead volumes in the pump are not as critical if gas can be kept out of the liquid. A survey was made of 1 HP size positive displacement liquid pumps to determine possible efficiencies and operating ranges now realized. Table 14 shows the results. This information is readily available since hydraulic transmissions use this type of hardware in which efficiency is important. The standard line of hydraulic pumps for high efficiency use do not usually go down to 1 HP. On the other hand, experience with a Stirling engine powered hydraulic pump for the artificial heart shows that the pump hydraulics is greater than 95% efficient at 5 watts output (Ref. 20b).

3.3.3 Oscillating Mechanical Power

Since much of the cost, weight and reliability problems associated with both "Otto" and "Stirling" cycle engines have to do with converting energy applied to the piston to rotary motion, it is natural to look for machines that do not require this transformation. Liquid and gas pumps are in this category. Mechanical power can be applied directly to a special oscillating electric generator. No available engine generator operates on this principle but there are a number of patents issued on the idea (Ref. 21). At the present time ERDA is sponsoring a program to develop a Sitrling engine and an oscillating electric generator to build a 700 watt isotope powered electric generator for space. Don Morrow of ERDA at Germantown, Maryland (phone 353-4203) is project engineer and Mechanical Technology Incorporated of Latham, New York is the prime contractor and developer of the generator, Bruce Goldwater, principal investigator. Sunpower of Athens, Ohio is the engine developer.

TABLE 14

CHARACTERISTICS OF AVAILABLE POSITIVE

DISPLACEMENT LIQUID PUMPS

Make & Model	Ref.	Speed rpm	Power in watts	Power out watts	Efficiency %	Comments
Lucas IP60	(1)	2600	2618	2409	92	Includes mechanical linkage losses
Vickers MVB5	(2)	1800	3285	2895	88	

(1) Lucas Vendor Literature

(2) Vickers Vendor Literature

3.3.4 Shaft Power (Cranks and Seals)

Essentially all small heat engines convert pressure-volume energy at the piston to rotary mechanical energy at the output shaft. Since the early days of steam engines, it has been realized that there is an important loss for this part of the engine. Table 15 summarizes some representative references which indicate the attainable mechanical efficiency for a conventional Stirling engine at its maximum efficiency points for three different heat input temperatures. These data indicate that a mechanical efficiency of about 80% can be obtained. Table 16 gives additional data for piston engines to show what mechanical efficiency can generally be obtained. Experience shows that 80 to 90% can be expected.

3.4 Conversion Mechanisms

Figure 1 identifies some final conversion mechanisms that eventually get to electricity. These are:

1. a small very high speed gas turbine.
2. a hydraulic turbine or "water wheel"
3. a positive displacement hydraulic motor.

All three of the above are coupled directly to a:

4. rotary electric generator.

Finally is the direct operation of an:

5. oscillating electric generator.

These components will now be discussed.

3.4.1 Gas Turbines

A number of small turbines have been made and tested that are in the 1 HP size range. Table 17 shows the results of a literature search in this area. Although this table is brief, it does indicate that the state-of-the-art for small turbines is on the order of 80% efficiency with 84% peak reported for a new vane expander.

TABLE 15

CHARACTERISTICS OF A PHILIPS 93 cm^3 DISPLACEMENT RHOMBIC DRIVE STIRLING ENGINE (Ref. 38) HYDROGEN CHARGE

Heater Temperature, ^oC	850	400	250
Cooler Temperature, ^oC	0	0	0
Heat Input, watts	9259	3571	2941
Indicated Power Out, watts	5000	1500	1000
Brake Power Out, watts	4250	1250	764
Carnot Efficiency	0.76	0.59	0.48
Indicated Efficiency	0.54	0.42	0.34
Fraction of Carnot	0.71	0.71	0.71
Mechanical Efficiency	0.85	0.83	0.76
Overall Efficiency	0.46	0.35	0.26

TABLE 16

MECHANICAL EFFICIENIES FOR

SMALL PISTON ENGINES

Engine Type	Speed rpm	Ref.	Indicated Power HP	Power HP	Mechanical Efficiency
Rankine	1500	23	38.2	34.3 HP	0.90
	2000		43.1	38.4 HP	0.89
Rankine	3200	24	Not given		0.80
Positive Displacement Brayton		25		6.6 HP	0.84

TABLE 17

CHARACTERISTICS OF SMALL TURBOEXPANDERS

Working Fluid	Ref.	Output Power watts	Speed rpm	Efficiency %
Toluene	26	3108 KW(m)	8000	78.3%
Toluene	27	1213 KW(m)	55000	59.8%
Various	28	--	--	80%
Rotary Vane R-11	29	2230 KW(m)	800	84%

3.4.2 Hydraulic Turbine (Water Wheel)

Hydraulic turbines in extremely large sizes are the mainstay of hydroelectric projects. The advantage they would have for this application is that some type could be designed for high speed operation for direct coupling to a light and high speed electric generator. This requirement might be filled by a Pelton wheel in which a jet of liquid impinges onto cup-shaped deflectors around the rim of a wheel. In large sizes 85 to 90% efficiency are common. In small sizes fluid viscosity would be more important. In the 1 HP size, 80% efficiency can probably be expected.

3.4.3 Positive Displacement Hydraulic Motor

This device is the inverse of the hydraulic pump and is equally efficient. Table 14 shows that about 90% efficiency as normally obtained. The weight of an axial piston, constant displacement hydraulic motor with an efficiency of 85 to 95% is 1.4 lb/HP (Ref. 30).

3.4.4 Rotary Electric Generators

Rotary electric generators are the common type of electric generators. They can be obtained in the 750 watt size at a variety of sizes and weights and qualities. Generally, the higher speed the generator can operate the lighter it is and the more efficient it becomes. Table 18 shows a representative sampling of current technology in electric generators. It would seem from this sampling that 90% efficiency is possible in a 10 lb., 750 w(e) generator.

3.4.5 Oscillating Electric Generators

Oscillating electric generators are not generally available. Neither are efficient oscillating electric motors. The electric solenoid and the dynamic speaker with the voice coil oscillating between the poles of a permanent magnet are as close as current technology comes.

Table 18

ROTATING ELECTRIC GENERATORS

Weight lb.	Ref.	Output watts	Speed rpm	Measured Efficiency
Not given	27	1,000	55,000	82.4%
Not given	31	8.7	100,050	96.27%
89.8	32	105,000	60,000	88.9%
14	33	1,000	12,000	82%

Mechanical Technology Incorporated, Latham, New York, has been developing efficient oscillating electric motors. They have just recently tested a generator. Information on MTI's first test of the electric generator was obtained by telephone (Ref. 22). Their generator operated at 60 Hz and 700 w(e) output with a measured efficiency of 80%. They think they can get to 90% by redesigning. The generator is 10" in diameter by 6" long. The stator weighs 70 lbs. and the plunger weighs 18 lbs, for a total of 88 lbs. Flight weight for this generator would be 61 lbs. Of course, higher efficiency and lighter weight can be obtained by operating at higher frequencies but the engine efficiency drops off. Sixty hertz was computed to be the optimum.

3.5 Energy Storage Mechanisms

The system will probably require some means of energy storage because the laser beam cannot always be directed at the energy converter. In the "Stirling" cycle systems, energy can be stored at the head end as heat (see Section 3.1.2.2). The "Otto" cycle systems energy must be stored by batteries. Nickel-cadmium batteries have been proved by many years of use in connection with solar cells in space power systems. Current technology seems to be using Ni-Cd batteries at 50% depth of discharge which gives a power density of 10 w-hr/Kg (Ref. 41). The energy efficiency is hardly ever stated but is estimated at 75%.

3.6 Heat Rejection Mechanisms

All heat engines must reject heat. In a space power system rejection must be by radiator. The radiator surface must have a high emissivity and must be either shielded from the sun or have a surface with also a low absorptivity to solar radiation. Low temperatures are much better for the engine but cause the size of the radiator to greatly increase. Light weight radiators are being developed which employ mulitple heat pipes so that meteorite puncture of one pipe will not be serious. Assume that the heat pipe has walls and wick

equivalent to a 0.015" thick steel sheet and also that the surface emissivity is 0.95. The capacity and weight of the radiator is then as shown in Table 19.

C-2

TABLE 19

ASSUMED CAPACITY OF LIGHT-WEIGHT

HEAT RADIATOR FOR SPACE

Temperature ^{o}K	Radiating Capacity Kw/m^2	Specific Weight* Kg/Kw
400	1.38	2.17
350	0.81	3.70
300	0.44	6.82
250	0.21	14.3
200	0.09	33.3

* for 3 Kg/m^2 radiator area

4. SYSTEM EVALUATION

In this section a preliminary evaluation will be given of a number of possible space electric power systems. These systems will be evaluated to a common set of specifications which are:

1. 750 w(e) power to be supplied on a continuous basis.
2. One hour of reserve power to allow for eclipse between laser and receiver engine each day.
3. Zero gravity deep space environment with capability of pointing the receiver mirror and of shading the radiator from the sun.
4. Greater than 50% overall efficiency desired.

It should be emphasized that the information on efficiencies and particularly weights of the various components of the system are very sketchy and in some cases are educated guesses. Particularly this observation is true for the engines. The system concepts presented in this section indicate general possibilities and are in no way definitive at this time.

In this section two systems will be diagrammed, one with the engine internally heated by laser pulses through a window directly into the helium working fluid seeded with a small fraction of absorber gas, the other with the engine externally heated by a thermal energy storage reservoir which obtains its heat from any type of radiant energy. Table 20 reviews the engine characteristics for two kinds of internally heated machines, the Garbuny and the Otty cycles, and one type of externally heated machine, the Stirling engine.

4.1 Internal Heated Systems

The Garbuny cycle was chosen because it promises to have the highest efficiency of any of the internally heated engines (see Section 3.2.1.4). It should be emphasized again that this efficiency is based upon an estimate of the top temperature attainable in a laser heated gas with no experimental evidence

Cycle Name	Garbuny	Otto	Stirling
Cycle Processes			
Compression	Isothermal	Adiabatic	Both*
Heating	Const. Vol.	Const. Vol.	Variable Vol.**
Expansion	Adiabatic	Adiabatic	Both*
Cooling	During Compression	By Gas Exchange	Variable Vol.**
Max. Metal Temp., °K (°F)	300 (80)	300 (80)	1600 (2420)
Max. Gas Temp., °K (°F)	3000 (4940)	3000 (4940)	1600 (2420)
Min. Metal, Gas Temp., °K (°F)	300 (80)	300 (80)	300 (80)
Max. Gas Pressure, atm	317	56	14
Min. Gas Pressure, atm	1	1	6
Gas Heating Method	Laser Pulses Through Window Directly to Seeded Gas		From Solid Heat Exchanger Heated by Radiant Energy
Possible Indicated Engine Efficiency, %	74	68	73

*Isothermal in some parts of engine, may be adiabatic in other parts.
**Because processes overlap.

TABLE 20. Thermodynamic Cycles to Convert Laser Energy to Mechanical Energy.

at all. The engine operates at an extreme compression ratio using an isothermalizer displacer. Figure 26 shows this concept. The 80% mechanical efficiency of the engine is based upon the information in Tables 15 and 16. The weight is an estimate as is the weight and efficiency of the required speed increaser. The electric generator characteristics are from Section 3.4.4. The rotary electric generator also must act as a starting motor after the one hour eclipse. There will be a severe control problem to be able to synchronize the engine with the incoming pulses of laser radiation. There is a possibility that the efficiency of the seals, engine crank and speed increaser combined can be increased to ~90% and the generator to ~95% (Ref. 31). In this case the overall efficiency would be 0.74(.90)(.95) = 63% for the basic machine.

The big weight penalty that any internally heated engine concept has is the weight of the batteries needed to take care of the eclipse time of one hour and the charge, discharge efficiency that goes with it.

The Otto cycle summarized in Table 20 and discussed in Section 3.2.1.5.2 is only slightly less efficient but would be technically easier to execute. It has a much lower pressure ratio which would make the window problem much easier and may reduce seal friction. It seems reasonable that it would weigh half of what the Garbuny cycle engine would weigh. Also, the Otto cycle engine is much closer to the current state-of-the-art. If the Otto cycle engine were to replace the Garbuny cycle engine in the system as shown in Figure 27, the overall efficiency would drop from 53 to 48% and the weight would not be changed significantly. After experimental work on laser heating of a confined gas through a window, the Otto cycle may be the only reasonable choice for an internally heated engine.

4.2 External Heated Systems

Two Stirling engine space electric power systems are diagrammed (Figures 27 and 28). One important thing to note is that the thermal energy storage is 98%

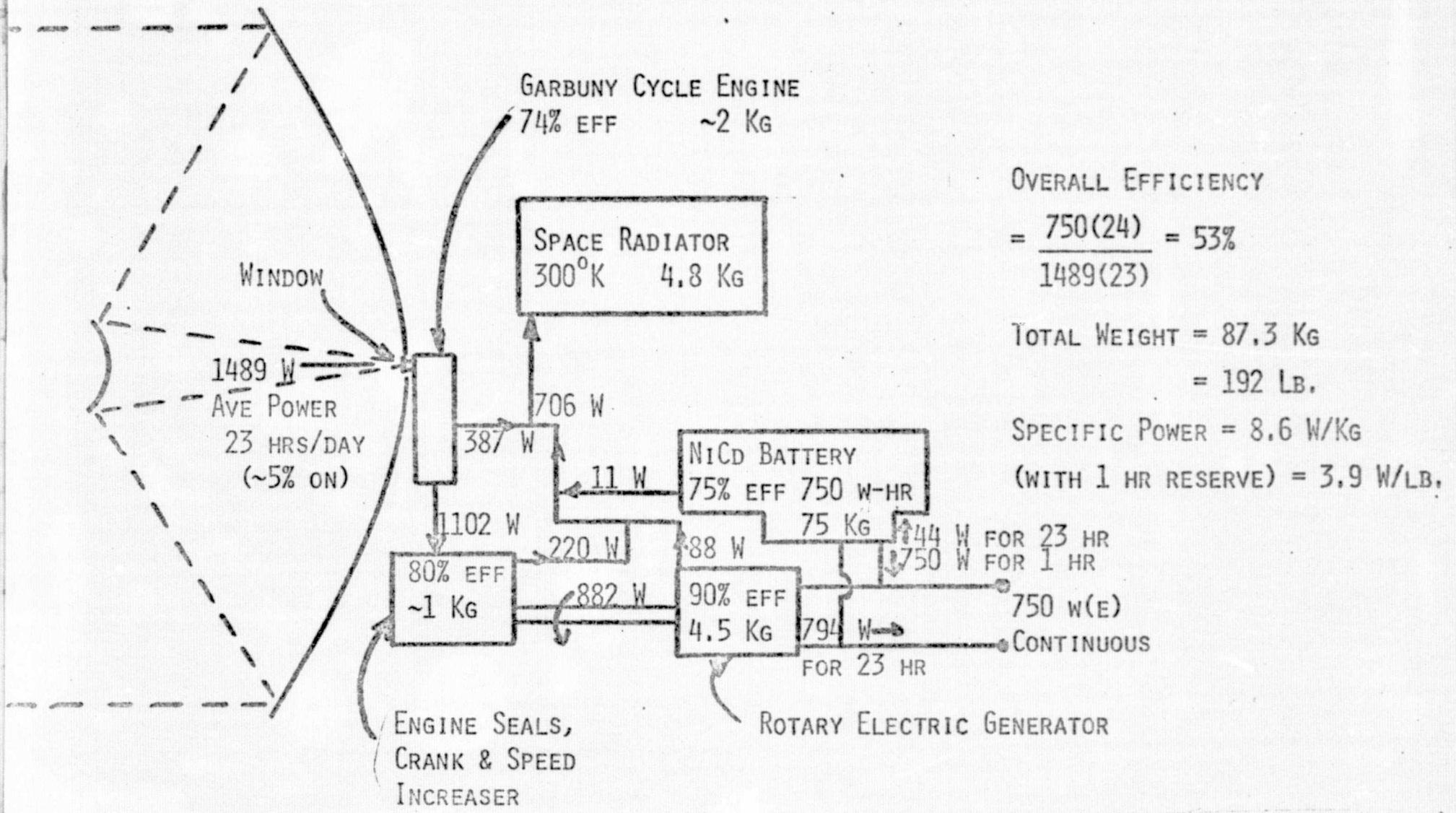

Figure 26. Garbuny Cycle Space Electric Power Concept.

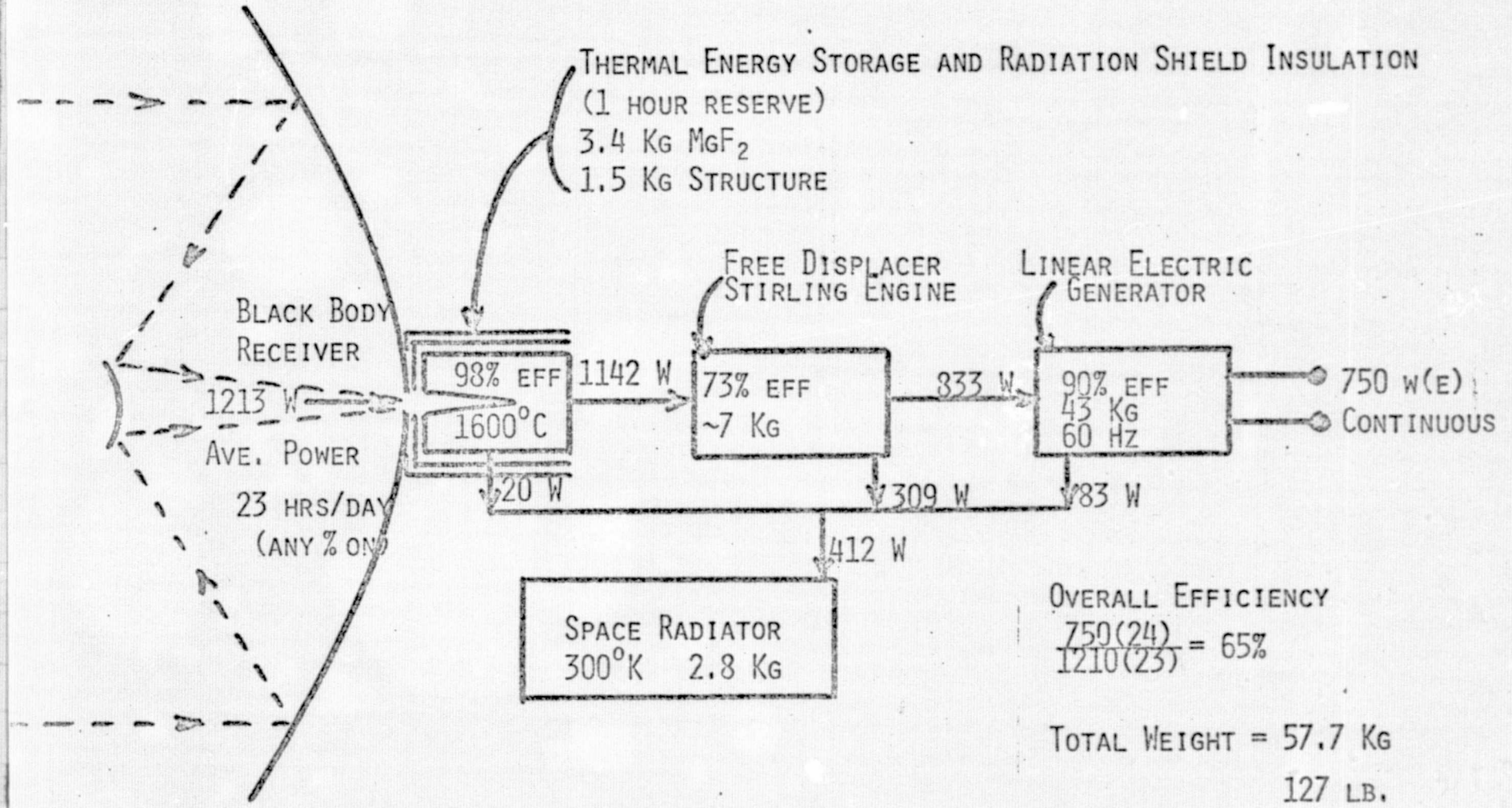

OVERALL EFFICIENCY

$$\frac{750(24)}{1210(23)} = 65\%$$

TOTAL WEIGHT = 57.7 KG

127 LB.

SPECIFIC POWER = 13 W/KG

(WITH 1 HR RESERVE) = 5.9 W/LB.

Figure 27. Stirling Cycle Space Electric Power Concept.

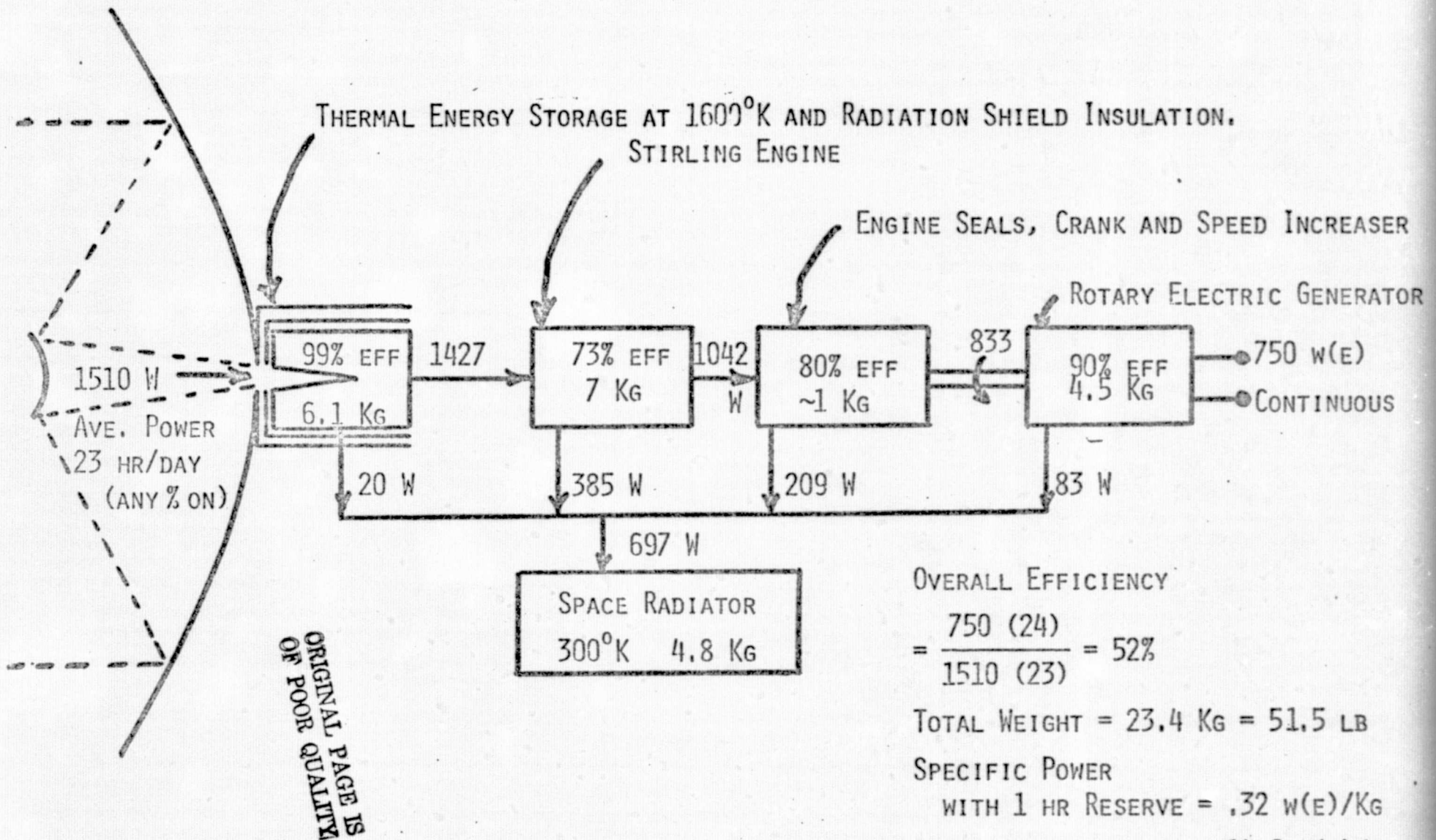

Figure 28. Stirling Cycle Space Electric Power Concept, Light Weight Version.

efficient and is much lighter weight than the batteries it replaces (4.9 Kg vs. 75 Kg). The Stirling engine considered in Figure 27 assumes that the engine can be made with refractory metal to operate at 1600^{o}K heat source temperature at 90% of Carnot efficiency. This is a considerable advance over current technology of 1123^{o}K heat source temperature and 75% of Carnot efficiency which results in an indicated efficiency of 55% instead of the 73% claimed as possible. Making an engine from refractory metal has not been done because it will not take atmospheric oxidation without special coatings which are not very reliable. A refractory metal Stirling engine would be even more expensive to build when the present emphasis is on reducing cost. Ceramics are being considered as a way of increasing temperature and at the same time reducing cost. The task of building a high temperature, high efficiency Stirling engine is probably easier than the development of a laser heated Garbuny cycle engine.

Figure 27 shows the Stirling engine coupled to the linear generator being developed by MTI (Ref. 22). This concept shows the highest efficiency (65%) and weighs less than the Garbuny cycle system.

Note that the weight of the Stirling cycle system is dominated by the linear electric generator (75% of the total). The 60 Hz chosen was a compromise between the characteristics of the engine and the generator. Possibly with isothermalizers, the flow losses can be reduced so that the optimum frequency can be higher and the electric generator can be lighter without sacrificing efficiency. If the operating frequency can thereby be increased to 120 Hz still with 73% efficiency for the engine, then the weight of the 90% efficient generator might be reduced to about 75% of 43 Kg or 28 Kg. This could increase the specific power from 13 w(e)/Kg to 17.6 w(e)/Kg.

What might be desired is a combination of the light weight, efficient but high speed electric generator used in the Garbuny system (See Figure 26) with the light weight thermal energy storage system of the Stirling system

(Figure 27). The combination diagrammed in Figure 28 shows an overall efficiency of 52%, essentially equivalent to the Garbuny cycle system with a specific power of 32 w(e)/Kg which is over 3 times better than the Garbuny cycle system.

5. SUMMARY AND CONCLUSIONS

Before this study was made, it was generally agreed that there was only one reasonable way of converting laser energy to electricity by use of an engine (Ref. 1). In this study the original way of internally heating involving heating a confined gas seeded to absorb the laser radiation coming through a window was considered in more depth as far as the required engines were concerned. The original way was still found to be a reasonable one, but it was found to have the following key problems from an engine and system point of view:

1. Nothing is known experimentally about how hot a confined gas can be heated by a laser through a window and how fast this gas will cool off.
2. Little is known about the ability of the laser window to withstand the combined pressure and thermal stress as it would be used in the engine.
3. Little is known about the seal life, friction and leakage at very high compression ratios in relatively small sizes using a helium gas.
4. The task of keeping the engine synchronized with the incoming pulses of laser energy appears to be difficult.
5. If system design requires energy storage the electrochemical energy storage requires in an internally heated system is about 15 times heavier than thermal energy storage usable in an externally heated system.
6. Long lived reciprocating machines must operate slowly. Low weight, high efficiency generators must turn at high speeds. A reliable speed increaser is therefore necessary.

In this study a new way of converting laser radiation into electrical energy using an engine has been evaluated to the same level as the original way. The new way of external heat involves using the heat from any type of incident radiation being absorbed into a black body and stored in a thermal energy storage reservoir. The heat is then applied to a Stirling engine.

Although the temperature cannot be as high (1600 vs. 3000°K), the efficiency is expected to be about the same (73 vs. 74%). Then the seal friction and speed increaser gearing losses can be eliminated by using an oscillating electric generator which unfortunately is much heavier. This new way is considered by the author to have fewer and less severe problems than the original way but the following key problems are seen from an engine and system point of view:

1. Some advances are needed in Stirling engine design. Indicated efficiency needs to be increased from 75% of Carnot to 90% of Carnot by using isothermalizers and more efficiency regenerators.
2. Some advances are needed in Stirling engine fabrication to build the engine out of refractory metal instead of stainless steel. However, many similar things have been made from refractory metal.
3. Although direct driving of an oscillating electric generator with the Stirling engine led to high efficiency, the system needs to be carefully optimized to reduce weight by increasing efficiency as high as practical.
4. A MgF_2-refractory metal thermal energy storage needs to be developed.

At this point the results from both evaluations are very preliminary but the general magnitudes are expected to be indicative. Table 21 summarizes the results.

The conclusion appears to be that the Stirling engine system is better both from a system performance and from an effort to develop point of view. However, there are so many uncertainties on both sides that a definite conclusion cannot be made.

TABLE 21

SUMMARY OF PRELIMINARY LASER-ELECTRIC

GENERATION SYSTEM DESIGNS

Method of Heating	Cycle	Generator Type	Overall Efficiency,%	Specific Power w(e)/Kg
Internal	Garbuny	Rotary	53	8.6
Internal	Otto	Rotary	48	8.6
External	Stirling	Oscillating	65	13.0
External	Stirling	Rotary	52	32.0

6. RECOMMENDATION

If the total system for laser energy transmission in space is considered worthy of development in comparison to micorwave energy transmission, it is recommended that a more thorough study and design be made of both the internal and external heated systems. It is also recommended that laser heating of a confined gas space be evaluated experimentally to see if the expected gas pressures can be attained without rupturing the laser window. If this can be done to an interesting level, then construction of an engine should be considered. In parallel with the internal heated engine experimental program, it is recommended that a test Stirling engine and a test thermal energy storage system and a test oscillating electric generator be built and evaluated at full temperature to determine if the promised efficiencies can indeed be realized. Life tests on the chemical compatabilities involved in the thermal energy storage should also be started. After the results of the experiments and the additional study are in, a much more certain choice can be made for an efficient and reliable laser-to-electricity energy converter.

REFERENCES

1. M. Garbuny and M. J. Pechersky, "Laser Engines Operating by Resonance Absorption," Applied Optics, May 1976, Vol. 15, No. 5.

2. A. Borucka, "Survey and Selection of Inorganic Salts for Application to Thermal Energy Storage," ERDA-59.

3. J. Schröder, "Thermal Energy Storage and Control," ASME Paper 74-WA/Oct-1.

4. R. C. Svedberg and R. W. Buckman, Jr., "Artificial Heart System Thermal Insulation Component Development," 1975 IECEC Record, pp. 1489-1495.

5. M. F. Patterson, D. J. Webster and J. O. Spragge, "Improved Multilayer Insulation for Compact High Temperature Power Source," 1975 IECEC Record, pp. 1554-1557.

6. W. R. Martini, et al., "Mechanical Engineering Problems in Energetics--Stirling Engines." ASME Paper 69-WA/Ener-15.

7. W. R. Martini, "A Stirling Engine Module to Power Circulatory Assist Devices," ASME Paper 68-WA/Ener-2.

8. W. R. Martini, "Developments in Stirling Engines." ASME Paper 72-WA/Ener-9.

9. J. C. Moise, R. J. Faeser, V. F. Russo, "Thermo-Compressor Powered Artificial Heart Assist System," 1976 IECEC Record, pp. 150-156.

10. R. P. Johnston, et al., "A Stirling/Hydraulic Power Source for Artificial Hearts," 1976 IECEC Record, pp. 143-149.

11. C. F. Hansen, G. Lee, "Laser Power Stations in Orbit," Astronautics and Aeronautics, July 1972, pp. 42-55.

12. R. S. Reylek, et al., "Thermoelectric Module Designed for a Wide Range of Applications Using High Performance Selenide Materials," 1976 IECEC Record, pp. 1599-1605.

13. W. D. Kenney, H. W. Longee, D. L. Adland and R. J. Henler, "Brayton Isotope Power System Ground Demonstrator," 1976 IECEC, pp. 201-207.

14. F. Horrigan, C. Klein, R. Rudko, D. Wilson,"Windows for High-Power Lasers," Laser Technology, Jan. 1969, Published by Laser Optics, P.O. Box 3, Danbury, Connecticut 06810.

15. Vendor Literature, Oriel Optics Corp., Stanford, Connecticut.

16. E. D. Waters, "The Heat Pipe - A Tool and a Challenge," 1976 IECEC Record, pp, 874-875.

17. N. E. Polster, W. R. Martini, "Self-Starting, Intrinsically Controlled Stirling Engine," 1976 IECEC Record, pp. 1511-1518.

18. W. R. Martini, "The Free-Displacer, Free-Piston Stirling Engine--Potential Energy Conserver." 1975 IECEC Record, pp. 995-1002.

19. W. T. Beale, "Free Piston Stirling Engines--Some Model Tests and Simulation," SAE Paper 690230.

20a. J. H. Perry, "Chemical Engineers Handbook," Third Edition, p. 1260.

20b. Personal Communication with W. R. Griffith, McDonnell Douglas Corp.

21. Turner, U.S. Patent 2,899,565; Colgate, U.S. Patent 3,234,395; James, Jr., U.S. Patent 3,105,153.

22. Personal Communication with S. Pitter, MTI, 518-785-2458.

23. R. D. Brooks, S. E. Eckard, R. G. Frank, K. F. Barber, "Design of Reciprocating Single Cylinder Expanders for Rankine Cycle Engines," 1972 IECEC Record, pp. 269-278.

24. C. A. Amann, D. C. Sheridan, C. J. Sagi, and G. D. Skellenger, "The Uniflow Steam Expander--Its Relation to Efficiency of the SE-101 Powerplant," 1972 IECEC Record, pp. 960-970.

25. B. C. Fryer, J. L. Smith, Jr., "Design,Construction and Testing of a New Valved Hot-Gas Engine," 1973 IECEC Record, pp. 174-181.

26. A. B. Martin, "Subsea Nuclear Power Systems for Future Offshore Production Operations," 1976 IECEC Record, pp. 1102-1109.

27. J. Monahan, Ron McKenna, "Development of a 1 KW Organic Rankine Cycle Power Plant for Remote Applications," 1976 IECEC Record, pp. 1148-1156.

28. R. E. Barber, "Solar Powered Organic Rankine Cycle Engines--Characteristics and Costs," 1976 IECEC Record, pp. 1151-1156.

29. S. E. Eckard, "Multi-Vane Expander as Prime Mover in Low Temperature Solar or Waste Heat Applications," 1975 IECEC Record, pp. 1399-1405.

30. Basic Course in Hydraulic Systems Machine Design, Pentor Publishing Co., Cleveland, Ohio, 1968.

31. D. B. Colyer, "Design and Development of Cryogenic Turbo Refrigerator Systems," AFFDL-TR-74-93, April 1974.

32. E. F. Hammond, Jr., A. E. King, A. L. Jokl, "Permanent Magnet Generators for Portable Military Power," SAE Paper 710565.

33. TKM Electric Corporation, Rochester, NY, Vendor Literature, Model A4.

34. P. D. Dunn, G. Rice, R. H. Thring,"Hydraulic and Rotary Drive Stirling Engines with Fluidized Bed Combustion/Heat Pipe System," 1975 IECEC Record, p. 942.

35. G. Schmidt, "Theory of Lehmann's Heat Machine, Journal of the German Engineers' Union, Vol. XV, No. 1 (1871).

36. R. B. Goranson, R. P. Johnston, W. R. Martini, M. A. White, "Development of a Simplified Stirling Engine to Power Circulatory Assist Devices," 1968 IECEC Record, pp. 733-749.

37. W. R. Martini, M. A. White, "How Unconventional Stirling Engines Can Help Conserve Energy," 1974 IECEC Record, pp. 1092-1099.

38. A. P. J. Michels, "The Philips Stirling Engine: A Study of its Efficiency as a Function of Operating Temperatures and Working Fluids," 1976 IECEC Record, pp. 1506-1510.

39. E. A. Paste and R. O. Whitaker, "Investigation of a 3 KW Stirling Cycle Solar Power System," WADD-TR-61-122, Vol. I to X.

40. GMR Stirling Engines, F. E. Heffner, General Motors Research Laboratory, Warren, Michigan (sales literature).

41. T. A. LaVigna, F. L. Hornbuckle, "The ATS-6 Power System: Hardware Implimentation and Orbital Performance," 1976 IECEC Record, pp. 1414-1421.

APPENDIX A

DERIVATION OF EQUATIONS FOR HEAT FLOW FROM VOLUMES WHICH ARE HEATED UNIFORMLY

During expansion and compression of a gas, the gas temperature of the entire volume changes uniformly before thermal-conductivity makes a difference. Laser heating also approximates this. For the purpose of evaluation the equations will be derived for heat flow from a slab and from a cylinder.

From a Slab

In Figure A1 the gas is being cooled from both sides. The heat flow at x is:

$$Q_x = Q_w \frac{x}{(s/2)} = -k_G A \frac{dT}{dx} \tag{A1}$$

where Q_w = heat flow at wall, watts

x = distance from centerline, m

k_G = thermal conductivity of gas, w/m ^oC

A = area for heat flow, m^2

T = gas temperature, ^oC

Integrating,

$$\frac{2Q_w}{s} \int_0^{s/2} x\,dx = -k_G A \int_{T_\ell}^{T_M} dT \tag{A2}$$

So

$$Q_w = \frac{4k_G A}{s} (T_\ell - T_M) \tag{A3}$$

However, we need to know the average gas temperature, T_A, instead of the centerline temperature, T_ℓ. T_A is defined by the equation

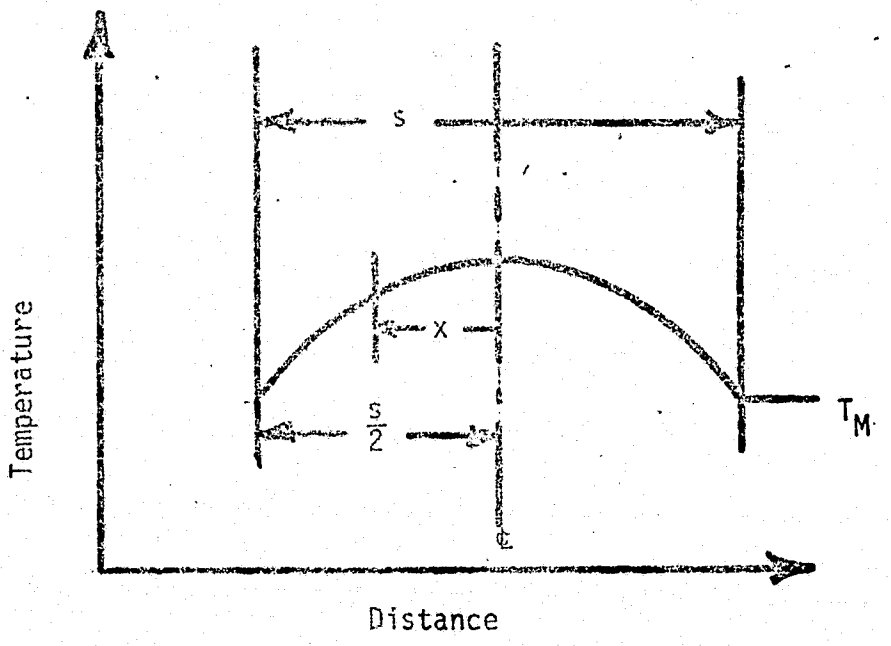

Figure A1. Assumed Gas Conduction in a Slab.

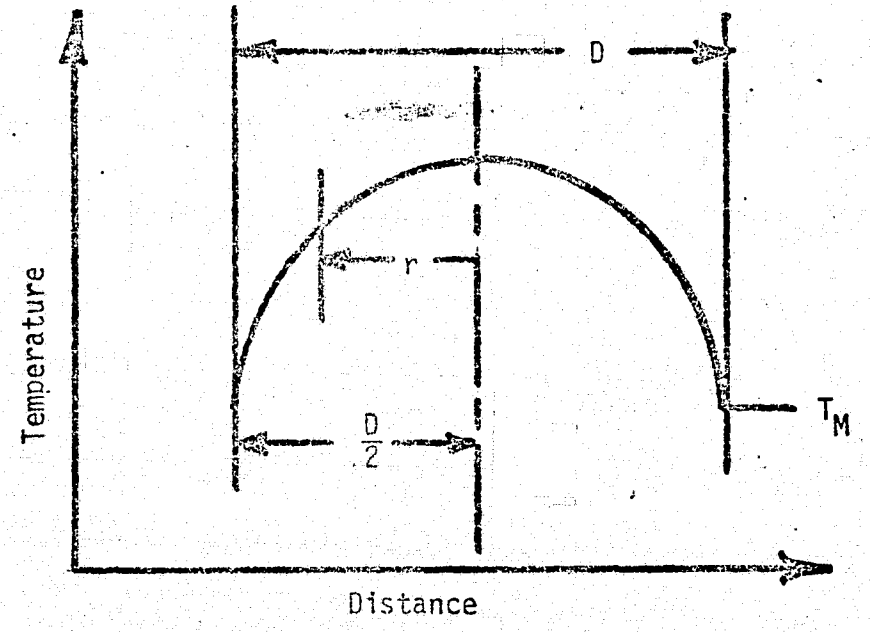

Figure A2. Assumed Gas Conduction in a Cylinder.

$$(T_A - T_{\text{¢}})\frac{s}{2} = \int_0^{s/2} (T - T_{\text{¢}})dx \qquad (A4)$$

Using different limits on Equation A2:

$$\frac{2Q_w}{s}\int_0^x x\,dx = -k_G A \int_{T_{\text{¢}}}^{T} dT \qquad (A5)$$

$$\frac{2Q_w}{s}\frac{x^2}{2} = -k_G A(T - T_{\text{¢}}) \qquad (A6)$$

$$T - T_{\text{¢}} = -\frac{Q_w x^2}{sk_G A} \qquad (A7)$$

So

$$T_A - T_{\text{¢}} = \frac{\int_0^{s/2} -\frac{Q_w}{sk_G A}x^2 dx}{s/2} = -\frac{Q_w s}{12k_G A} \qquad (A8)$$

From Equation A3

$$T_{\text{¢}} - T_M = \frac{Q_w s}{4k_G A} \qquad (A9)$$

Therefore,

$$T_A - T_M = T_A - T_{\text{¢}} + (T_{\text{¢}} - T_M) \qquad (A10)$$

$$= -\frac{Q_w s}{12k_G A} + \frac{Q_w s}{4k_G A} = \frac{Q_w s}{6k_G A}$$

or

$$Q_w = \frac{6k_G A}{s}(T_A - T_M) \qquad (A11)$$

Also, from the standpoint of heat capacity,

$$Q_w = -\rho V C_v \frac{dT_A}{d\theta}$$

where ρ = gas density, kg/m^3

V = gas volume, m^3

C_v = heat capacity at constant volume, $j/kg\ ^oC$

T_A = average gas temperature, ^oC

θ = time, seconds

From a Cylinder

In Figure A2 the gas is being cooled from the cylindrical surface. The heat flow at r is:

$$Q_r = Q_w \frac{\pi r^2}{\frac{\pi}{4}D^2} = -k_G(2\pi r\ell)\left(\frac{dT}{dr}\right)_r \qquad (A12)$$

where ℓ = length of cylinder.

Integrating:

$$\int_0^{D/2} \frac{4Q_w r^2\, dr}{D^2(2\pi r\ell k_G)} = -\int_{T_\ell}^{T_M} dT \qquad (A13)$$

$$\frac{2Q_w}{\pi\ell k_G D^2}\left[\frac{r^2}{2}\right]_0^{D/2} = -\left[T\right]_{T_\ell}^{T_M}$$

$$\frac{Q_w D^2}{\pi\ell k_G D^2 4} = T_\ell - T_M$$

$$\frac{Q_w}{4\pi\ell k_G} = T_\ell - T_M \qquad (A14)$$

However, what is needed is the integrated average gas temperature, T_A. By definition,

$$(T_A - T_\ell)\frac{\pi}{4}D^2 = \int_0^{D/2} (T - T_\ell)2\pi r dr \qquad (A15)$$

Using different limits for Equation A13,

$$\frac{2Q_w}{\pi\ell k_G D^2}\int_0^r r dr = -\int_{T_\ell}^{T} dT \qquad (A16)$$

or

$$\frac{Q_w r^2}{\pi \ell k_G D^2} = T_{\ell} - T \tag{A17}$$

Substituting into Equation A15,

$$(T_A - T_{\ell}) \frac{\pi}{4} D^2 = \int_0^{D/2} - \frac{Q_w r^2}{\pi \ell k_G D^2} \, 2\pi r dr \tag{A18}$$

$$= - \frac{2Q_w}{\ell k_G D^2 \pi} \int_0^r r^3 dr$$

$$T_A - T_{\ell} = - \frac{2Q_w(4)}{\ell k_G D^2 D^2 \pi} \left[\frac{r^4}{4}\right]_0^{D/2}$$

$$= - \frac{2Q_w(4)D^4}{\ell k_G D^4 \pi (4)(16)}$$

$$= - \frac{Q_w}{8\ell k_G \pi} \tag{A19}$$

Therefore:

$$T_A - T_M = T_A - T_{\ell} + T_{\ell} - T_M \tag{A20}$$

Substituting Equation A14 and A19 in Equation A20:

$$T_A - T_M = - \frac{Q_w}{8\pi \ell k_G} + \frac{Q_w}{4\pi \ell k_G} = \frac{Q_w}{8\pi \ell k_G} \tag{A21}$$

or

$$Q_w = 8\pi \ell k_G (T_A - T_M) \tag{A22}$$

APPENDIX B

COMPUTER PROGRAMS USED IN ENGINE ANALYSIS

Title HEAT TRANSFER

SWITCH TO W/PRGM. PRESS [f] [PRGM] TO CLEAR MEMORY.

Page ____ of ____

KEY ENTRY	CODE SHOWN	COMMENTS
LBL	23	
A	11	
RCL 1	3401	
R/S.	84	COPY Θ_0.
B	12	
R/S	84	COPY V_0
STO 2	33 02	
RCL 3	3403	
R/S.	84	COPY T_0.
10 C	13	
R/S.	84	COPY P
LBL	23	
1	01	RETURN LABLE
RCL 6	3406	
RCL 1	3401	
+	61	
R/S.	84	COPY Θ.
STO 1	3301	
RCL 2	3402	
20 B	12	
R/S.	84	COPY V_1
STO 2	3302	
÷	81	
2	02	
↑	41	
3	03	
÷	81	
9	35	
0	05	
30 RCL 3	3403	
X	71	
R/S.	84	COPY T_1
RCL 7	3407	
−	51	
RCL 5	3405	
RCL 2	3402	
÷	81	
RCL 4	3404	
RCL 2	3402	
40 X	71	
+	61	
ℓ^{-1}	32	
LN	07	
÷	81	
RCL 7	3407	
+	61	
R/S.	84	COPY T_1'
STO 3.	3303	
C	13	
50 R/S.	84	COPY P.

KEY ENTRY	CODE SHOWN	COMMENTS
GTO	22	
1	01	
RTN.	24	
LBL	23	GAS VOLUME SUBROUTINE
B	12	
RCL 1	3401	
ℓ	31	
COS.	05	(AFTER Θ=180 CHANGE TO 360)
CHS	42	
60 1	01	
÷	61	
2(3)	02(03)	
⊙	83	
6(7)	06(07)	$\Theta = 0$ TO 180, 2.505×10^{-3}
6(0)	06(05)	Θ 180 TO 360, 1.746×10^{-5}
EEX	43	
5	05	
CHS	42	
X	71	
70 1	01	
⊙	83	
7(11)	07(04)	
3(0)	03(03)	
EEX	43	
6(5)	06(05)	
CHS	42	
+	61	
RTN	24	
LBL	23	
80 C	13	PRESSURE SUB ROUT
⊙	83	
0	00	
1(2)	01(02)	
2(6)	02(06)	
3(0)	03(00)	
RCL 3	3403	
X	71	
RCL 2	3402	
÷	81	
90 RTN.		

REGISTERS

R1 Θ (START WITH 0)

R2 V_0, V_1

R3 T_0 (START WITH 300)

R4 13 362 (516.4)

R5 A (2.641 x 10^5)

R6 $\Delta\Theta$ 10

R7 T_P 300

R8

R9

LABELS

A ✓
B ✓
C ✓
D
E
0
1 ✓
2
3
4
5
6
7
8
9

FLAGS

1
2

ORIGINAL PAGE IS OF POOR QUALITY

TO RECORD PROGRAM INSERT MAGNETIC CARD WITH SWITCH SET AT W/PRGM.

Title GARBONY (OTTO) CYCLE Page ____ of ____

Programmer ____ Date ____

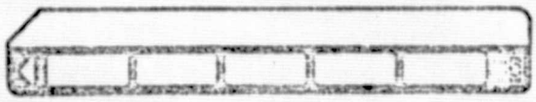

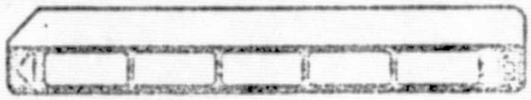

STEP	INSTRUCTIONS	INPUT DATA/UNITS	KEYS	OUTPUT DATA/UNITS
1	FEED IN APPROPRIATE CARD			
2.	CHARGE REGISTERS 1, 3, 4, 5, 6, +7 WITH APPROPRIATE CONSTANTS.			
3.	START.		A	
4.	COPY.			
	θ, V_0 T_0 $-T_1'$	P.		
	— — —	—		
	— — — —	—		
	! ! ! !	!		
	! ! ! !	!		
	! ! ! !			
5.	CHANGE R5 AFTER θ=180 LINE			
	(CHANGE R3 " " " ")			

HEWLETT-PACKARD

APPENDIX C

Errata to 1976 IECEC Paper 769259

SELF-STARTING, INTRINSICALLY CONTROLLED STIRLING ENGINE

Eratta to Self-Starting, Intrinsically Controlled Stirling Engine

The calculations of the TES-Stirling automotive propulsion system given in the published paper was found to be in error by a large factor at one point. As a result of this mistake the computation procedure has been thoroughly re-examined and corrected and has been computerized. An adequate but not optimum design is presented below to substitute for the one that was in error. Table IIIN substitutes for Table III in the published paper. The major differences are that the maximum displacer stroke and the power piston stroke have been reduced from 2" (5.1 cm) to 1" (2.54 cm) with a compensating increase in gas pressure. The length of the displacer stroke has been made variable and the gearing ratio between the engine and the wheels has been fixed at 4 to 1.

These changes result in a simple automobile propulsion system that can climb hills and accelerate and also cruise efficiently on the level. Figure 8.1N compares the traction force generated by the specified engine with the drag force which is the sum of rolling friction, air friction and the force needed to climb a hill. For instance, at 65 kph (40 mph) the drag force on the level is 340 N (76 lbs). The engine can produce this traction force at 65 kph (40 mph) by operating with a 10% displacer stroke. Figure 8.2N shows the heat demand. For the example operating point, 11 KW are required. Therefore, the charge of 73 KWH is expended in 6.64 hours resulting in a range of 431 km (263 mi). Figure 8.3N shows the vehicle range for other vehicle speeds. The fuel cost of operating the vehicle in terms of ¢/Km or ¢/mile is also given on Figure 8.3N as a function of speed and heat cost. Electricity is a convenient source for this heat but heat can be derived from any source that can produce heat at 1200 to 1400°F (650-760°C). For instance, heat derived from coal or wood obtained at a fuel price of $1.5/$10^6$ BTU ($38/ton for coal) might be supplied at a price of $2.93/$10^6$ BTU (1¢/KWH) which is also about the retail price of electricity in some areas. Therefore, at 65 kph (40 mph) the fuel cost would be 0.2¢/km (0.3¢/mile). In contrast a vehicle attaining 30 miles/gallon of gasoline at 40 mph and using 60¢/gallon gasoline would have a fuel cost of 2¢/mile.

Table IIN gives the revised vehicle acceleration capability and top speed. This design meets or exceeds all specifications. This engine promises to be so much better than current internal combustion engines that careful optimization is not needed until the accuracy of the computational procedure is verified by measurement.

Table IIN. Vehicle Performance.

	EPA Specification	Calculation This Paper
Ground covered in 10 seconds from standing start	440 ft. (134 m.)	436 ft. (133 m.)
Time to reach 60 mph (97 kph) from standing start	13.5 sec.	11.3 sec.
Time to accelerate from 25 mph (40 kph) to 70 mph (113 kph)	15 sec.	10 sec.
Climb 30% grade at 5 mph (8 kph)	yes	yes
Climb 5% grade at 65 mph (105 kph)	yes	yes
Top speed on level	85 mph (137 kph)	120 mph (195 kph)

Table IIIN. Specifications and Calculations for a TES-Stirling Automotive Propulsion System.

Specifications

Overall		
Length	50 in.	(1.27 M)
Diameter	32 in.	(0.81 M)
Weight	572 lbs.	(260 kg)
Engine		
Displacers		
number	4	
ID of cylinder	11 in.	(27.9 cm)
maximum stroke	1 in.	(2.5 cm)
cylinder length	12 in.	(30.5 cm)
drive rod diameter	0.5 in.	(1.2 cm)
Regenerator*		
number of spaces	20	
thickness each space	0.010 in.	(0.25 mm)
thickness of foil	0.0005 in.	(0.012 mm)
Power Pistons		
number	4	
effective diameter	11 in.	(27.9 cm)
stroke	1 in.	(2.5 cm)
Isothermalizers**		
fin thickness	0.050 in.	(1.27 mm)
fin length	1 in.	(2.5 cm)
end clearance	0.005 in.	(0.12 mm)

*Foils wrapped around displacer and attached to it. Foils embossed to maintain spacing.
**Interleaving square fins with slight taper.

Transmission
- Efficiency--90%
- Gear reduction engine/wheels 4
- Wheel diameter--22 in. (56 cm)

Thermal Energy Storage

Number	2
Weight both TES Containers (includes heat pipe)	99 lb. (45 Kg)
Weight all LiF salt	341 lb. (115 Kg)
Volume of all LiF salt	85 liters
Volume of each TES assuming 50 v/o LiF	5,815 $in.^3$ (85 liters)
TES container diameter	29 in. (73.5 cm)
Maximum temperature	1561°F (850°C)
Minimum temperature	1021°F (550°C)
Capacity, together	250,000 BTU (73 KWH)

Calculated Performance

Assumed hot gas temp.	1200°F	(649°C)
Assumed cold gas temp.	150°F	(66°C)
Maximum gas pressure	197 psia	(1.36×10^6 Pa)
Minimum gas pressure	91 psia	(6.27×10^5 Pa)
% of full stroke	8.3	
Vehicle speed	30 mph	(49 kph)

Heat Required, KW

Carnot Heat	6.30
Reheat Loss	0.14
Shuttle Conduction	0.01
Metal Conduction	0.15
Gas Conduction	0.20
Insulation Loss	0.11
Regenerator Windage Credit	-0.03
Isothermalizer " "	-0.02
Net	6.86

Power Generated, KW

Basic	3.98
Regenerator Windage	-0.06
Isothermalizer Windage	-0.03
Net	3.89

Heat Source Superheat (°C)		
Due to gas conduction	24	
Due to fin conduction	8	
Hot Metal Temperature	955°K	(1259°F)
Heat Sink Subheat (°C)		
Due to gas conduction	2	
Due to fin conduction	1	
Cold Metal Temperature	336°K	(145°F)
% of Carnot Efficiency*	87	
Predicted Motive Force	258 N	(58 lb)
Computed Vehicle Drag	258 N	(58 lb)
Range	521 Km	(318 mi)
Stand Time**	6.3 days	

*Based upon metal temperatures.
**Time that the 73 KWH capacity will be dissipated by the 472 watt constant heat leak.

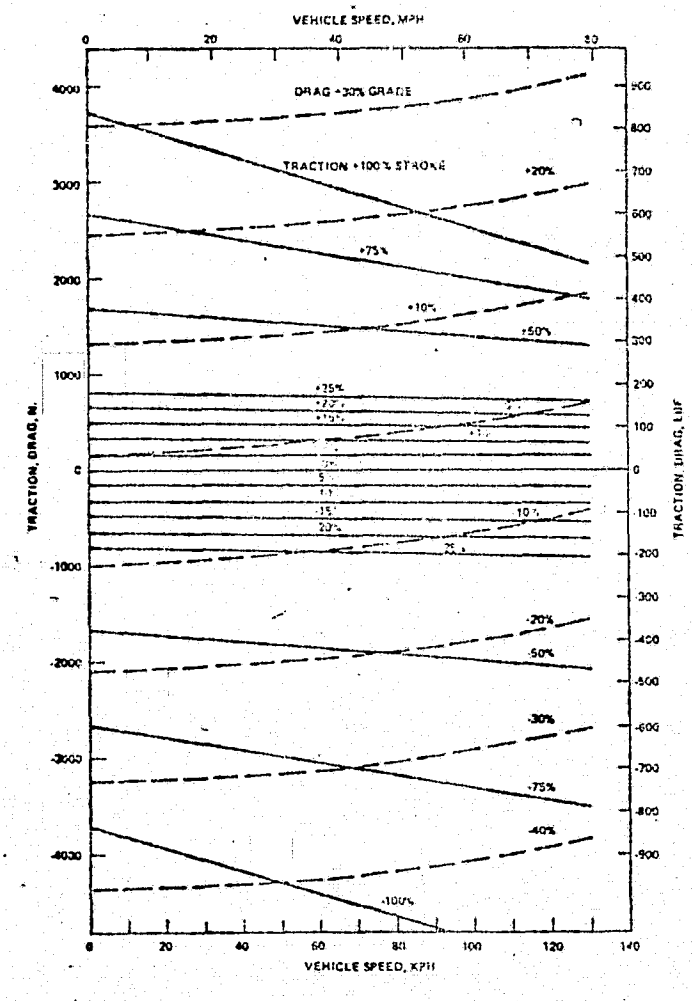

Figure 8.1N. Traction and Drag Force for Vehicle.

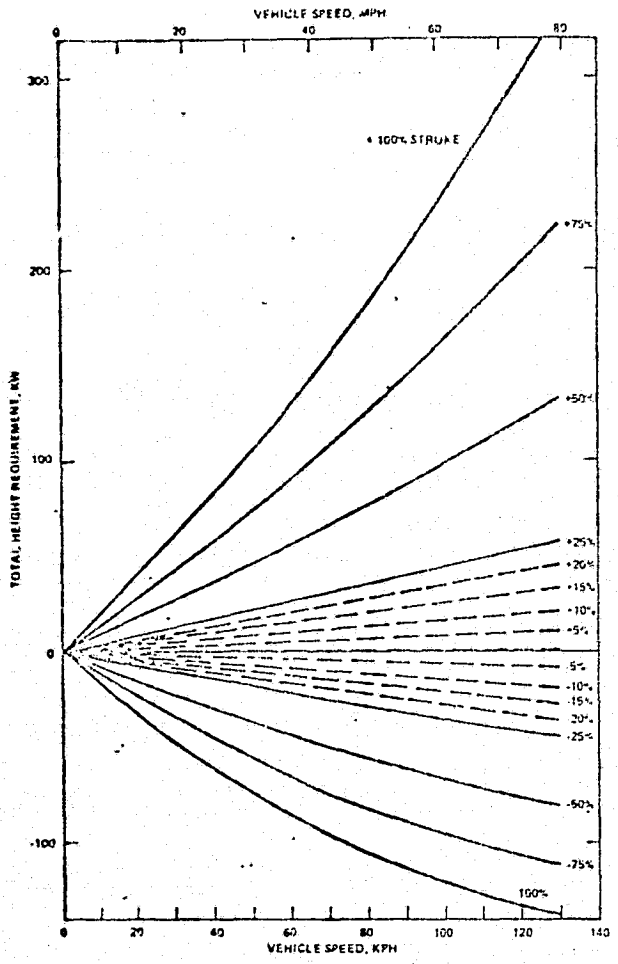

Figure 8.2N. Total Heat Requirement for Vehicle.

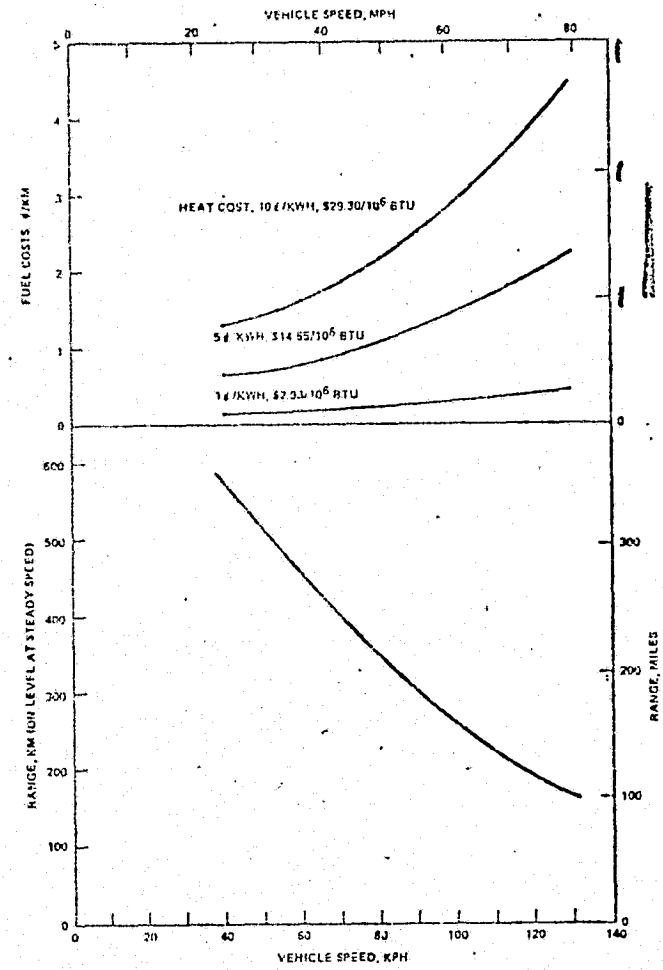

Figure 8.3N. Calculated Range and Fuel Cost.